Technische Universität München
TUM School of Engineering and Design

Distortion Control after Grinding by computer-aided Design of Distortion Compensation Strategies

Christian Schieber

Vollständiger Abdruck der von der TUM School of Engineering and Design der Technischen Universität München zur Erlangung eines

Doktors der Ingenieurwissenschaften (Dr.-Ing.)

genehmigten Dissertation.

Vorsitz: Prof. Wolfgang Polifke, Ph.D.

Prüfende der Dissertation:

1. Prof. Dr.-Ing. Michael F. Zäh
2. Prof. Dr.-Ing. Michael Schmidt

Die Dissertation wurde am 10.01.2024 bei der Technischen Universität München eingereicht und durch die TUM School of Engineering and Design am 27.05.2024 angenommen.

Editors' Preface

In times of global challenges, such as climate change, the transformation of mobility, and an ongoing demographic change, production engineering is crucial for the sustainable advancement of our industrial society. The impact of manufacturing companies on the environment and society is highly dependent on the equipment and resources employed, the production processes applied, and the established manufacturing organization. The company's full potential for corporate success can only be taken advantage of by optimizing the interaction between humans, operational structures, and technologies. The greatest attention must be paid to becoming as resource-saving, efficient, and resilient as possible to operate flexibly in the volatile production environment.

Remaining competitive while balancing the varying and often conflicting priorities of sustainability, complexity, cost, time, and quality requires constant thought, adaptation, and the development of new manufacturing structures. Thus, there is an essential need to reduce the complexity of products, manufacturing processes, and systems. Yet, at the same time, it is also vital to gain a better understanding and command of these aspects.

The research activities at the Institute for Machine Tools and Industrial Management (*iwb*) aim to continuously improve product development and manufacturing planning systems, manufacturing processes, and production facilities. A company's organizational, manufacturing, and work structures, as well as the underlying systems for order processing, are developed under strict consideration of employee-related requirements and sustainability issues. However, the use of computer-aided and artificial intelligence-based methods and the necessary increasing degree of automation must not lead to inflexible and rigid work organization structures. Thus, questions concerning the optimal integration of ecological and social aspects in all planning and development processes are of utmost importance.

The volumes published in this book series reflect and report the results from the research conducted at *iwb*. Research areas covered span from the design and development of manufacturing systems to the application of technologies in manufacturing and assembly. The management and operation of manufacturing systems, quality assurance, availability, and

autonomy are overarching topics affecting all areas of our research. In this series, the latest results and insights from our application-oriented research are published, and it is intended to improve knowledge transfer between academia and a wide industrial sector.

Rüdiger Daub *Gunther Reinhart* *Michael Zaeh*

Acknowledgments

This dissertation was written during my employment as a research associate at the Institute for Machine Tools and Industrial Management (*iwb*) at the Technical University of Munich (TUM), funded by the German Research Foundation (DFG).
First, I would like to express my sincere gratitude to Prof. Dr.-Ing. Michael Zaeh, the head of the Chair for Machine Tools and Manufacturing Technology, for his benevolent encouragement and generous assistance at every research project stage. I express my most profound appreciation to Prof. Dr.-Ing. habil. Carsten Heinzel and Matthias Hettig of the Leibniz Institute for Material-Oriented Technologies (IWT) for the always fruitful technical discussions and suggestions concerning the topic of this thesis. I would like to extend my sincere thanks to my second examiner, Prof. Dr.-Ing. Michael Schmidt, and the examination board chairman, Prof. Dr. Wolfgang Polifke.

This endeavor would also not have been possible without my colleagues Matthias Wimmer, Christian Bernauer, and Xiao Fan Zhao, who contributed to the success of this thesis with their essential and helpful comments. Aside from that, I would like to thank all my colleagues for the numerous professional discussions on my topic, and also all students, especially Wenzhe Liu and Valentin Müller, who supported me in the elaboration and implementation of the method in the context of their student research projects or their activities as student assistants. Additionally, I want to sincerely thank my office colleagues, Christian Fritz, Sophie Grabmann, and Avelino Zapata, for the numerous discussions on equally essential topics apart from work.

Finally, I would like to thank my parents, who contributed to the success of my work through their patience and loving support.

Straubing, December 2023 *Christian Schieber*

Table of Contents

List of Abbreviations

2D	two-dimensional
3D	three-dimensional
AISI	American Iron and Steel Institute
BPP	Beam parameter product
CIRP	Collège International pour la Recherche en Productique (English: The International Academy for Production Engineering)
CMMO	Conference on Modeling of Machining Operations
CNC	Computerized numerical control
Cr	Chromium (chemical element)
CP	Conceptional Phase
DFG	Deutsche Forschungsgemeinschaft (English: German Research Foundation)
DIN	Deutsches Institut für Normung (English: German Institute for Standardization)
E modulus	Elastic modulus or Young's modulus
e.g.	exempli gratia (English: for example)
EN	European norm
et al.	et alii (English: and others)
F	Main Findings
FE	Finite element
FEM	Finite element method
FWHM	Full Width at Half Maximum
i.e.	id est (English: that is)
ISO	International Organization for Standardization

iwb	Institut für Werkzeugmaschinen und Betriebswissenschaften (English: Institute for Machine Tools and Industrial Management)
IWT	Leibniz-Institut für Werkstofforientierte Technologien (English: Leibniz Institute for Material-Oriented Technologies) (at University of Bremen, Germany)
Mo	Molybdenum (chemical element)
No	Numero sign
NC	Numerical control
P	Publication
p.	Page
pp.	Pages
Ph.D.	Doctor of Philosophy
QT	Quenched and tempered
SO	Sub-objective
TUM	Technical University of Munich
VDI	Verein Deutscher Ingenieure (English: Association of German Engineers)

List of Symbols

Latin Symbols

Variable	Unit	Description
a	mm	Geometric parameter for the width of a double elliptical heat source
A_C	€	Total costs for the computer-aided distortion control
a_e	mm	(Radial) depth of cut
a_{ed}	µm	Dressing depth
A_M	€/a	Total annual costs for manual flame straightening
a_{se}	mm	(Radial) effective depth of cut
b	mm	Geometric parameter for the depth of a double elliptical heat source
b_s	mm	Grinding wheel width
c	J/(kg · K)	Specific heat capacity
C_C	€	Costs for a computer cluster
C_D	€	Costs for the deep rolling tool
c_f	mm	Geometric parameter for the front part of a double elliptical heat source
C_{FE}	€	Costs for an FEM software
C_L	€	Costs for the laser equipment
c_r	mm	Geometric parameter for the rear part of a double elliptical heat source
d_L	mm	Laser spot diameter on the workpiece
d_l	mm	Diameter of the ring-shaped laser spot
d_{L0}	mm	Laser focus diameter
d_s	mm	Grinding wheel diameter
d_{se}	mm	Effective grinding wheel diameter
E	MPa	Elastic modulus
e_c	J/mm³	Total specific grinding energy
e_{ch}	J/mm³	Specific chip formation energy
e_{pl}	J/mm³	Specific plowing energy

e_{sl}	J/mm³	Specific sliding energy
E_t	MPa	Tangent modulus
F	N	Total grinding force
$F_{F_{dr}}$	N	Frictional force during deep rolling
$F_{n,S}$	N	Normal force of a plowing grain
$F_{N_{dr}}$	N	Deep rolling normal force
$F_{t,S}$	N	Tangential force of a plowing grain
f_a	mm/min	Traverse feed rate of the grinding wheel
F_{dr}	N	Deep rolling force
f_{dr}	mm	Lateral feed perpendicular to the deep rolling velocity
F_n	N	Normal grinding force
F_t	N	Tangential grinding force
h	W/(mm² · K)	Heat transfer coefficient
h_m	mm	Maximum uncut chip thickness
h_v	mm	V-groove height
h_w	mm	Workpiece height
HV	HRC	Surface hardness
I_L	W/mm²	Laser beam intensity
$I_L(r_L, z_L)$	W	Local laser beam intensity
I_{L0}	W/mm²	Intensity at the beam waist center
k	W/(mm · K)	Thermal conductivity
l_g	mm	Grinding contact length
l_w	mm	Workpiece length
M^2	-	Beam quality factor
M_f	°C	Martensite finish temperature
M_G	€/h	Costs for flame straightening material
M_L	€/a	Annual maintenance costs for the laser equipment
M_s	°C	Martensite start temperature
N_{dr}	-	Number of deep rolling passes
N_l	-	Number of laser spot passes
$P_{l,abs}$	W	Absorbed laser power
P_c	W	Grinding power
p_{dr}	bar	Deep rolling pressure
P_{FE}	€/h	Costs for an FEM engineer
P_g	W/mm²	Specific grinding power
P_l	W	Laser power
P_{WS}	€/h	Costs for a welding specialist

$\dot{Q}_{\infty}$	W	Heat flux via radiation and convection at the workpiece surface
$\dot{Q}_{ch}$	W	Heat flux to the chip
$\dot{Q}_{f}$	W	Heat flux to the fluid
$\dot{Q}_{s}$	W	Heat flux to the grinding wheel
$\dot{Q}_{total}$	W	Total heat flux generated in the grinding zone
$\dot{Q}_{w}$	W	Heat flux to the workpiece
q_d	-	Speed ratio during dressing
Q_w	mm³/s	Material removal rate
q_w	W/mm²	Heat flux density
Q'_w	mm³/(mm · s)	Specific material removal rate
R_a	µm	Arithmetic average roughness
r_L	mm	Radial distance to the laser beam axis
$R_{p0.2}$	MPa	Offset yield strength at 0.2 % strain
R_t	µm	Peak-to-valley roughness
S	m²	Finite surface
T	°C	Temperature
t	s	Time
$T(x, y)$	°C	Quasi-stationary two-dimensional temperature field
$T(x, y, z, t)$	°C	Transient three-dimensional temperature field
T_{∞}	°C	Ambient temperature
t_C	h	Simulation time
t_M	h/a	Annual working hours of a welding specialist
V	m³	Finite Volume
v_c	m/s	Cutting speed
v_{dr}	mm/min	Deep rolling velocity
v_{ft}	mm/min	Grinding feed rate
v_{jet}	l/min	Lubricant flow rate
v_l	m/min	Laser feed rate
v_s	m/s	Peripheral wheel speed
V_w	mm³	Removed workpiece material volume
v_w	mm/min	Workpiece feed rate
w_v	mm	V-groove width
w_w	mm	Workpiece width
x	mm	General spatial coordinate
y	mm	General spatial coordinate
z	mm	General spatial coordinate

z_L	mm	Distance to the beam waist
z_R	mm	Rayleigh length

Greek Symbols

Variable	Unit	Description
β	°	Angle of the V-groove
ΔPV	mm	Workpiece distortion difference (peak to valley)
ε	-	Strain
$\boldsymbol{\varepsilon_{cr}}$	-	Creep strain vector
$\boldsymbol{\varepsilon_{el}}$	-	Elastic strain vector
ε_{ep}	-	Grinding energy fraction entering the workpiece
$\boldsymbol{\varepsilon_{pl}}$	-	Plastic strain vector
$\boldsymbol{\varepsilon_{th}}$	-	Thermal strain vector
$\boldsymbol{\varepsilon_{total}}$	-	Total strain vector
$\boldsymbol{\varepsilon_{tp}}$	-	Transformation plasticity vector
$\boldsymbol{\varepsilon_{tr}}$	-	Phase transformation strain vector
η_{abs}	-	Degree of absorption
Θ_f	°	Aperture angle
λ	µm	Wavelength of the laser radiation
μ	-	Coefficient of friction
ρ	kg/mm³	Material density
σ	MPa	Normal stress
$\boldsymbol{\sigma}$	MPa	Stress tensor
$\sigma_{\parallel}$	MPa	Surface residual stress distribution along the grinding direction
$\sigma_{\perp}$	MPa	Surface residual stress distribution perpendicular to the grinding direction
σ_{ij}	MPa	Normal stress component ij of the stress tensor
σ_m	MPa	Mechanically-induced residual stress
σ_{max}	MPa	Tensile strength
σ_{res}	MPa	Residual stress
σ_t	MPa	Thermally-induced residual stress
σ_Y	MPa	Yield strength
τ	MPa	Shear stress
τ_{ij}	MPa	Shear stress component ij of the stress tensor

1 Introduction

1.1 Motivation, objective, and methodology

Linear guide rails, as they are for example used in machine tools, require the highest quality in industrial applications; even slight deviations in shape can render them unusable. They are usually manufactured from quenched and tempered steel by roughing and finishing, followed by peripheral milling. The removal of material layers and the generation of residual stresses due to high thermal and mechanical loads during the grinding of these slender and long steel components lead to unwanted distortions. Significant degradation of the workpiece quality is in some cases nearly inevitable. Particular clamping strategies and straightening processes are chosen to minimize form deviations, resulting in disadvantages that make these processes time-consuming and costly. For example, straightening in the industry is still not automated, due to a lack of knowledge about the process-specific residual stress generation and the resulting dimensional and shape changes. The selection and design of suitable clamping strategies and straightening processes are currently mainly iterative and based on the long-term experience of experts. A few proven techniques, such as flame and bend straightening, are typically used. A better understanding of the complex physical interactions involved in grinding in an industrial environment would significantly contribute to optimizing straightening processes. In the literature, thermal and mechanical stresses have been identified as sources of workpiece deformation. Elastoplastic deformation in the material boundary zone creates an asymmetric residual stress state (MITZE 2010), which is a severe problem, especially when manufacturing precision components (Figure 1). Targeted elastoplastic deformations of the workpiece allow for compensation of the distortion (JÖNSSON 1998).

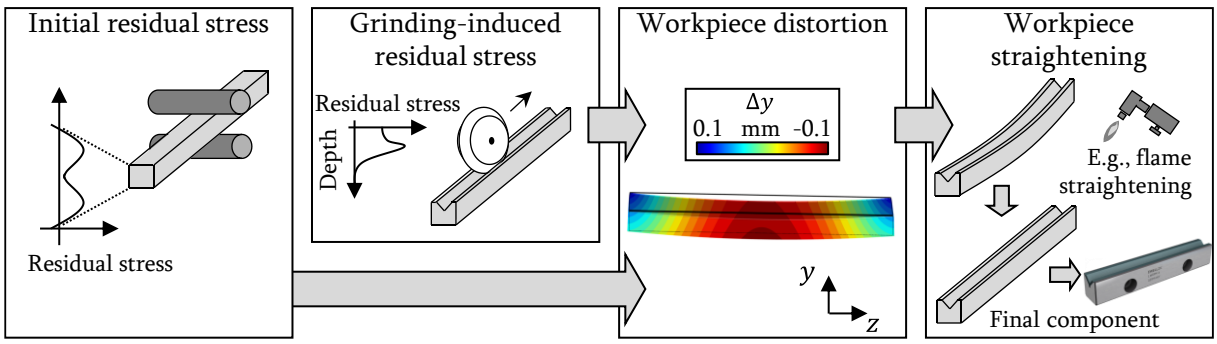

Figure 1: Causes of a workpiece distortion in linear guide rails after profile grinding in a V-groove and a subsequent straightening (based on DREIER ET AL. (2016) and EWELLIX (2023))

A prime example is the machining of steel structures in shipbuilding. A manual flame straightening process is used here to compensate for distortion in steel structures (KOERDT ET AL. 2008). In addition, laser sources in the aerospace industry allow for process-integrated correction of joined workpieces (HORNFECK 2008). In both cases, it is essential to note that these thermal loads generate tensile stresses on the surface that promote crack initiation (BERSTEIN & FUCHSBAUER 1982, SEYFFARTH 2007). More complex workpiece geometries exhibit distortion and usually require the targeted application of compressive stresses to the surface. Shot peening and deep rolling increase fatigue strength and offer the possibility of surface hardening and other applications during forming processes of thin-walled structures (BERSTEIN & FUCHSBAUER 1982, JOHANSSON 1998). There is a distinct disadvantage of the mechanical straightening process compared with the thermal one. The flexibility of application in a production line is limited; therefore, it is not yet utilized. However, combining techniques, such as targeted thermal or mechanical post-treatments, is also possible. Single straightening processes often do not allow a complete distortion compensation. Consistent methods enable efficient selection and design of thermal and mechanical processes and process parameters in grinding, thus opening up new options. These methods are particularly effective when considering the interactions between thermal and mechanical processes.

Finite element (FE) simulation is suitable for predicting distortion during grinding because it allows for the calculation of component-related residual stresses based on thermomechanical boundary conditions, transient temperature fields, and phase transformations. FE-based structural simulation is advantageous for macroscopic analysis and provides a precise temperature- and phase-dependent modeling of the underlying material behavior (HEINZEL 2009, MOULIK ET AL. 2001, MAHDI & ZHANG 1999, 1998, CHOI 1986).

High thermal and mechanical loads are applied on the workpiece surface layer during the grinding process, leading to residual stresses and distortions. To predict these effects accurately, all thermometallurgical and thermomechanical effects must be modeled to a sufficient extent, which can be achieved by an FE simulation (DUSCHA ET AL. 2010, DUSCHA ET AL. 2011).

FE simulation allows for the modeling and solving of coupled, highly nonlinear differential equations that describe the transient effects, thereby providing a comprehensive understanding of the complex physical phenomena that occur during the grinding process. While a numerical calculation can be time-consuming, the immense scope and high quality of the results make it a valuable tool for predicting distortion during grinding (ZHANG & MAHDI 1995, MAHDI & ZHANG 2000).

This dissertation aims to extend knowledge of the relevant mechanisms of distortion generation during profile grinding of slender workpieces with a V-profile as a replacement

component of a linear guide rail made of AISI 4140 steel. The focus is on a feasibility analysis of the distortion compensation, the verification of its suitability, and the further development of simulation approaches for modeling the compensation methods. The aim is to identify and implement procedures and approaches for post-treatment processes, consisting of laser machining and deep rolling, for efficient distortion compensation after the grinding of slender workpieces with V-grooves by a targeted generation of residual stresses. The coupling of experiments and validated finite element (FE) simulation models forms the basis for the computer-aided design of compensation strategies. It allows for the analysis of distortion phenomena, the control of process-specific interactions, and thus the elimination of current limitations in post-treatment processes. The findings are to be transferrable to industrial production at a low cost, enabling improved product quality and significant time and cost savings for manufacturing companies.

1.2 Structure of the thesis

This dissertation is based on the contents of five publications whose scientific results are presented in this study. First, Chapter 2 explains the technical and methodological principles necessary for understanding the state of the art described in Chapter 3. Chapter 4 subsequently identifies the essential need for action and the procedure to be followed. Thereafter, Chapter 5 briefly summarizes the publications produced for the dissertation. The discussion of the results is followed by an assessment of the economic benefits and a summary in Chapter 6.

2 Fundamentals

2.1 Chapter overview

In this chapter, the fundamentals of profile grinding and the distortion compensation processes are presented. In addition, the thermomechanical effects that occur both during machining and during the thermal and mechanical post-treatment of an AISI 4140 V-groove workpiece are explained along with their material-specific causes. The fundamentals chapter continues – after this overview – with the properties of the workpiece surface to be machined and the formation of distortions due to the change of residual stresses (Section 2.2). The grinding basics are detailed in Section 2.3, including kinematics and chip formation during machining. Energy partitioning in the contact zone between the tool and workpiece forms the thematic conclusion of this chapter, which explains the boundary zone influence resulting from thermomechanical interaction. The fundamentals of the two compensation strategies, meaning laser machining and deep rolling, are described in Sections 2.4 and 2.5. In each case, references are made to the process characteristics as well as the effects on the workpiece material and the distortion. The finite element method (FEM) is used to simulate the complex processes explained in Section 2.6. This section presents essential numerical approaches to heat transfer and structural problems.

2.2 Material properties of steel

2.2.1 Properties of the steel surfaces

The surface and subsurface layers of a steel workpiece exhibit variations in mechanical, metallurgical, thermal, and other properties. These variations are determined based on the topography of the layers and may include shape defects and surface roughness. Layer properties, such as plastic deformation, residual stress distribution, and material recrystallization, can significantly impact the fatigue life of manufactured components (SOMMER ET AL. 2014, ZUM GAHR 1983).

Figure 2 shows typical surface properties after a machining process such as grinding. Here, the surface roughness is characterized by the arithmetic average roughness R_a and peak-to-valley roughness R_t. After a machining step, changes in residual stresses $\sigma_\perp$ and $\sigma_\parallel$, sub-

surface hardness HV, and microstructure occur (SCHOLTES & MACHERAUCH 1986, MALKIN & GUO 2008).

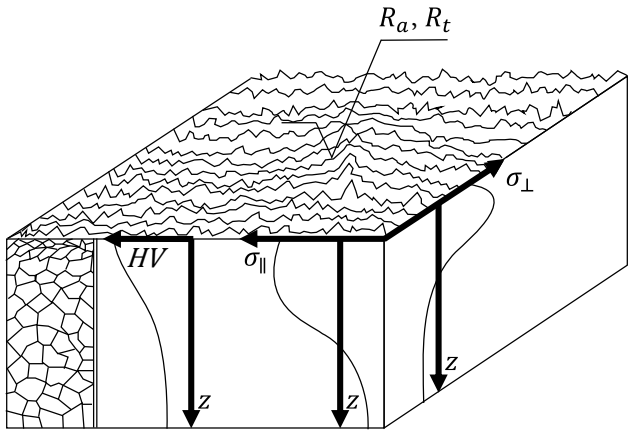

Figure 2: Workpiece surface with boundary zone and subsurface properties, affected by machining processes (based on SCHOLTES & MACHERAUCH (1986))

For many workpieces, a high hardness is preferred because it increases strength. This results in greater material resistance to plastic deformation (SCHOLTES & MACHERAUCH 1986, ZUM GAHR 1983).

Changes in surface roughness can be considered as an alteration in material properties. The valleys in the surface profile are analogous to microcracks. Thus, a lower surface roughness results in a higher fatigue strength. This factor is crucial for the deliberate enhancement of mechanical properties, which also encompasses improved wear resistance and reduced energy losses due to decreased friction (SCHOLTES & MACHERAUCH 1986, RABINOWICZ 1995).

The surface properties of a workpiece, such as hardness and roughness, are important indicators of its quality and performance (SCHOLTES & MACHERAUCH 1986). The following sections of Chapter 2 discuss the effects of grinding on these surface properties in the context of an AISI 4140 component. This steel is a commonly used alloy in industrial applications and, therefore, for linear guide rails. However, in order to fully understand the changes that occur during grinding and that cause workpiece distortion, it is necessary to investigate the changes in the material's microstructure and residual stress state. By examining the interplay between surface properties and microstructural changes, one can gain a complete picture of the effects during this process.

2.2.2 The material structure of AISI 4140 steel

During grinding, AISI 4140, a low-alloy steel, undergoes microstructural changes that affect the properties of a workpiece and vary depending on the specific heat treatment used. Therefore, it is essential to consider them when predicting distortion later in this

dissertation. Microstructural transformations can have several effects: surface hardening, hardening in untreated steels, and rehardening in already hardened steels. In addition, during tempering, the hardness of the surface layer can be reduced by high temperatures. A corresponding cooling gradient causes rehardening. A microstructural transformation in steel depends on the carbon content and the alloying elements (ROOS & MAILE 2004, TOTTEN 2007).

Annealing can improve the ductility of AISI 4140. It involves heating the steel to recrystallization temperature and maintaining it for a specified time to allow the microstructure to become fully austenitic. The steel is then slowly cooled to room temperature, producing a soft, ductile structure known as ferrite-pearlite (ROOS & MAILE 2004).

The rehardening principle involves first heating and then holding at the hardening temperature. This austenitizing is followed by cooling (ROOS & MAILE 2004). The transformation from a ferritic-pearlitic microstructure to austenite (γ-solid solution) by nucleation and growth (recrystallization) involves the diffusion of carbon. If a critical cooling rate is exceeded during a subsequent quenching process, martensite is formed as a very hard microstructure. The critical cooling rate must be reached for a complete transformation by diffusionless folding of the γ-lattice into a tetragonally distorted α-lattice (Figure 3) (LIEDTKE 2004), otherwise a hardness-reducing residual austenite content remains in the microstructure.

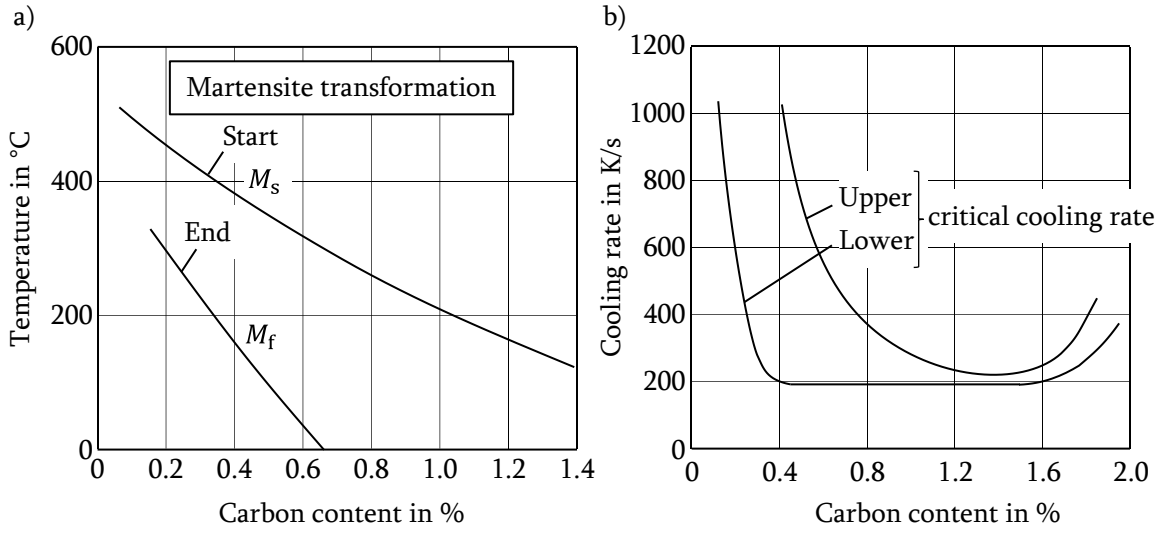

Figure 3: Critical temperatures and cooling rates during martensite formation; (a) influence of carbon content on martensite finish (M_f) and martensite start temperature (M_s) and (b) critical cooling rates as a function of the carbon content (based on ROOS & MAILE (2004))

In Figure 3, the start temperature of the martensite transformation is indicated by M_S, and the martensite finish temperature by M_F. Both are dependent on the carbon content and the alloying elements, as are the necessary cooling rates. The high hardness of the martensite is caused by a diffusionless transformation, which leads to an oversaturation of carbon

with solid solution hardening. It is increased by a high lattice defect density and internal strains (ROOS & MAILE 2004).

Tempering of the steel associated with a reduction in hardness occurs when the temperature falls below the austenitizing temperature. Therefore, tempering temperatures should be avoided when machining already quenched and tempered workpieces. In this work, AISI 4140 workpieces were used for grinding. They were quenched and tempered, usually at 540–680 °C after hardening. This process reduces the brittleness caused by hardening and allows for higher ductility (ROOS & MAILE 2004).

2.2.3 Residual stress

Residual stresses are internal stresses in materials without thermal gradients or external loads. A distinction is made between compressive and tensile stresses. Both are in equilibrium throughout the material (TOTTEN ET AL. 2002). If the tensile stresses are changed in one part of the workpiece, the compressive ones change elsewhere. The residual stress state as a material property is essential for this work since it causes workpiece deformations.

In contrast to compressive residual stresses, tensile ones that dominate after the grinding process have a positive sign. They favor the formation of cracks due to aging and, thus, the reduction of the component strength (ENGEIL & SPEIDEL 1969). Furthermore, residual compressive stresses increase fatigue strength and surface quality (ENGEIL & SPEIDEL 1969, TÖNSHOFF 1965, BÜHLER & BUCHHOLTZ 1933).

The result of a changing residual stress state is a material-dependent response of the shape of the workpiece indicated by ε. This so called strain ε has a direct correlation with the normal stress σ (GROSS & HAUGER 1998). The elastic range of deformation, described by Hook's law, is defined with the elastic modulus E as follows (BEER & JOHNSTON 2002):

$$\sigma = E \cdot \varepsilon. \tag{2-1}$$

Workpieces can be affected by load stresses, which occur when external loads are applied to a body, and by residual stresses resulting from non-uniform elastoplastic deformations in the material (ZOCH 1995, ZOCH 2012).

The yield strength of a workpiece limits the residual stresses. If this limit is exceeded, they are reduced by plastic deformation (PEITER 1992, DENKENA & TÖNSHOFF 2011).

Stress is defined vectorially and is divided into two components: the normal stress σ and the shear stress τ. Figure 4 illustrates that three vectors describe the stress state in a point. These are located on three perpendicular surfaces (BREIDENSTEIN 2011).

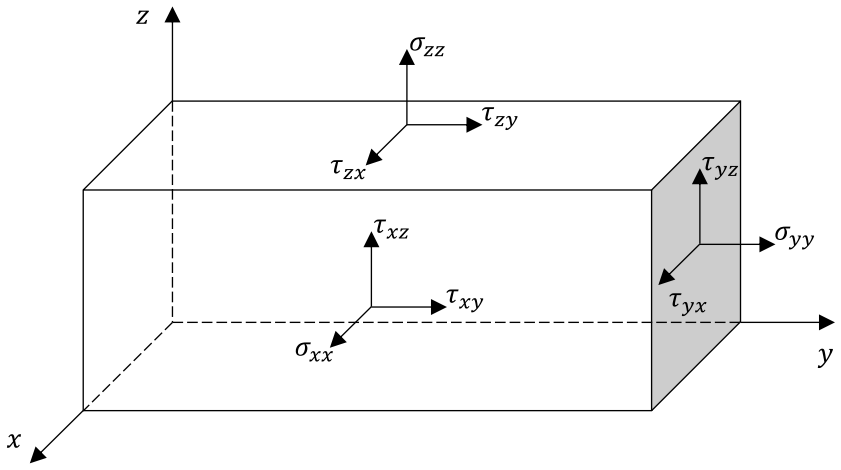

Figure 4: Components of the stress tensor $\boldsymbol{\sigma}$ (BREIDENSTEIN 2011)

The stress tensor $\boldsymbol{\sigma}$ includes all different stress vectors:

$$\boldsymbol{\sigma} = \begin{bmatrix} \sigma_{xx} & \tau_{xy} & \tau_{xz} \\ \tau_{yx} & \sigma_{yy} & \tau_{yz} \\ \tau_{zx} & \tau_{zy} & \sigma_{zz} \end{bmatrix} = \begin{bmatrix} \sigma_{xx} & \tau_{xy} & \tau_{xz} \\ \tau_{xy} & \sigma_{yy} & \tau_{yz} \\ \tau_{xz} & \tau_{yz} & \sigma_{zz} \end{bmatrix}. \tag{2-2}$$

The symmetric matrix contains the normal stresses σ_{ii} in the main diagonal and the shear stresses τ_{ij} in the remaining positions (GROSS & HAUGER 1998).

During the production of steel components, residual stresses are usually introduced by various manufacturing processes (TÖNSHOFF 1965, SÖLTER 2010). Since semi-finished products have different geometric and material properties, the stresses can have different characteristics and forms during machining. During grinding, residual stresses are mainly caused by thermal effects such as temperature gradients, or by microstructural changes (MITZE 2010).

The grinding process is classified according to DIN EN 8580:2003-09 as cutting with an undefined cutting edge. Other methods defined in the standard, such as forming, joining, or coating, also induce residual stresses in the treated workpieces by changing the material properties. Other important aspects of this influence are an inhomogeneous cooling temperature and a strain gradient. These arise during casting and grinding, leading to a changed residual stress profile (SADROSSADAT & JOHANSSON 2008).

While thermal stresses dominate in grinding, cutting processes (e.g., milling and turning) generate predominantly mechanical ones. If the heat is dissipated strongly enough by a high thermal conductivity of the grinding tool, or if the process is performed with a high cutting force, compressive stresses can be generated on the surface. The situation changes if the cutting speed, the feed rate, or the depth of cut is increased. With the increase, predominantly tensile stresses on the surface can be caused (SCHOLTES 1991, GAO ET AL. 2020).

As previously mentioned, one of the main properties of residual stresses is stress equilibrium since the workpiece has reached the state with the lowest potential energy due to elastic

deformations (TÖNSHOFF 1965, GROSS & HAUGER 1998, BRINKSMEIER ET AL. 1982). An ablation of residual stress layers during machining also influences the equilibrium in the workpiece. The state shifts accordingly to restore the lowest potential energy level (GROSS & HAUGER 1998).

Although these macroscopic shape changes are more noticeable in the case of long and slender workpieces than in thicker ones (TÖNSHOFF 1965). The scientific results in Chapter 5 also show this. After grinding and the resulting unintentional and undesired change of the residual stress state leading to distortion, slender components such as linear guide rails require reworking by straightening to preserve their usability (TÖNSHOFF 1965, SIM 2010).

2.2.4 Elastoplastic material behavior

For the description of the deformation of a workpiece, an exact definition and an analysis of the elastoplastic behavior by the classical plasticity theory are necessary. Mechanical and thermal loads change during the manufacturing process. Materials initially deform elastically until the yield strength is reached (TÖNSHOFF 1965).

During the grinding process, the thermal load initially causes the structure to expand, resulting in temporary compressive stresses until the yield strength of the material is exceeded. These stresses are nonlinearly related to the strain through a path-dependent relationship. Thus, the residual stress state is also related to the strain history. Three essential components of plastic analysis are relevant for defining plasticity models that can be used in a simulation for predicting workpiece distortions: a yield criterion, a yield rule, and a hardening rule (COOK ET AL. 2002).

The sum of several strain components, consisting of the elastic strain vector $\boldsymbol{\varepsilon_{el}}$, the thermal strain vector $\boldsymbol{\varepsilon_{th}}$, the plastic strain vector $\boldsymbol{\varepsilon_{pl}}$, the phase transformation strain vector $\boldsymbol{\varepsilon_{tr}}$, the transformation plasticity vector $\boldsymbol{\varepsilon_{tp}}$ and the creep strain vector $\boldsymbol{\varepsilon_{cr}}$, describes the total strain vector $\boldsymbol{\varepsilon_{total}}$ (INOUE & ARIMOTO 1997):

$$\boldsymbol{\varepsilon_{total}} = \boldsymbol{\varepsilon_{el}} + \boldsymbol{\varepsilon_{th}} + \boldsymbol{\varepsilon_{pl}} + \boldsymbol{\varepsilon_{tr}} + \boldsymbol{\varepsilon_{tp}} + \boldsymbol{\varepsilon_{cr}}. \tag{2-3}$$

Figure 5 illustrates the dependence of stress σ on strain ε for a one-dimensional elastoplastic material behavior. The technical tensile stress–strain curve represents the relationship between stress and strain in a material subjected to a static load. It is obtained by controlling the loading rate of a standard specimen in a materials testing machine (AVALLONE & BAUMEISTER 1996). The curve usually consists of an initial linear elastic region (A) in which the material behaves elastically and reversibly, with the slope corresponding to the elastic modulus E. Beyond this region, the curve begins to deviate from a straight line (B), and plastic deformation occurs, which can lead to permanent deformation. The yield strength

of the material is marked by σ_Y at C (AVALLONE & BAUMEISTER 1996). A workpiece can withstand large deformations until rupture. After a decrease in load, the stress and strain decrease linearly (D) (BEER & JOHNSTON 2002). A strain offset of 0.2 %, denoted by $R_{p0.2}$, is termed by default for some ductile materials due to the ambiguous definition of yield strength. The offset is often selected as a reference point to determine yield strength in materials testing since it is a reasonable trade-off between accuracy and practicality (ROSS 1999).

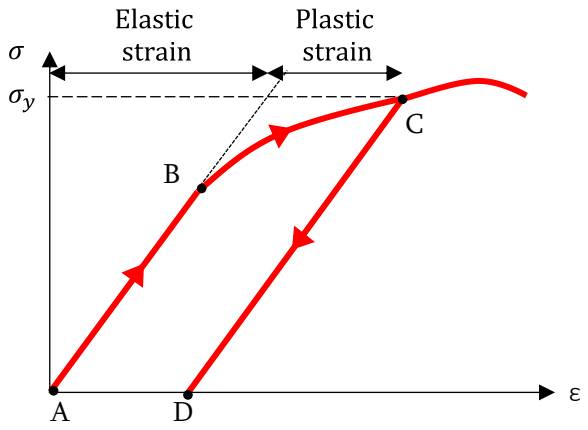

Figure 5: General stress–strain diagram for one-dimensional elastoplastic material behavior loaded (A–B–C) beyond yield and unloaded (C–D) (based on AVALLONE & BAUMEISTER (1996) and BEER & JOHNSTON (2002))

The yield strength is the elastic limit and, thus, the largest stress value at which the material behaves elastically. The curve may have a well-defined yield strength for some materials. Therefore, plastic deformation is a function of the maximum stress level, for which the preceding time-dependent stress change becomes irrelevant. Slip and creep are the terms used to describe the stress- and time-dependent parts of plastic deformation (BEER & JOHNSTON 2002).

When the strain exceeds the initial yield, the hardening rule applies. It describes how the material's yielding behavior evolves, with a distinction between isotropic and kinematic strain hardening (Figure 6). Both types occur together under uniaxial stress (COOK ET AL. 2002). The proportional and elastic limits increase while the ductility decreases when the specimen is loaded twice in the same direction. If the second load is applied in the opposite direction, this is referred to as the Bauschinger effect, where the material has no clearly defined yield strength (BEER & JOHNSTON 2002).

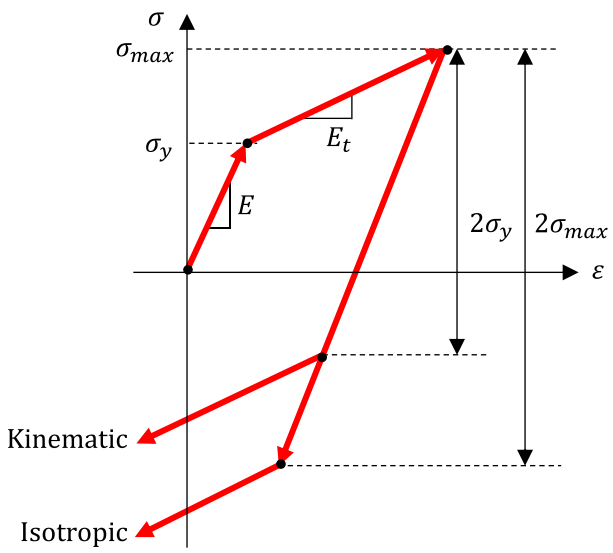

Figure 6: Stress–strain curve with isotropic and kinematic hardening rules under uniaxial stress (based on COOK ET AL. (2002))

Characterized by a uniform expansion of the initial yield surface, the shape changes during isotropic hardening. In this context, the term "yield surface" refers to the boundary in stress-strain space where yielding or plastic deformation begins. The elastic region expands from the initial value of $2\sigma_y$ to $2\sigma_{max}$ after the tensile strength is reached at the initial load σ_{max}, where E describes the elastic modulus, while E_t represents the tangent modulus. The total stress change between two loads in opposite directions equals twice the yield strength. Kinematic hardening is the direct translation of the original yield surface without changing its shape (COOK ET AL. 2002, BEER & JOHNSTON 2002).

2.3 Fundamentals of profile grinding

2.3.1 General remarks

This dissertation addresses the computer-aided process design of distortion control after profile grinding of steel workpieces. Section 2.3 provides an overview of the process characteristics during grinding (Subsection 2.3.2). Based on the technological process fundamentals, the known workpiece-related mechanisms and thermomechanical effects are presented to describe grinding processes and to simulate the resulting workpiece distortions (Subsections 2.3.3 and 2.3.4). A detailed discussion of the technological and physical dynamics during the grinding process concerning the tool–workpiece relationship is given in Subsection 2.3.5 and in the integrated publications P1 to P5.

2.3.2 Process parameters

In machining, a distinction is made between the manufacturing process with geometrically defined and undefined cutting edge. Grinding, which, according to DIN 8589-11:2003-09, in contrast to turning, milling, or drilling, belongs to the second category, uses a high number of cutting edges at high cutting speed, and is a standard method for finishing surfaces of linear guide rails to increase component quality. The abrasive grains used in the tool, including hard materials such as corundum, boron carbide, and diamond, exhibit variability in terms of their number, geometry, and positioning relative to each other. According to DIN EN ISO 6507-1:2018-07, the grain size may vary between 40 µm and 1,180 µm. Because of their high number and the penetration of a few micrometers into the material during the process at high cutting speeds, higher surface quality is generally achieved with finer grain size. Increased thermal conductivity of high-hardness grinding wheels reduces the heat flux into the workpiece (DENKENA & TÖNSHOFF 2011).

Many control variables are involved in grinding. The basic ones are the radial depth of cut a_e, the feed rate v_{ft}, the cutting speed v_c, and the cooling lubricant flow rate v_{jet} (Figure 7).

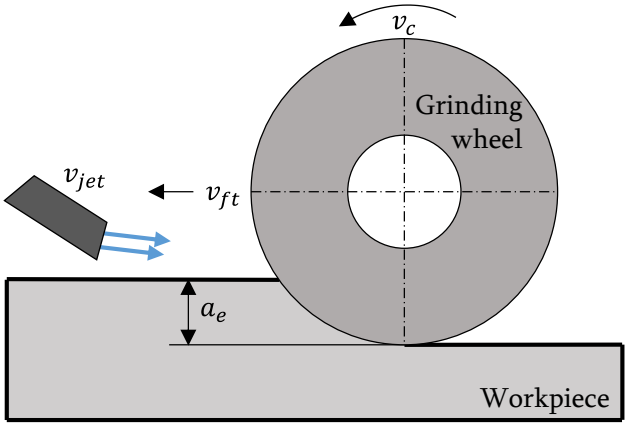

Figure 7: Example of a grinding process with different control variables

Various disturbance variables also exist, such as temperature fluctuations and vibrations. Both, in combination, influence the result after grinding. The relationships are depicted in Figure 8.

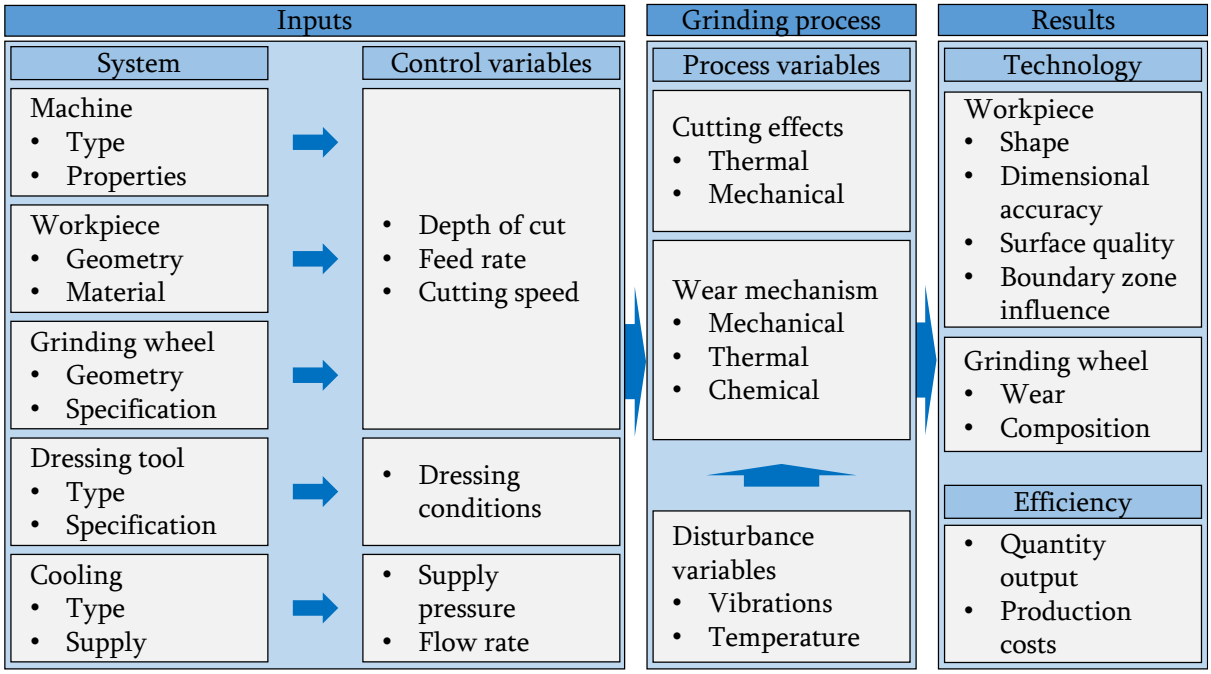

Figure 8: Process input variables and results during grinding (based on KLOCKE (2018))

The grinding process can be subdivided according to the surface produced. Surface grinding, cylindrical grinding, generating grinding, profile grinding, and form grinding are the typical processes whereby the workpiece performs either a rotational or a translational movement during the grinding wheel rotation (DIN EN 8580:2003-09). DIN EN 8580:2003-09 also describes different types of grinding based on where the tool interacts with the workpiece, what the shape of the machined surface is, and how the tool moves relative to the workpiece. These types include peripheral and side grinding, external and internal grinding, and different ways of moving the tool, such as longitudinal, transverse, angular, and free-form grinding. For the final surface quality improvement, conventional grinding is performed with low depths of cut, metal removal rates, and cutting speeds (VDI 3411).

Superabrasive grinding wheels are usually used in high-performance grinding. The process is carried out at large cutting speeds and high depths of cut. To be suitable for those variables, the base body, which defines the macro-geometry and the strength of the grinding wheel, is usually made of steel to withstand the mechanical loads. Furthermore, superabrasive grinding wheels consist of a coating with grain and bond. A distinction is made between single-layer coatings, usually made of electroplated nickel, and multilayer coatings made of ceramics. For profile grinding, only the second variant is suitable due to its profiling capability and the inclusion of abrasive grains in the volume bond (DENKENA & TÖNSHOFF 2011, BRINKSMEIER & BROCKHOFF 1994, KLOCKE & KÖNIG 2005).

For the exact modeling of the grinding process, which was carried out for this dissertation, a comprehensive identification of the equipment- and process-specific system and control

variables was necessary. These represent the input variables of the formal system model. In the literature, there are clear distinctions between the system and control variables of grinding processes (DENKENA & TÖNSHOFF 2011, BRINKSMEIER & BROCKHOFF 1994, KLOCKE 2018). On the one hand, the physical aspects of all process components, such as the cooling lubricant, the grinding wheel, the machine tool, and the workpiece to be machined, form the system variables. On the other hand, control variables can, to a certain extent, be freely selected as manufacturing parameters that are directly included in the system model as input variables. As briefly mentioned, these variables are the cutting speed v_c, the radial depth of cut a_e, the feed rate v_{ft}, and the cooling lubricant volume flow rate v_{jet} (STÖHR 2008, TOTTEN ET AL. 2002).

2.3.3 Kinematics and chip formation mechanisms during grinding

The tool spindle regulates the kinematic control variables, which determine the movement of the single grain relative to the workpiece surface during grinding. This involves the wheel's axial movement along a clamped workpiece at a cutting speed v_c, and a feed rate v_{ft}, in contrast to profile grinding, where the peripheral speed v_s is locally variable at the outer part of the grinding wheel due to the locally changing diameter. The difference corresponds to the cutting speed v_c in surface grinding. The depths of cut of the grinding wheel are defined in the normal direction of the workpiece surface (BROCKHOFF 1998).

By forming the differential quotient, consisting of the removed workpiece material volume V_w and the time t, the material removal rate Q_w is calculated. The volumes are machined per time unit (BROCKHOFF 1998):

$$Q_w = \frac{dV_w}{dt}. \tag{2-4}$$

For surface grinding, where the wheel profile forms a straight line parallel to the wheel axis over the grinding width, V_w is defined by the width of the active grinding wheel profile b_s. The machining is performed over a contact length l_g. The relationship is shown in the following equation (KLOCKE 2018):

$$V_w = a_e \cdot b_s \cdot l_g. \tag{2-5}$$

If this equation is inserted into the equation of the material removal rate Q_w (2-4), the following equation results under the assumption of a constant feed rate v_{ft} (KLOCKE 2018):

$$Q_w = a_e \cdot b_s \cdot v_{ft}. \tag{2-6}$$

In terms of transferability to other grinding processes, such as profile grinding, comparing process variables to the width of the active grinding wheel profile is relevant. For this

purpose, the previously considered control variable of the material removal rate Q_w in relation to the tool width can be extended to the specific material removal rate Q'_w (KLOCKE 2018) as follows:

$$Q'_w = \frac{Q_w}{b_s} = a_e \cdot v_{ft}. \tag{2-7}$$

When profile grinding a V-groove for a linear guide rail, the constant stock removal distribution in an equidistant direction along the two flanks within the profile must be observed (KLOCKE & KÖNIG 2005). Here, the grinding wheel has symmetrically flat surfaces, which are inclined at an angle β with the depth of cut a_e. Figure 9 shows, on the left side, the xy-plane of one half of a workpiece with a V-groove during profile grinding. The feed rate is perpendicular to the xy-plane. The right side depicts an inclined projected view of a circular section through the wheel looking parallel to the workpiece surface and perpendicular to one half of a V-goove flank. The depth of cut a_e and the grinding wheel diameter d_s can be converted to effective values (MALKIN & GUO 2008). The shape of the tool in the projected view results in an elliptical shape with the length of the major axis d_s and minor axis:

$$d_{se} = \frac{d_s}{cos\beta}. \tag{2-8}$$

The effective depth of cut a_{se} perpendicular to the flank with the angle β is as follows (MALKIN & GUO 2008):

$$a_{se} = a_e \cdot cos\beta. \tag{2-9}$$

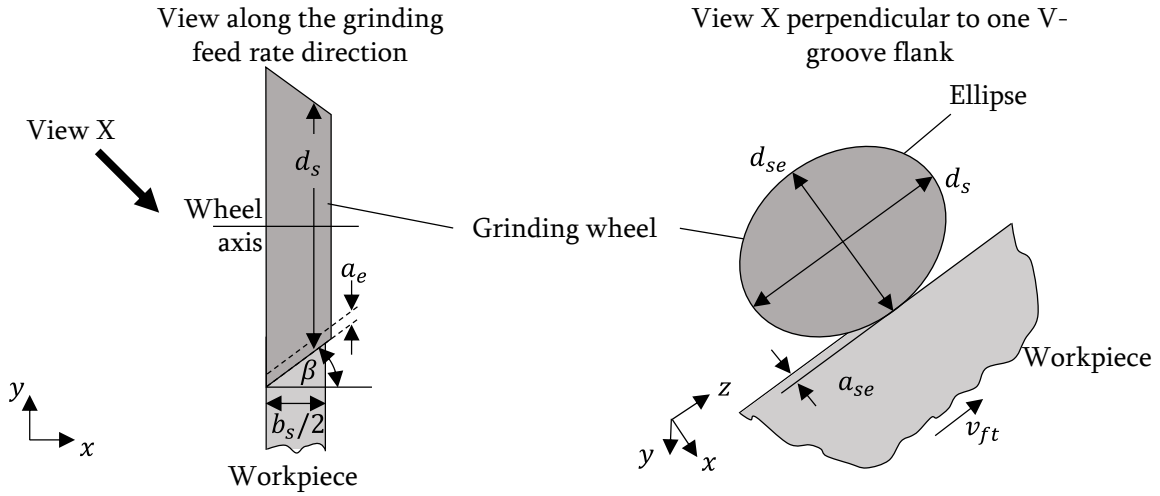

Figure 9: View along the grinding feed rate direction (left) and inclined (right) view of a profile grinding process perpendicular to one half of a V-groove flank (based on MALKIN & GUO (2008))

To illustrate the geometry, the setting, and result variables, Figure 10 shows a schematic representation of the surface grinding and a model of the cutting-edge engagement during regular up-grinding. This demonstrates the trajectory-based principle of surface grinding with peripheral wheel speed v_s, where the cutting edge of a grain follows a specific path as it penetrates into the workpiece. The model of cutting-edge engagement can be divided into phases (KLOCKE 2018).

In Phase ①, the grain enters the workpiece. During this process, the material deforms elastically due to the tangential and normal forces on the cutting edge ($F_{t,S}$, $F_{n,S}$) with a flat entry angle. The total grinding force thus results from the overall tangential force F_t and the normal force F_n. These effects arise from microscopic effects (LORTZ 1975, KLOCKE & KÖNIG 2005, DENKENA & TÖNSHOFF 2011).

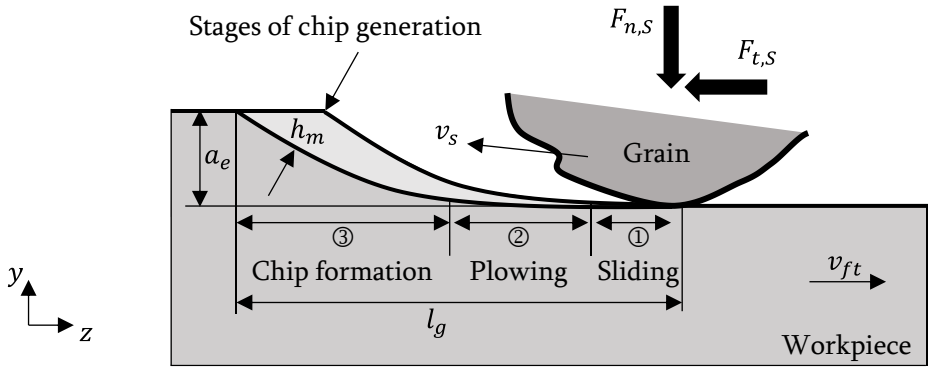

Figure 10: Model of the cutting-edge engagement during grinding with the three stages of chip formation (based on KLOCKE (2018))

As shown in Figure 10, the uncut chip thickness increases during plowing in Phase ②. The material is deformed elastically and plastically, before chip removal follows in Phase ③. The grains of the grinding wheel move continuously along the geometric contact length l_g with increasing chip thicknesses. This leads to a material flow underneath the cutting edges toward their free surfaces and to lateral material displacements. The maximum uncut chip thickness h_m is reached at the end of the depicted grain engagement path. Given the typically shallow depth of cut a_e, the length of the contact arc can be approximated reasonably as the geometric contact length l_g. For this purpose, the equivalent grinding wheel diameter d_s is used in addition to a_e and the angle of the V-groove β based on the geometrical definitions of a_{se} and d_{se} in Figure 9 (MALKIN & GUO 2008, KLOCKE 2018):

$$l_g \approx [a_{se} \cdot d_{se}]^{\frac{1}{2}} = \left[(a_e \cdot cos\beta)\left(\frac{d_s}{cos\beta}\right)\right]^{\frac{1}{2}} = (a_e \cdot d_s)^{\frac{1}{2}}. \tag{2-10}$$

Regardless of the angle β, the contact length is the same as for surface grinding. However, the local variation in grinding wheel diameter on the inclined surface also leads to localized

changes in the contact length (MALKIN & GUO 2008). This leads to a variable thermal load on the workpiece within the grinding zone.

Lubrication during the grinding process influences the macroscopic effects in the contact zone and the friction conditions on the single grain and hence affects the chip formation. The presence of a cooling lubricant has a lubricating effect that reduces frictional shear stresses between the grain and the material. This effect shifts the separation point closer to the surface of the workpiece. VITS (1985) demonstrated that this increases the depth of cut at which chip removal begins. Thus, lower effective chip thicknesses are present due to the elastoplastic deformation processes under the grain cutting edge. The result is an improved surface quality (BRINKSMEIER & HEINZEL 1998, WITTMANN ET AL. 2006). A disadvantage is the additional energy required for shear and deformation due to the high lubricating effect. This, in turn, leads to a higher thermal load on the workpiece. However, a lower surface roughness can be achieved (MARTIN & YEGENOGLU 1992, VITS 1985).

Not only increased energy input but also the high proportion of elastic and plastic displacement or the high friction component based on the stochastic distribution of the abrasive grains in the coating leads to intense heat generation during grinding processes. The grain sizes, protrusions, and geometry within the grinding wheel vary, resulting in the simultaneous presence of all chip formation mechanisms, each occurring with different frequencies (DENKENA ET AL. 2012). YEGENOGLU & THURNBICHLER (1995) demonstrated that high cutting speeds shift the prevalence of these mechanisms towards micro-chipping. However, geometrical conditions usually prevent microchip formation (YEGENOGLU & THURNBICHLER 1995).

2.3.4 Energy partitioning in grinding processes

The energy conversion in the contact zone significantly influences the developing heat flux, leading to residual stresses and, thus, distortions in the workpiece. Chip formation is primarily responsible for this effect (WERNER 1971). The total specific grinding energy e_c describes the mechanical energy transformed during machining per unit volume (ZEPPENFELD 2005). The energy converted during chip formation transferred to a single chip is related to the chip volume. KANNAPPAN & MALKIN (1972) and MALKIN & GUO (2008) decomposed the specific grinding energy into three main components. A detailed consideration of the previously shown three phases in chip formation can consequently be made (KÖNIG ET AL. 1978, HAHN 1966):

$$e_c = e_{ch} + e_{pl} + e_{sl}. \tag{2-11}$$

The equation contains the specific chip formation energy e_{ch}, the specific plowing energy e_{pl}, and the specific sliding energy e_{sl} (MALKIN & GUO 2008).

The first component of the total specific energy is e_{ch}, which accounts for chip formation. According to the literature, this value can be assumed to remain nearly constant because the energy required for chip formation is constrained by the rapid reduction of shear stress upon reaching the melting temperature. Two methods for estimating this value are employed. Firstly, one approach involves calculating the enthalpy difference required to liquefy a material from the solid state at room temperature. Secondly, this approximation must be further adjusted by considering the melting enthalpy, as not all chips undergo complete melting (MALKIN & GUO 2008, MARINESCU ET AL. 2004).

Similarly to kinetic energy, other energy components not listed, such as the energy for generating the surface and the energy remaining in the surface layers, can be neglected in this energetic consideration. Their amount is negligible, or the energy introduced into the process is almost completely converted into heat (MAIER 2008, ZEPPENFELD 2005).

So, this heat generation is not of interest for chip formation, but for the residual stress state and the deformation of the workpiece. The rotation of the grinding wheel is responsible for the mechanical friction, deformation, cutting, and shearing operations required during machining. These process-specific mechanisms for Phase ③ are presented in Figure 11 (KLOCKE & KÖNIG 2005).

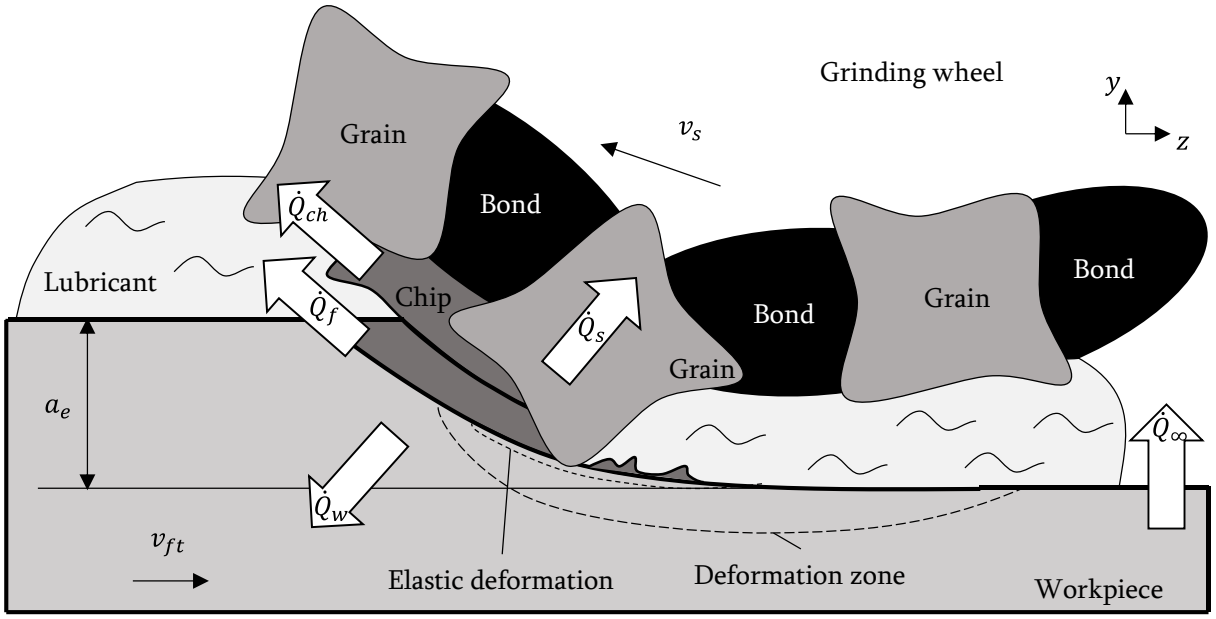

Figure 11: Energy conversion and heat distribution into the components during grinding (based on KLOCKE (2018))

During chip formation, the abrasive grain interacts with the material. This results in separation and shearing. During chip removal, friction along the cutting surface and elastic-plastic deformation occur due to displacement from the shear zone. Friction also occurs at the wear surface of the tool due to lateral material displacement below the cutting zone. All elastically deformed parts regain their original shape after termination of the grain contact (KLOCKE & KÖNIG 2005).

MALKIN and GUO established a basic equation for energy partitioning ε_{ep}, i.e., for the proportion of heat that goes into the workpiece during grinding (overall fraction of the grinding energy conducted to the workpiece) (MALKIN & GUO 2008):

$$\varepsilon_{ep} = \frac{e_{pl} + e_{sl} + 0.55e_{ch}}{e_c} = \frac{e_c - 0.45e_{ch}}{e_c}. \tag{2-12}$$

They assumed that almost all the sliding and plowing energy on the workpiece surface is transferred to the workpiece as heat because these actions involve deformation without material removal. Approximately 55 % of e_{ch}, the energy associated with chip formation, was considered to be conducted as heat. This assumption aligns with the expectations derived from a heat transfer analysis of the chip formation process. Therefore, all of the grinding energy, except for about 45 % of e_{ch}, is conducted into the workpiece as heat (MALKIN & GUO 2008).

All process-specific mechanisms affect the heat flux distribution in the contact zone. The thermal components are shown in Figure 11 and consist of the heat flux into the workpiece $\dot{Q}_w$, into the grinding wheel $\dot{Q}_s$, into the cooling lubricant $\dot{Q}_f$, and into the chips $\dot{Q}_{ch}$. In addition, heat flux components $\dot{Q}_\infty$ are emitted via radiation and convection at the workpiece surface. The total heat flux $\dot{Q}_{total}$ results from the following sum (GUO & MALKIN 1995, KLOCKE & KÖNIG 2005):

$$\dot{Q}_{total} = \dot{Q}_w + \dot{Q}_s + \dot{Q}_f + \dot{Q}_{ch} + \dot{Q}_\infty. \tag{2-13}$$

Furthermore, the type and condition of the grinding wheel and the cooling lubrication influence the distribution of the heat flux. However, the majority of heat is transferred to the workpiece (LOWIN 1980, HADAD & SADEGHI 2012).

Assuming that the total kinetic energy of the grinding wheel is almost completely converted into heat, the total heat flux is calculated from the applied power P_c. In turn, $\dot{Q}_{total}$ is derived from the tangential grinding force F_t and the cutting speed v_c (SHAW 1992):

$$\dot{Q}_{total} = P_c = F_t \cdot v_c. \tag{2-14}$$

Jin et al. described the transfer of this general equation, valid for surface grinding, to the machining of profiled surfaces. They used the approach of local energy partitioning in the

contact zone between the grinding wheel and the workpiece. This was possible by splitting the power to locally limited areas due to the position-dependent varying cutting speed (JIN ET AL. 2017).

2.3.5 Boundary zone influence from grinding processes

In addition to the previously presented heat-caused thermal stress by F_t, the normal forces F_n influence the material mechanically during the grinding process (ROWE 2001, MALKIN & GUO 2007). Together with the grain interactions, the microstructure is affected, resulting in structural transformations. The change of residual stresses in the workpiece surface layer arises from thermomechanical effects which are dependent on the process variables. The properties of the final workpiece change due to friction within the cutting zone (JERMOLAJEV ET AL. 2016).

For this dissertation, the material AISI 4140 in hardened condition was used. During the grinding of steel materials, there is a short-term, high thermomechanical stress in the workpiece boundary zone with significant heat penetration depths and energy densities, which limits the realizable material removal rates Q_w and thus the performance of conventional grinding processes (MALKIN 1974, SNOEYS ET AL. 1978, ROWE ET AL. 1996, KLOCKE 2018). Typical high-temperature gradients create rehardening zones (BROCKHOFF & BRINKSMEIER 1999). These exhibit brittleness, which affects the quality of the workpiece by reducing its structural integrity (BRINKSMEIER & BROCKHOFF 1997, DENKENA ET AL. 2003, KLOCKE ET AL. 2005). While there is a superposition of the thermal effects with the mechanical influences, the former predominate, and overstressing occurs in the form of stains on the workpiece surface. If the surface rehardens and the reaustenitization temperature is exceeded, grinding burn occurs (GUO & MALKIN 2000, MALKIN 1978). This result is a limiting feature for the process and the material removal rates. Figure 12 presents a comparison between hardened materials and soft-annealed materials, illustrating their influence on the boundary zones.

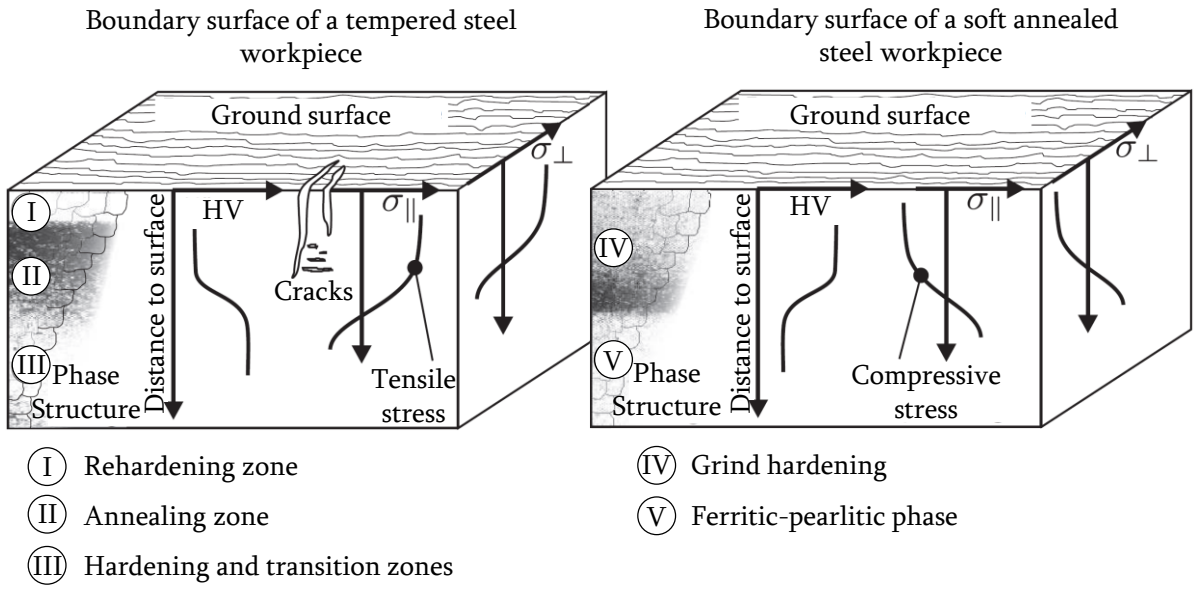

Figure 12: Representation of qualitative curves for the analysis of the thermometallurgical and thermomechanical influence on the boundary zones from the grinding of hardened and soft-annealed steel materials as a function of the distance to the machined workpiece surface (based on BRINKSMEIER ET AL. (2005) and FÖCKERER (2015))

Thermomechanical and metallurgical influences on the surface due to the grinding process lead to a residual stress generation due to plastic deformation, which manifests itself in distortions, especially in slender workpieces (MAHDI & ZHANG 1999, CHEN ET AL. 2000, ZHANG ET AL. 1992). Both the thermally (σ_t) and mechanically (σ_m) induced residual stresses superpose, according to the superposition principle, to form the resulting σ_{res}. The residual stresses induced by microstructural transformation are also added. Figure 13 shows the superposition as a function of the specific grinding power P_g (BRINKSMEIER 1990, BRINKSMEIER 1991).

The used grinding control variables, such as the depth of cut, the feed rate, and the cutting speed, determine the specific grinding power. Less heat is introduced when the material removal rate is reduced. Thus, for example, the thermal input time can be reduced if the feed rate is increased (BRINKSMEIER & MINKE 1993). In addition, if necessary, the lubricant supply can change the dissipated heat and thus, to a limited extent, the influence on the boundary zones. Depending on the choice, different residual stresses dominate. At low power values, these stresses are thermally induced by the external friction that arises (BRINKSMEIER 1990). The expansion of the boundary zone opposes the non-expanding deeper workpiece layers, and compressive stresses occur in the heated zone. Subsequent cooling after plastic compression leads to thermally induced tensile stresses σ_t (SCHREIBER 1973).

If the specific grinding power P_g increases, the mechanical influence on the surface layer intensifies, with a simultaneous continuous rise in temperature. The compressive stresses

increase abruptly. From this point, a coinciding increase of σ_t and, again, a decrease of σ_m follow, as illustrated in Figure 13. The deformations due to mechanical stress have less influence on the boundary layer (BRINKSMEIER 1990).

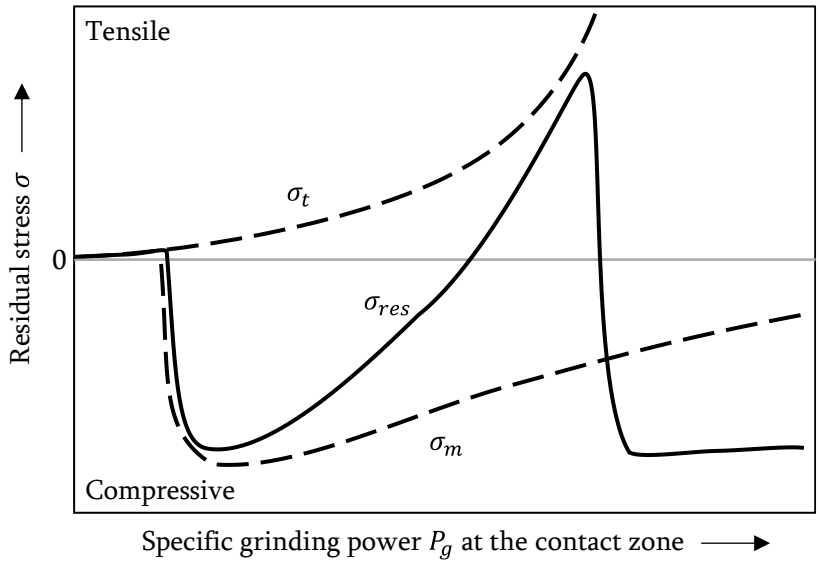

Figure 13: Dependence of residual stresses in the workpiece boundary zone on the contact area-related grinding power P_g due to superposition of thermal, mechanical, and metallurgical effects (based on SÖLTER (2010) and BRINKSMEIER (1990))

If the grinding power is increased beyond the range where dominant tensile stresses are observed, grinding hardening occurs during grinding in the surface layer due to microstructural transformations with a tendency to lower crack formation (WILKE 2008). The resulting martensite during this heat treatment has a higher specific volume than the ferritic-pearlitic microstructure in deeper layers of the material (BRINKSMEIER & BROCKHOFF 1996, BROCKHOFF 1998). The associated microstructural expansion leads to compressive stresses in the workpiece. Since this part of the residual stress generation was not part of this work, reference is made here to the relevant literature (WILKE 2008, HEEß 2012, KEßLER ET AL. 1998).

The region with dominating tensile stress in particular is relevant for the distortion analysis of hardened steel over the further course of this dissertation. With this grinding power located in the middle, significant distortions occur in slender workpieces because of the strongly dominating tensile stresses at σ_{res}. Crackings in the surface layer, as in Figure 12, are also possible (NACHMANI 2008, SÖLTER 2010, DENKENA & TÖNSHOFF 2011).

2.4 Laser processing

2.4.1 Properties of laser radiation

Straightening processes with thermal effects are suitable to counteract unwanted workpiece deformation caused by a manufacturing process, such as grinding (KOERDT ET AL. 2008). During laser processing of surfaces, the laser beam must first be focused using an optical lens. Figure 14 shows the geometric relationships and the beam caustics (HINTZE 2021).

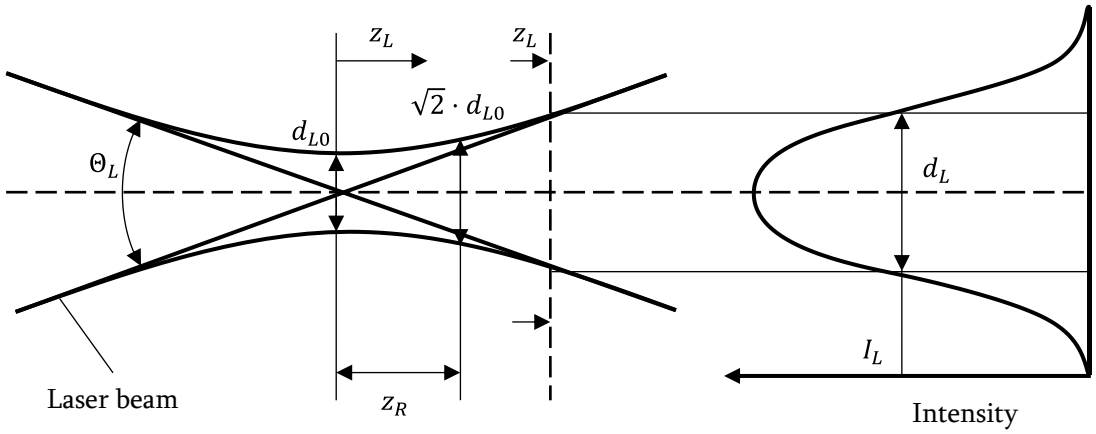

Figure 14: Illustration of the laser beam caustics with characteristic parameters (based on HINTZE (2021))

With the focal length as the distance from the lens center, the focus diameter d_{L0} is defined, at which the highest beam intensity I_L is achieved. The Rayleigh length z_R is the distance measured along the optical axis from the focus point, encompassing double the cross-sectional area of the laser beam. This z_R is calculated from the aperture angle Θ_L and the focus diameter d_{L0} (HINTZE 2021):

$$z_R = \frac{d_{L0}}{\Theta_L}. \tag{2-15}$$

The beam parameter product BPP is used to describe a low divergence angle with a simultaneously considerable Rayleigh length, which is required for many laser beam processing applications (HÜGEL & GRAF 2009):

$$BPP = \frac{d_{L0} \cdot \Theta_L}{4} = M^2 \cdot \frac{\lambda}{\pi}, \tag{2-16}$$

where M^2 is the beam quality factor and λ is the wavelength of the used radiation. If the laser power P_l is increased during the application, I_L increases. The same effect occurs when the cross-sectional area of the beam in the focal plane is reduced with d_L as the diameter of the laser spot on the workpiece. A homogeneous intensity distribution is assumed (HÜGEL & GRAF 2009):

$$I_L = \frac{4 \cdot P_l}{\pi \cdot d_L^2} \tag{2-17}$$

Different operating modes are used in laser processing depending on the application area. In contrast to a pulsed laser operation, continuous waves, in which radiation is permanently emitted by continuous excitation of the laser resonator, were used for this work. Given a different influence on the laser energy input targeting the workpiece, this mode enables welding and cutting applications at a power of up to several kilowatts (HÜGEL & GRAF 2009). For a continuous laser beam, the local intensity $I_L(r_L, z_L)$ decreases progressively with the radial distance r_L to the beam axis and with the axial distance z_L to the beam waist. The beam has a rotationally symmetric profile (HÜGEL & GRAF 2009):

$$I_L(r_L, z_L) = I_{L0} \left(\frac{d_{L0}}{d_L(z_L)} \right)^2 e^{-\left(\frac{8r_L^2}{d_L^2(z_L)} \right)} \tag{2-18}$$

2.4.2 Thermomechanical interaction between laser beam and workpiece

The radiation energy interacts with the material during the laser processing of steel workpieces. On the one hand, one part of the radiation is absorbed and reflected. On the other hand, another part is transmitted for certain materials if the material is transparent to the corresponding wavelength. Depending on the absorbed laser power $P_{l,abs}$, structural changes occur on the workpiece. Mainly two factors influence this effect (HÜGEL & GRAF 2009):

$$P_{l,abs} = P_l \cdot \eta_{abs}, \tag{2-19}$$

where P_l is the laser power and η_{abs} is the degree of absorption. Furthermore, at a point on the workpiece surface, the local intensity $I_L(r_L, z_L)$ must also be considered. The degree of absorption is mainly influenced by the wavelength λ, the temperature, and the material with its surface properties (HÜGEL & GRAF 2009).

The temperature field is an important point when considering the development of distortion. Together with the temperature gradient, it influences the residual stress state of the heat-affected zone. Depending on the absorption rate and energy loss, the material heats up as a function of time. At the atomic level, electrons are excited during absorption by interaction with the incident photons (MISHRA & YADAVA 2015). The heat propagates through the workpiece by thermal conduction, causing microstructural changes (LIU ET AL. 1997, MISHRA & YADAVA 2015). A boundary between the phase-changed and the unaffected material zones is created. On the surface of the workpiece, depending on the laser intensity, vapor bubbles can develop due to the exceeding of the boiling temperature or tempering and rehardening zones (CHICHKOV ET AL. 1996, ZOCH 1995). Introduced transformation

stresses influence the mechanical equilibrium of the entire workpiece. As a result of the volume expansion due to the thermal load of the boundary zone material during laser processing, the residual stress state is influenced, and dimensional and shape changes to the workpiece consequently occur. The counteraction of the lower layer introduces a bending moment, which follows the same scheme as during grinding. First, compressive stresses are introduced with a possible exceeding of yield strength. Cooling follows with a contraction of the material and an emergence of tensile stresses in the plastically compressed region (FANINGER 1976, SCHREIBER 1973). Changes in distortion behavior are also generated by the clamping of the workpiece with resulting high tensile stresses in the outer regions. Differences in the coefficient of thermal expansion also lead to a similar response (SOCHALSKI-KOLBUS ET AL. 2015, BAYERLEIN ET AL. 2016, BAYERLEIN ET AL. 2018).

2.5 Deep rolling

2.5.1 Classification of deep rolling tools

In addition to the previously presented laser processing for the systematic induction of tensile stresses into the deformed workpiece, the dissertation aims to illustrate the possibilities of deep rolling experimentally and numerically for distortion control. The required fundamentals are presented in this section.

Deep rolling tools have different classifications, each with variable effects of a contact pressure p_{dr} and a force F_{dr}. For this dissertation, a type with hydrostatic pressure was chosen. By ensuring low wear due to both fewer components and operation with hydraulic fluid allowing constant pressure, this tool is the most commonly used. Another advantage is minimizing workpiece roughness after machining (ABRÃO ET AL. 2014).

Aside from the hydrostatic load application, there are other options for deep rolling tools. These usually use elastic forces through a preloaded spring or generate a load by a tool displacement on the processed workpiece (ABRÃO ET AL. 2014).

2.5.2 Structural interaction between the deep rolling tool and the workpiece

Deep rolling generally produces a smooth surface by employing a mechanical treatment. A corresponding tool establishes contact with the workpiece with a defined pressure in this process. Hertzian pressure causes stresses to exceed the yield strength of the material at a certain point, resulting in plasticization. Depending on the applied pressure as well as the geometry of the used tool, the consequent compressive stresses and the work-hardening layer can be influenced (SCHOLTES & MACHERAUCH 1986). The material must be plasticized

to enable this process to be used for distortion compensation. A purely elastic deformation of the boundary layer zone is not sufficient. The resulting stresses during machining in the contact zone must be high enough to prevent complete relaxation of the material layer. For these to be selectively induced in a workpiece, tool movement follows a defined trajectory along the surface. Rolling friction between the material and tool causes a smoothing effect with a freely rotating tooltip, whereas sliding friction occurs with a fixed one (SCHOLTES & MACHERAUCH 1986). During deep rolling, a distinction is made between tangential and normal forces acting on the surface. A combination of the two causes Hertzian pressure and plastic strain (SPINU ET AL. 2011), which results in compressive stresses within the subsurface with high plastic deformations. Hertzian pressure usually dominates for hard materials such as quenched and tempered AISI 4140 steel used for linear guide rails. For medium-hard materials, both effects overlap. In addition, Figure 15 shows that an occurring sliding friction caused by the slip between the tool and the workpiece can result in maximum compressive stresses close to the surface (SCHOLTES & MACHERAUCH 1986).

A detailed understanding of the frictional effects during the deep rolling process is necessary for the numerical modeling discussed later in this dissertation. The surfaces of the tool and the workpiece interact, initially generating adhesive friction and, as the rotating process progresses, a combination of sliding and rolling friction at the tip of the ball. Here, the influence of the lubricant must be considered.

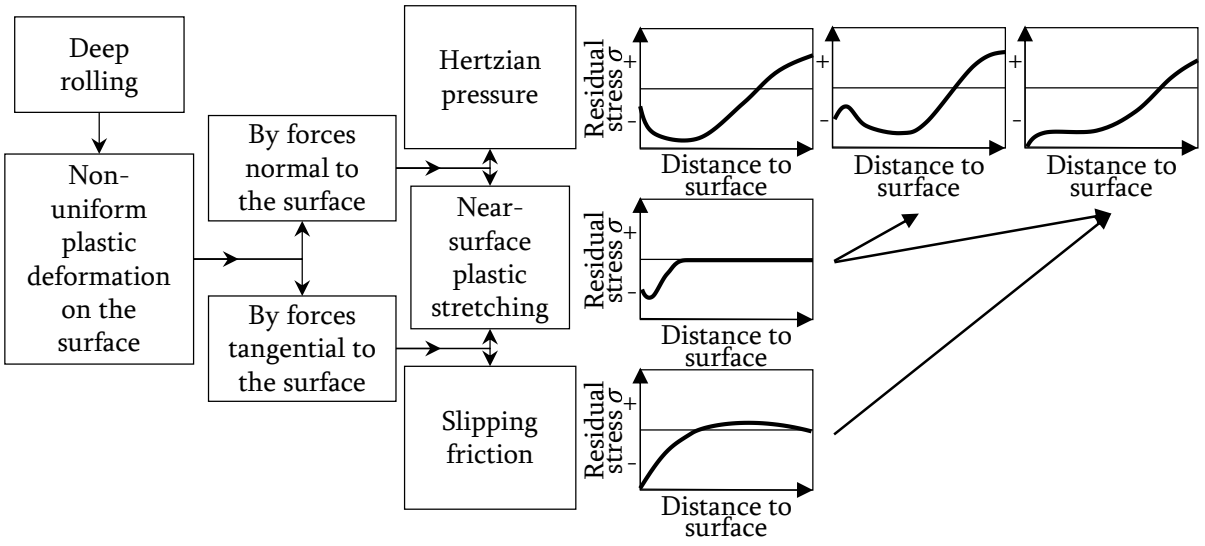

Figure 15: Simplified representation of the deep rolling effects on the residual stress state (based on SCHOLTES & MACHERAUCH (1986) and LYUBENOVA (2020))

The coefficient of friction μ results from the so-called Stribeck curve and is defined as the quotient of the frictional force $F_{F_{dr}}$ and the normal force $F_{N_{dr}}$ (ROBINSON ET AL. 2016):

$$\mu = \frac{F_{F_{dr}}}{F_{N_{dr}}}. \tag{2-20}$$

In this case, there is a dependency on the relative speed between the tool and the workpiece at higher deep rolling velocities v_{dr} (Figure 16). At low ones, there is no influence because of a lack of lubrication. However, at medium velocities, the coefficient of friction decreases (ROBINSON ET AL. 2016).

Mixed lubrication occurs when one part penetrates the material during loading due to the low roughness profile of the tool and the workpiece. As in this dissertation's application, it typically appears during deep rolling with hydrostatic pressure. A polished tool tip opposes the rough surface of the workpiece. During this operation, there is always mechanical contact (ROBINSON ET AL. 2016).

At high rolling velocities v_{dr}, the roughness profiles continue to decrease, as does the thickness of the lubricating film. However, direct contact of the tool with the workpiece is not possible. The entire normal load is on the lubricating film. However, the increased friction is usually lower than that caused by boundary lubrication (ROBINSON ET AL. 2016).

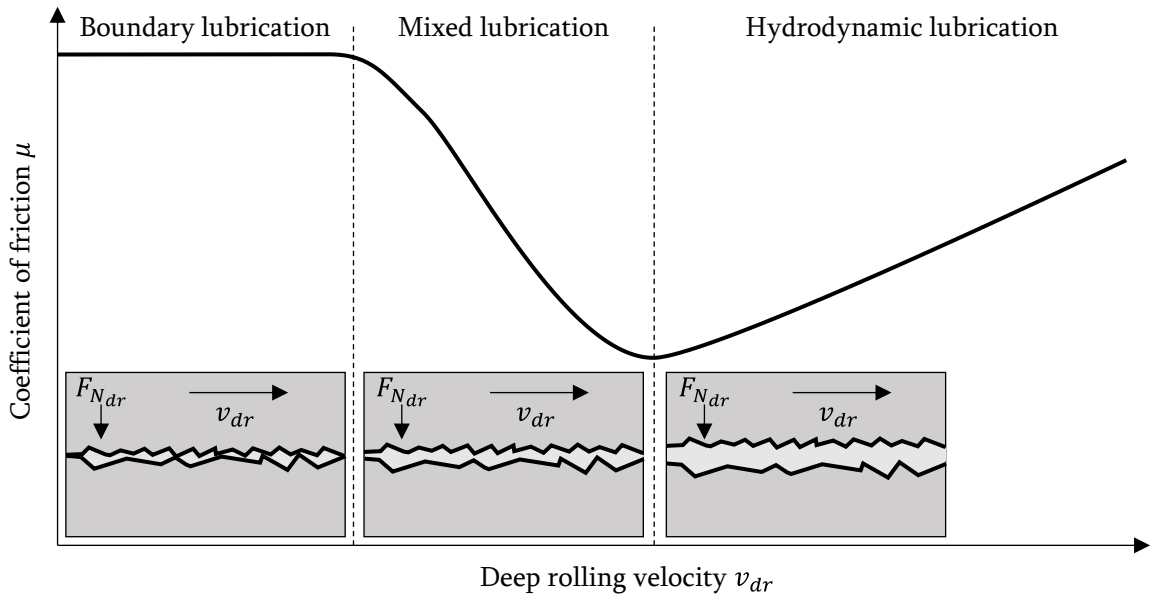

Figure 16: Stribeck curve describing the coefficient of friction depending on the deep rolling velocity v_{dr} and the type of lubrication (based on ROBINSON ET AL. (2016))

Due to the possibility of a targeted application of compressive stresses, deep rolling is used in the automotive (e.g., crankshafts or engine valves) and aerospace industries (e.g., turbine blades). However, tensile stresses caused by a thermal process can also be reduced in welded

structures (RÖTTGER & FRICKE 2014). The process kinematics often limit the application possibilities due to the inaccessibility of certain workpiece surfaces.

2.6 Modeling of processes

2.6.1 Finite element method

For the computer-based analysis and prediction of component-related thermomechanical effects during and after the grinding of steel components, FE-based structural simulation and analytical approaches have proven particularly useful for macroscopic observation (HEINZEL 2009). Thus, the change in residual stress and resulting distortion development can be modeled. Complex nonlinear phenomena can be described and numerically calculated via differential equations. A typical example is transient heat conduction in solids. The process of meshing is utilized to simulate and represent transient temperature fields, phase transformations, and existing mechanical boundary conditions. It involves creating a structure that can accurately capture and model these dynamic systems, enabling precise analysis of the system's behavior. The defined finite elements are coupled at discrete nodes, and a simulation program solves the differential equations numerically at these points. Although the relevant phenomena can be arbitrarily complex, all thermometallurgical and thermomechanical effects must be represented sufficiently (ZAEH ET AL. 2009). That applies particularly to the simulation of residual stresses and distortions resulting from grinding, allowing the creation of a valid model for predictions (BRINKSMEIER ET AL. 2006, DOMAN ET AL. 2009, HEINZEL 2009). Despite the large scale and the high quality of FE-based simulation results, a significant amount of time is required to model and solve the coupled, highly nonlinear differential equations.

Detailed approaches can be found in BATHE's (2002) work. Nonetheless, some crucial approaches for numerical modeling of the relevant processes are discussed below. These are necessary to predict the distortion behavior in profile grinding and the two compensation strategies, namely laser processing and deep rolling.

Distortion modeling involves the problem of an elastic-plastic solid subject to large dynamic deformations. To obtain a robust mathematical basis for mesh fitting and error estimation from a minimal principle, time discretization and a constitutive model approach must be combined for the time-discretized incremental problem of the processes to be modeled. Formulated as a variational problem in the FEM, the motion of the solid can be characterized as a solution to a series of minimization problems (FRIESECKE & DOLZMANN 1997, JORDAN ET AL. 1998, ORTIZ & REPETTO 1999, KANE ET AL. 1999). For the further step formulation of variable constitutive updates for elastic-plastic solids in this dissertation, reference is

made to RADOVITZKY & ORTIZ (1999) and ORTIZ & STAINIER (1999). The minimal incremental principle can hence be derived.

2.6.2 Thermal effects and the structural problem

Heat transfer occurs during grinding due to the dominant thermal effect in the contact zone. This results in different boundary conditions in the modeling, which must be considered. These consist of conduction within the workpiece as well as convection and radiation to the environment.

Regarding the corresponding heat transfer modes in a three-dimensional solid as boundary conditions for the FEM simulation, reference is made to Föckerer et al. They provide the exact analytical definitions of radiant heat flux, heat loss by radiation, and heat loss by surface convection, which are relevant for a thermomechanical process simulation (FOECKERER ET AL. 2013).

Corresponding temperature distributions in the material can be calculated by the sufficiently accurate description of occurring thermometallurgical and thermomechanical effects with the FEM. They are defined by the formulation of the heat transfer problem from the conservation law for thermal energy (CAMACHO & ORTIZ 1997). The non-steady-state three-dimensional heat conduction equation in a moving solid describes the thermomechanical coupling and the interaction between the friction, the temperature, and the plasticity as an equilibrium (FOECKERER ET AL. 2013):

$$\rho c \left(\frac{\partial T}{\partial t} - v_{ft} \frac{\partial T}{\partial x} \right) = k \left(\frac{\partial^2 T}{\partial x^2} + \frac{\partial^2 T}{\partial y^2} + \frac{\partial^2 T}{\partial z^2} \right), \tag{2-21}$$

where ρ is the material density; c is the specific heat capacity; $T = T(x, y, z, t)$ is the temperature field depending on the coordinates x, y, and z; t is the interaction time; and k is the thermal conductivity. Thus, the significant mechanical and thermal behavior of the workpiece during machining can be described (FOECKERER ET AL. 2013).

The thermal problem, originating in friction and plastic work, is coupled with the mechanical one. On the one hand, the distortion of the material due to plastic deformation causes a significant amount of heat (CAMACHO & ORTIZ 1997). On the other hand, softening due to temperature affects yield strength (MARUSICH & ORTIZ 1995).

Large plastic strains in the steel workpiece are generated due to mechanical stresses and thermal expansion caused by the heat flux in a grinding contact area. Moreover, the thermal expansion initiated during laser processing for a distortion compensation is sufficient to generate large plastic strains in workpieces via a mechanical process. The elastoplastic

element formulation must be addressed to integrate the mechanical problem into the FEM to predict deformations numerically.

3 State of the Art

3.1 Chapter overview

Building upon the theoretical foundation established in Chapter 2, Chapter 3 presents existing concepts and approaches concerning distortion control after machining processes. These served as a basis for the publications of this dissertation. Since distortion during profile grinding largely depends on the change of the residual stress state in the material, the machining effects on workpiece deformation are explained in Section 3.2, followed by a presentation of the numerical prediction possibilities using simulations of the grinding process in Section 3.3. Literature-based options subsequently describe how specific workpiece deformations have been generated by laser machining and numerically modeled. In Section 3.4, the effects of deep rolling on the workpiece material are discussed as approaches for controlling distortion after grinding. Before the need for action is debated, the concepts for deformation minimization according to literature are presented.

3.2 Boundary zone influence and distortion formation during grinding

This section provides essential investigations into changes of material properties in a defined volume of the boundary area of a newly created surface, and how these changes lead to distortion formation. For this purpose, a presentation of different studies on simulation and, thus, on the prediction of the workpiece deformation is given. The effect of process-induced residual stresses is also considered. During the grinding process, the boundary zone is significantly influenced by external mechanical, thermal, and chemical factors affecting the material to a depth of up to several millimeters. The hardness, microstructure, and residual stress state are changed by the process (ZHANG ET AL. 2017).

Residual stress-induced workpiece distortion

LEÓN GARCÍA (2010) determined workpiece deformations, which occur due to the thermal load of the boundary zone material during the one-sided machining of plate components. An empirical model introduced and incorporated as a boundary condition of an FE model was provided to predict residual stresses.

RATCHEV ET AL. (2011) used a mathematical algorithm employing an FE simulation to determine workpiece distortion due to micro-scale and near-surface residual stresses after

turning. With this method, stresses and resulting distortions were reproduced in the boundary zones of an axially symmetric FE model during the cutting process of a tie rod.

WIMMER ET AL. (2018) provided another means of characterizing boundary zone effects during machining. In their study, the distortions of machined thin-walled samples were investigated. The deformation was calculated utilizing the finite element method (FEM) for a whole workpiece.

Concerning the precision workpieces used in this dissertation, the work of MARUSICH ET AL. (2008) on a simulated distortion of thin-walled aerospace structural components should also be mentioned. Based on the manufacturing history of the semi-finished product, initial residual stresses were first determined empirically, and process-induced ones were then determined using an FEM machining simulation. The numerically calculated distortions of these thin-walled components showed only a slight deviation from those determined experimentally.

ZHONGYI & YUNQIAO (2010) also investigated aerospace structural components manufactured by cutting utilizing thermomechanical coupling in an FE simulation. However, they extended previously known models by selectively deactivating finite elements to predict workpiece distortion after machining. They also achieved a proper match between experimental and simulative results.

MA ET AL. (2010) investigated the manufacturing history of metallic workpieces. The distortions due to initial residual stresses before the actual machining are essential for consideration of the resulting geometrical deviations. Through the creation of a simulation chain, distortions after each production step, in which several heat treatments of the workpiece took place, were predicted with an error of only ± 20 %. For the FE simulation, the authors two-dimensionally mapped the model, thereby reducing both complexity and computational time. Through a subsequent optimization, the distortion of the engine components was proven to be minimized.

Thermal modeling of the grinding process

The boundary zone influence depends on the energy input at the surface of the machined workpiece. In particular, the heat input, temperature fields, and residual stresses could be modeled sufficiently accurately for processes such as grinding. A variety of approaches exist for modeling the relevant thermal processes (KOLKWITZ ET AL. 2011, JERMOLAJEV ET AL. 2016). The basic models are discussed below.

In the literature, the simulation of the heat flux within the contact zone into the workpiece during grinding was mainly based on the approaches of JAEGER (1942) and CARSLAW &

JAEGER (1959) for calculating a two-dimensional temperature field in a semi-infinite body. These approaches have been refined over time to include other thermal effects (e.g., temperature changes and energy losses). The assumption of an adiabatic surface with a constant feed rate v_{ft} of the heat source along the surface to be machined remained unchanged. A constant heat flux density $q_w(x,y)$ with a quasi-stationary temperature field $T(x,y)$ was assumed by MISHRA & PRASAD (1985). The model was subsequently extended to include the temperature reduction in the workpiece due to radiation and convection at the surface through the heat transfer coefficients h and the ambient temperature T_∞ (FOECKERER ET AL. 2013). In their experiments, the commonly used cooling lubricant transported most heat away during grinding. This heat partitioning has been studied analytically by WITTMANN (2007) and WILKE (2008). Figure 17 illustrates the basic model with the combined effects of a heat source with a heat flux density $q_w(x,y)$ along the contact length l_g, radiation, and convection at the surface.

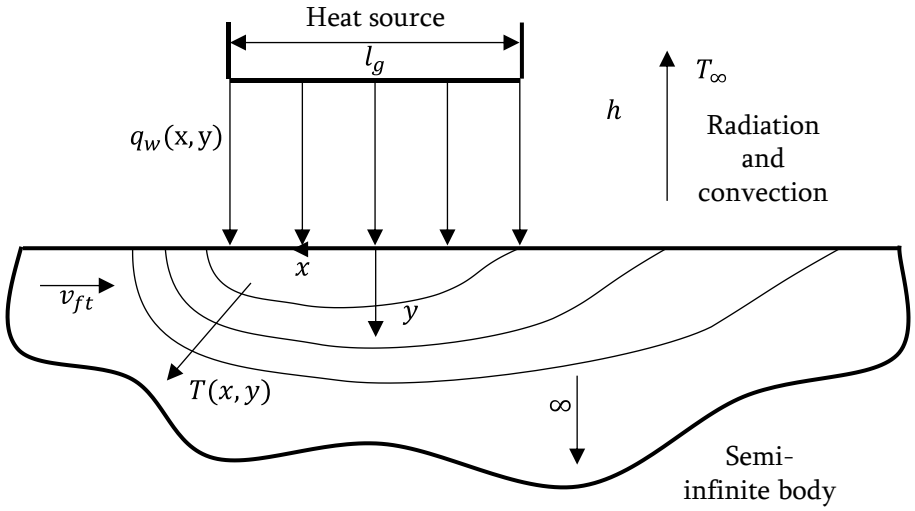

Figure 17: Schematic representation of a quasi-stationary temperature field in a semi-infinite body with a machining feed rate v_{ft} due to a heat source with a length l_g and a heat flux density q_w as well as the resulting radiation and convection at the surface (based on JAEGER (1942), Carslaw & Jaeger (1959), and DES RUISSEAUX & ZERKLE (1970))

In addition, the thermal interactions between the workpiece, the grinding wheel, the chips, and the cooling lubricant have not yet been considered. LIAO ET AL. (2000) and MAKSOUD (2005) pursued this approach in their analytical models. The amount of heat converted grows proportional to the increasing uncut chip thickness. Thus, a triangular heat flux density distribution can be assumed along the contact zone (SNOEYS ET AL. 1978). The basic model was accurately adapted to the actual grinding process based on experiments by JIN & CAI (2001), JIN ET AL. (2002), ROWE (2001), and ROWE & JIN (2001). However, these modelings only refer to surface grinding with a triangular heat source on an inclined plane.

Furthermore, in the numerical results of BRINKSMEIER ET AL. (2003), who compared heat sources with different heat flux density distributions for surface grinding hardening, heat input via a triangular heat flux density distribution showed good agreement with the results of the performed experiments. This geometry was used in further publications to model and simulate other different grinding processes (FOECKERER ET AL. 2013), such as profile grinding (JIN ET AL. 2017).

A different approach was chosen by TAKAZAWA (1966). Due to the coupling of various thermal effects, the models' computing times and complexities increase. Therefore, to reduce computational demands, it is also possible to calculate approximately one-dimensional temperature fields in grinding processes with a low depth of cut.

In addition, the model of CARSLAW & JAEGER (1959) can be modified to include heat conduction transverse to the feed direction. For this purpose, the heat source was extended from a line contact surface to a rectangular surface (NGUYEN & ZHANG 2010).

For residual stress or distortion prediction during grinding using FEM, analytical heat flow calculations allow for the definition of boundary conditions in the contact zone (SCHUHMANN & BIERMANN 2012). These computations enable the simulation of thermal expansion in the workpiece. Thus, the increased computational effort for calculating the energy and the temperature distribution in the workpiece can be reduced, as these were previously primarily based on empirical investigations (KARPUSCHEWSKI ET AL. 2008). Moreover, determined temperature fields can be coupled with material models. In this way, any microstructural changes in the boundary zone layer can be predicted (FOECKERER ET AL. 2010).

Especially for the three-dimensional analysis of plastic workpiece deformation during profile grinding processes, the energetic consideration within the contact zone is essential (JIN ET AL. 2017). The yield strength limits the specific plowing and sliding energies. With a larger depth of cut, their values increase (DOMAN 2008), whereas a higher cutting speed leads to decay. The cutting force ratio is determined from the quotient of the tangential and the normal force components (ANDERSON ET AL. 2011). As mentioned in Subsection 2.3.4, the cooling lubricant significantly influences the specific grinding energy components. The proportion of the specific deformation energy in the grain engagement increases with more lubrication, which means that the specific grinding energy is higher in the range of low engagement depths (MALKIN & GUO 2008). However, it is smaller for a higher depth of cut since the influence of the reduced sliding energy dominates (KÖNIG ET AL. 1985, VITS 1985).

In DOMAN's (2008) study, while the grinding energy rose at low cutting speeds and with an increasing depth of cut, this increase in energy consumption only occurred at higher speeds

until plastic deformation emerged. VUČETIĆ (2008) explained this effect with the influence of the chip thickness. This effect decreased with a lower cutting speed because of a higher temperature formation in the contact zone. According to him, a reversed influence occurred with larger chip thicknesses.

The most common opinion in the literature is that, as the cutting speed increases, the specific grinding energy decreases (BRINKSMEIER ET AL. 2002, BRINKSMEIER & GIWERZEW 2003, GIWERZEW 2003, HAMDI ET AL. 2003, ZHAO ET AL. 2013).

BRINKSMEIER (1982, 1991) also presented the relationship between grinding energy and the residual stress change of the component boundary zone for conventional grinding processes. However, there are many applications and modifications of process-dependent energetic model approaches for describing the boundary zone influence. Based on ZEPPENFELD's (2005) publication on this topic for the speed stroke grinding of gamma titanium aluminides, NACHMANI (2008) focused on modifying the model for hardened steel materials. Expanding on material, geometric, and kinematic boundary conditions in grinding high-hardness 100Cr6 bearing steel, MAIER (2008) derived a calculation method for predicting the rehardening zone considering thermal effects.

JIANG ET AL. (2016) and JIN ET AL. (2017) considered more complex contact surfaces in their model approaches for profile grinding. They analyzed the machining of gear teeth and tooth flanks and confirmed GORGELS's (2011) assumption that existing models must be adapted in each case for the specific application in profile grinding since the process kinematics and, thus, the load variables can change.

Process variables, which are relevant for grinding, are physically coupled and must be modeled using hybrid simulation systems in the FEM and the definition of actual boundary conditions. Depending on the application, this modeling is done by adapting substitute models to describe the heat flux into the workpiece (NOYEN 2008, DOMAN ET AL. 2009, FÖCKERER 2015). Thus, the temperature- and phase-dependent material behavior can be simulatively analyzed with a numerical calculation of the microstructural transformation (FOECKERER ET AL. 2012). Modeled transient temperature fields and thermomechanical process phenomena allow for the prediction of residual stress generation and the resulting workpiece distortions (SHAH ET AL. 2012, FOECKERER ET AL. 2013, KUSCHEL ET AL. 2016). Because these complex effects can only be inadequately predicted in the two-dimensional space, the published FE models are mostly three-dimensional thermometallurgical approaches (ZHANG ET AL., LI & AXINTE 2017).

Interim conclusions

In this section on the state of the art, various studies on the material changes of the workpiece properties in a defined volume of the boundary zone of a newly created surface and the resulting distortion after the grinding process are discussed. The changes are significantly affected by external mechanical and thermal influences on the material, whereby the depth of impact can be up to several millimeters. The hardness, microstructure, and residual stress are affected. Researchers have used FE simulations to model the resulting stresses and deformations and have developed various algorithms to predict thermomechanical effects. Empirical models have been developed to predict residual stresses, and the resulting deformations have been calculated for entire workpieces. Some studies have investigated the effects of thermal and mechanical stresses on thin-walled aircraft components. The energy input at the surface of the workpiece is a crucial factor in the resulting changes, and the thermal effects can be modeled using a variety of approaches. The simulation of heat flux in the contact zone during grinding is based on the work of JAEGER (1942) and CARSLAW & JAEGER (1959), which has been refined over time to include other thermal effects, such as heat dissipation into the surrounding environment, material phase changes, and cooling lubricant effects. Adiabatic surface assumptions and a constant feed rate were used in these models.

3.3 Numerical approaches for heat transfer and distortion modeling during laser processing

Thermomechanical simulation

Flame straightening, which is performed manually, is often used for distortion compensation on steel structures. This straightening process with a thermal deformation source is usually utilized in shipbuilding (KOERDT ET AL. 2008).

A laser offers the possibility for automation. It can be used as a heat source to selectively generate local heat spots on steel plates requiring straightening. Furthermore, hybrid welding is already used in the aerospace industry. Process-integrated operations on the joined structures straighten the workpieces (HORNFECK 2008). A significant disadvantage is the favoring of crack initiation by the thermal load, which generates tensile stresses at the surface (BERSTEIN & FUCHSBAUER 1982, SEYFFARTH 2007). A reduction in the component lifetime can be the consequence and must be considered in the design of thermal straightening processes.

A structure simulation is suitable for the distortion prediction in this dissertation, equivalent to the grinding process described above. The literature offers a variety of approaches,

especially in the area of joining processes (KOMERLA ET AL. 2020). Appropriate heat source models must be selected, for which the correct setting of the parameters is decisive. Using such equivalent heat sources as boundary conditions in the simulation allows for a highly accurate prediction of the temperature field in the workpiece. RADAJ (2002) described structural decoupling of the process simulation and the material simulation. This proven approach enables this differentiation due to the high complexity of the individual topics.

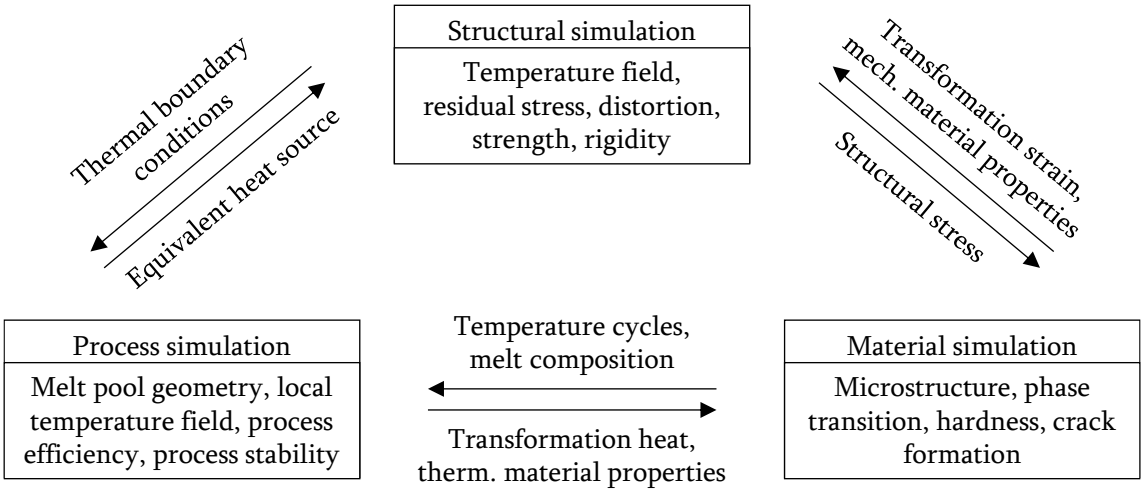

Figure 18: Distinction and mutual influencing of structural, process, and material simulations (based on RADAJ (2002))

Limiting the investigation of a numerical problem to only one part, for example by focusing on the workpiece distortion, as in this dissertation, can massively reduce the computational effort. This simplification of the model is made possible by the coupling of corresponding parameters. The structural simulation method is discussed briefly below before the numerical and analytical approaches to laser machining known from the literature are presented.

The structural approach calculates residual stresses and workpiece distortions. In addition to determining the temperature field, considering initial loadings from previous processing steps or the clamping conditions is also possible (PAPADAKIS 2008, SCHENK 2011). The establishment of equivalent heat sources in the distortion analysis must be sufficiently accurate so that the modeling of indirect effects can be neglected. This is the only way to decouple the process from the structural simulation. The same applies to the material models. These approaches are only necessary when time-dependent microstructural transformations and the heat they generate are responsible for residual stresses and workpiece distortions (KOISTINEN & MARBURGER 1959, LEBLOND & DEVAUX 1984).

Substitute heat sources are used in the simulation of laser processing, as shown in the previous section on grinding. Therefore, it is necessary to recalibrate their parameters for

different processes. For a sufficiently accurate solution, the literature offers numerical and analytical approaches aiming at an efficient and accurate prediction of the temperature field.

In their publications, RYKALIN (1957) and ROSENTHAL (1946) described the difficulties in solving the partial differential equations determining the temperature field during laser processing. They explained that various simplifications had to be made in this approach, such as the assumption of adiabatic boundary conditions and a constant laser feed rate. The temperature gradient in the material significantly influenced the resulting microstructure state and the distortions (RYKALIN 1957, ROSENTHAL 1946, POPRAWE 2005).

Substitute heat sources in the modeling of thermal processing can be distinguished according to the linear superposition principle (GOLDAK ET AL. 1984). Thus, based on Green's functions, according to CARSLAW & JAEGER (1959), the entire temperature field can be constructed from individual distributions in the workpiece. The Goldak heat source is most frequently used in analytical considerations. PITTNER ET AL. (2010) established a temperature equation depending on the spatial coordinates x, y, and z and the time t. The analytical equation depends on the heat flux $\dot{Q}_w$, the thermal conductivity k, the material density ρ, and the specific heat capacity c. The variables c_f, c_r, a, and b are geometrical parameters of a double elliptical heat source according to GOLDAK ET AL. (1984) with a heat flux density q_w (Figure 19).

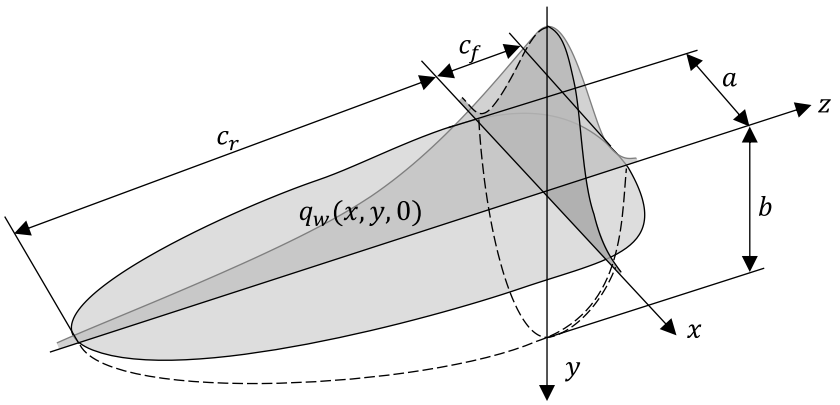

Figure 19: Double elliptical heat source (based on GOLDAK ET AL. (1984))

This parameter set determines the temperature field in an infinite continuum, which considers neither an adiabatic boundary layer nor a heat source movement (GOLDAK ET AL. 1984). It must be supplemented for an approximate solution based on actual thermal process conditions.

From a superposition of the partial results calculated with the help of numerical integration at a certain point in time, SCHLATHER ET AL. (2019) obtained the entire temperature field in the workpiece. In discrete time steps, they performed a time-dependent activation of heat

sinks. Thus, they numerically modeled a moving heat source with a simultaneous variation of the computational effort depending on the degree of discretization. This approach allowed them to meet the defined convergence criteria crucial for Finite Element Method (FEM) simulations.

Distortion modeling

Finite Element (FE) simulations are widely employed for modeling laser processing, owing to their adaptability and high precision throughout all steps of the process. Analytical calculations offer results at specific points but frequently involve model simplifications that may compromise result quality.

An illustrative case, presented by THATER ET AL. (2015), involved a weld distortion simulation in the context of an injection valve. They effectively minimized radial distortion after the thermal laser machining process by employing multiple concurrent heat sources on the workpiece's surface. This systematic method aimed to introduce residual stresses so that they counteracted each other, thus mitigating distortion.

Distortion minimization in a metal plate using a moving laser source was also achieved by DAI & SHAW (2002). Their approach involved a detailed FE analysis of the impact of laser scanning patterns on thermal residual stresses and distortions. Depending on the scanning direction, deformations on the plate surface were adjusted to eliminate both upward and downward distortions.

KRAUS (2020) systematically induced tensile stresses into steel profiles to counteract workpiece distortions. He employed an analytical process model, using a bending angle determination method. The author achieved controllable corrections by altering parameters such as laser power, feed rate, and sequential irradiation of an individual profile guided by numerical modeling. Depending on the generated stress fields, distortions were successfully minimized.

The FE method has been extensively applied in the literature not only to simulate temperature and residual stress fields but also to analyze microstructural changes in workpieces. Notably, the thickness of material layers significantly influences workpiece deformation. ZAEH & BRANNER (2010) investigated the effects of higher temperature fluctuations during selective laser melting, especially in thinner material layers, which led to more pronounced deformations.

BRUNA-ROSSO ET AL. (2021) transformed a complex three-dimensional numerical problem into a more manageable two-dimensional form. By generalizing plane strain conditions, they modeled deformation and transient stresses within material layers. This approach

allowed for a significant reduction in computational complexity, though it may offer a less comprehensive understanding of the process, especially when dealing with intricate workpiece geometries.

Interim conclusions

Thermal straightening processes are employed to rectify deformations in steel workpieces. However, manual execution of these processes can sometimes lead to structural stress-induced cracks. The utilization of a laser as a heat source presents an automated solution already in use in the aerospace industry, particularly for hybrid welding. Yet, it is important to recognize that thermal processes can potentially shorten a component's lifespan. Therefore, addressing the risk of cracking is crucial in the design of thermal straightening processes.

Structural simulations can help to analyze these processes using appropriate heat source models and parameter settings to accurately predict temperature fields within the workpiece. These simulations account for distortions or residual stresses, considering transient thermal loads on the workpiece and pre-stresses resulting from prior machining steps or clamping conditions. To effectively decouple the process from the structural simulation, it is vital to ensure the accuracy of heat source models and to neglect indirect effects.

Numerous numerical and analytical methods within the literature have been developed to predict temperature fields with precision during thermal processing. These include the linear superposition principle and Green's functions. RADAJ's (2002) has proposed a method to decouple structural simulation from process and material simulations, allowing for simplified assumptions in various aspects of numerical modeling. Often, the primary focus is on structural simulation in laser processing. Nevertheless, accurate assumptions must also be made for process and material simulations since these factors significantly influence the structure.

Modeling laser processing, therefore, necessitates an effective combination of process, material, and structural simulations to provide a reliable numerical tool for predicting workpiece distortion.

3.4 Structural effects during deep rolling and numerical approaches

General remarks

Deep rolling, a process that induces plastic deformation close to the surface (RÖTTGER 2003), is particularly valuable in applications involving workpieces, such as turbine blades in aerospace manufacturing (KLOCKE & MADER 2005). The mechanical load applied during deep

rolling can be precisely controlled, similar to laser beam straightening. This process imparts compressive stresses, and several parameters influence the resulting residual stress profile, with the initial condition of the workpiece, rolling pressure, and tool diameter being the most critical ones (PREVÉY, P., HOMBACH, D. & MASON 1997).

RÖTTGER (2003) explored the elastoplastic deformation zone created during deep rolling of 100Cr6V steel. Larger tool diameters led to deeper displacements without significantly altering the maximum compressive stresses. This observation held true for varying deep rolling pressures. SCHUH ET AL. (2007) conducted similar experiments with titanium workpieces, finding that higher rolling pressures led to deeper compressive stresses.

The number of machining cycles affects the generated compressive and tensile stresses during deep rolling. However, plastic deformation steadily decreases until it reaches a saturation point. ACHMUS (1999) analyzed this phenomenon's impact on surface integrity, considering axial residual stress distributions on rotationally symmetrical workpieces after a maximum of five passes.

Deep rolling interactions between the rolling ball and the workpiece adhere to Hertzian theory, predicting maximum equivalent stresses in rigid-body, point-contact scenarios. This model is suitable for hard materials but has limitations when workpiece elasticity is considered. To address this in numerical simulations, SPINU ET AL. (2011) used a rectangular cuboid with adjustments to the computational domain and a predefined exponential function to approximate the load profile.

The maximum compressive stress level in deep rolling is constrained by the material's yield strength and work-hardening state. Increasing the rolling force shifts the compression range to greater depths, simultaneously elevating subsurface hardness due to work-hardening effects (ZÖLTZER ET AL. 2001).

Experiments demonstrated that an increase in rolling tracks led to increased sub-surface compressive stresses in quenched specimens but not in soft-annealed workpieces (MAGALHÃES ET AL. 2017). SCHUH ET AL. (2007) also observed anisotropic behavior in residual stress measurements with stronger anisotropy in the axial direction, resulting in higher compressive stresses (SCHUH ET AL. 2007, BERSTEIN 1979). RODRÍGUEZ ET AL. (2012) highlighted strong anisotropies due to different plastic strains and shrinkages along and perpendicular to the rolling directions.

HETTIG & MEYER (2020) extended these approaches, specifically investigating sequential multistage deep rolling using AISI 4140 steel. Their research delved into the changes that occur in the material during the deep rolling process, considering various factors, including the effects of multiple contacts and the sequence of applied loads. The outcome of their

experiments and residual stress measurements revealed that the material's elastoplastic behavior and hardness led to significantly different residual stress depth distributions depending on the specific type of steel used. Moreover, for identical loads and geometric conditions, the material response remained consistent across repeated loading cycles (HETTIG & MEYER 2020).

The numerical approach of deep rolling

To simulate workpiece distortions due to deep rolling, adjustments to existing models were necessary. Time-dependent tool-workpiece interactions required analytical and finite element (FE) modeling to predict surface residual stress states at any process stage (JUNG ET AL. 1996, ACHMUS ET AL. 1997, ACHMUS 1999, JUNG 1996).

BROSZEIT (1984) laid the foundation for Hertzian theory-based models for roll peening. They prediced the sub-surface residual stress state in the rolling contact problem, although they omitted nonlinear elastoplastic deformations and friction effects.

ACHMUS (1999) demonstrated in his dissertation that the elasticity of the tool could be disregarded in simulations, even when assuming a rigid tool body.

PERENDA ET AL. (2015) successfully used an FE model in their deep rolling simulations to predict stress states in an AISI 4340 steel workpiece for torsion bar applications, saving time and resources. They matched their results with experimental data by implementing surface friction models and defining elastic-plastic boundary conditions with kinematic and isotropic hardening (PERENDA ET AL. 2015).

YEN ET AL. (2005) extended two-dimensional numerical models to three dimensions for predicting residual stresses and surface deformations. Their refined 2D model improved residual stress predictions, while the 3D model offered more realistic surface deformation insights and material flow (YEN ET AL. 2005).

According to ALTENBERGER (2002), the strain-dependent data may not be as critical as temperature-dependent data in defining boundary conditions for processes with lower strain rates.

Various material models are available for setting up deep rolling simulations. BROGGIATO ET AL. (2008) utilized a nonlinear linked isotropic-kinematic hardening rule, while the Johnson-Cook model was recommended for materials with large strains and high rates (JOHNSON & COOK 1983).

At the beginning of this section, the directional stress dependence in a workpiece during deep rolling was already described. PERENDA ET AL. (2016) used deep rolling to systematically induce residual stresses in torsion bars, positively impacting material fatigue life and

load capacity. They achieved control of residual stresses by combining deep rolling and preloading, leading to increased strength and durability (PERENDA ET AL. 2016).

Interim conclusions

Deep rolling enables plastic deformations close to the surface, resulting in hardened workpieces. This process, typically used in CNC machine tools, generates compressive stresses influenced by various parameters. The initial workpiece condition, rolling pressure, and tool diameter are crucial factors. Furthermore, the number of machining cycles impacts stress generation. Deep rolling can systematically control deformation and distortion in slender workpieces post-grinding. Numerical approaches in the literature offer the means to simulate the process by defining boundary conditions and adapting them to specific workpieces. In summary, deep rolling is a valuable method for influencing the stress state of steel parts, making it useful for distortion control.

3.5 Approaches for distortion compensation and minimization

During the production of slender workpieces, distortions arise from local plastic deformations. Various manufacturing processes, including grinding, affect the material's boundary zone, often leading to an asymmetric residual stress state. Subsequent straightening processes are essential, particularly in the manufacturing of precision components (MITZE 2010, JÖNSSON 1998). Deformations can be induced in workpieces through thermal and mechanical loading, either manually or semi-automatically.

Distortion minimization after machining

The effects of distortion resulting from the straightening processes depend on input parameters. The applicability of these processes is determined by the degree to which input parameters can be controlled and the magnitude of resulting deformations. Distortion engineering methodology allows a basic understanding of the involved mechanisms and estimation of workpiece deformations. As demonstrated, these processes can be divided into submodels for steel workpieces. A typical distinction is made between thermometallurgical and thermomechanical approaches, allowing the identification of influences on overall distortion. ZOCH (2012) examined workpieces for the gear industry, considering factors such as geometry, chemical composition, microstructure, and residual stresses, and how they affect the development of distortion. Thermal loads and mechanical stresses from preceding process steps also impact the material.

In controlled workpiece straightening, we differentiate between parameters that can be precisely adjusted for correction and those that cannot. However, the choice of machining

parameters can minimize the shape deviations of the finished workpiece during the grinding process, which causes undesirable deformations. Moreover, stress-induced distortion effects are more pronounced in slender geometries, making workpiece geometry a critical factor (MERCELIS & KRUTH 2006, SCHULZE 2009).

Microstructural transformations on the workpiece's surface are crucial for accurate distortion modeling. Omitting these can lead to inconsistent results, given the relationship between heat input and changing material parameters (MUGWAGWA ET AL. 2018). Similar to RADAJ (2002), KRAUSS & ZAEH (2013) acknowledge the need for simplifications in certain areas to maintain modeling efficiency. This shift in focus from microstructure and dimensional stability to distortion and residual stresses helps consider deformation magnitude in optimizing minimization strategies. The complex relationships between process parameter changes and distortion behavior are further complicated by different microstructural and mechanical properties. These become evident when thermal or mechanical loads are applied to a workpiece. In the context of manufacturing processes, such as grinding with a strong boundary zone influence, the development of minimization approaches as subsequent straightening options can help reduce unavoidable distortions. Simultaneously, this allows for the identification of the influences of these processes or a process chain.

SÖLTER ET AL. (2016) investigated the use of heat generation during chip removal for surface hardening, considering the influence of load stress conditions due to workpiece clamping. However, this process led to workpiece distortion, and the authors examined its causes and potential compensation methods. Their experiments revealed that higher feed rates increased distortion. To date, compensation through sequential grinding hardening of opposing workpiece surfaces has not yielded successful results.

Since it is often impractical to minimize distortion by altering machining steps at various points in the product development process, the literature offers recommendations for controlling workpiece deformations through additional thermal or mechanical machining steps (RADAJ 1988). Designing dedicated loads and manufacturing parameters for straightening processes, such as laser processing and deep rolling, can effectively influence residual stress generation during grinding. In this manner, boundary conditions can be precisely controlled, with consideration for heat flux and the occurring forces, allowing for the compensation of workpiece distortion (RADAJ 1988). LANGHORST (2016) subsequently describes additional options for minimizing distortion, including techniques for reducing shape deviation through local stretching, using rolling and the application of additional heat sources.

Experimental investigations are essential for deriving suitable strategies and selecting appropriate manufacturing parameters for straightening. They help reduce prediction errors resulting from the thermo-mechanical load interaction for selective stress induction of

residual stresses, which can counteract those from grinding and the material behavior of the steel. During laser processing, workpiece distortions can be specifically influenced by varying the laser power and feed rate (PRINZ ET AL. 2004, SCHIMANSKI ET AL. 2010). Similarly, the number of rolling tracks and the offset at the surfaces during deep rolling can affect the degree of distortion (HETTIG & MEYER 2020, ALTENBERGER 2005).

Computer-aided approaches

Efforts in analyzing thermomechanical effects in machining processes have traditionally involved time-consuming preliminary tests. However, the advent of computer-aided approaches has significantly reduced the need for extensive experimental testing, providing a more efficient way to characterize workpiece behavior during machining. These methods also facilitate practical design by minimizing the reliance on elaborate experimental plans, especially in critical areas where microstructural changes can significantly impact outcomes.

In addition to utilizing the finite element method and validating results through experimental data, researchers have successfully incorporated regression models and optimization algorithms to minimize workpiece distortion in computer-aided environments. Ensuring efficient simulations while maintaining reasonable computational times required advanced techniques, including the expansion of test domains within submodel extensions (BENYOUNIS & OLABI 2008).

Studies by LANGHORST ET AL. (2012) and SATHIYA ET AL. (2012) have demonstrated the potential of neural networks in welding applications. LANGHORST ET AL. (2012) predictes optimal process parameters in laser beam welding to maximize tensile strength. SATHIYA ET AL. (2012) explored angular distortion in stainless steel plates, subsequently identifying ideal parameter selections for heat source sequencing through neural networks and optimizing deformations using particle swarm algorithms. Both studies successfully achieved their objectives while meeting error tolerance requirements.

BELITZKI (2018) introduced a novel approach, combining numerical methods and artificial neural networks to maintain dimensional accuracy in welding-induced deformations. The method allowed for the efficient determination of deformation-optimized process parameters, particularly concerning the calibration of problem-specific heat sources. An artificial neural network and genetic algorithm were employed to identify optimized parameters, resulting in significant resource savings for complex welding tasks. While this computer-aided approach provided qualitative rather than quantitative solutions, its potential became evident when compared to conventional methods (BELITZKI 2018, BELITZKI & ZAEH 2016).

Accurate representation of geometric details and precise boundary conditions are essential not only for predicting workpiece distortions but also for implementing desired precompensation mechanisms. AFAZOV ET AL. (2017) illustrated this process in machining turbine blades, achieving results within defined tolerances. They accomplished this by refining the surface mesh of the FE problem in the tool-workpiece contact zone. Nevertheless, they encountered accuracy issues due to suboptimal mesh quality in representing the surfaces exposed to peak loads. As a result, they introduced boundary zone load calibration based on experimental data to reduce variations and uncertainties in nonlinear deformation behaviors.

Similarly, BAYERLEIN (2020) focused on achieving increased shape accuracy in laser beam melting by developing a thermomechanical FE model. Their research identified the inherent variability in material parameters and the lack of precise boundary conditions as contributors to the variability in experimental results. To address this, an iterative approach was used to generate a predeformed version of the input design, leading to a substantial reduction in maximum shape deviation. This study underlines the potential of simulation-based preforming for optimizing distortions, particularly in achieving substantial savings in manufacturing resources (BAYERLEIN 2020, BAYERLEIN ET AL. 2015).

Interim conclusions

Precision components often require subsequent straightening processes to minimize geometrical changes resulting from local plastic deformations. The distortion engineering methodology provides insights into these mechanisms and the estimation of workpiece deformations. The careful selection of machining parameters can effectively reduce shape deviations in finished workpieces, especially considering residual stresses' impact on geometric outcomes.

The control of stress-strain effects relies on controllable input parameters, and the quantity of deformation can be determined by simulating thermomechanical and thermometallurgical interactions. Microstructural transformations can profoundly affect distortion modeling, making their consideration vital for optimized minimization strategies. The utilization of submodels within simulations aids in identifying influences on overall workpiece shape deviations, with the potential for model efficiency through appropriate simplifications.

Computer-aided approaches have emerged as powerful tools, reducing the need for extensive experimental testing by characterizing workpiece reactions during machining processes. The FE method, regression models, and optimization algorithms contribute to the numerical minimization of workpiece distortion. Deep rolling and laser processing have

proven effective in influencing residual stress generation post-grinding, with controlled boundary conditions compensating for workpiece distortions.

In conclusion, the use of optimization algorithms and artificial neural networks in combination with numerical models has shown promise in reducing workpiece deformations resulting from thermal loads while providing valuable insights into the effects of machining processes.

3.6 Conclusion and need for action

In the manufacturing of metal components, ensuring precise dimensional accuracy is paramount. The issue of workpiece distortion must be addressed and minimized to meet the stringent quality standards. Traditional methods for achieving minimal distortion often involve design modifications or post-production thermal or mechanical corrections. However, alternative strategies already exist, leveraging lasers to apply controlled heat or adjust clamping conditions.

An analysis of the current state of the art reveals that straightening processes are employed in manufacturing, but their application is often based on empirical knowledge, and their effects are challenging to quantify. Grinding operations, in particular, can induce and exacerbate distortion effects in the component's boundary area, resulting in unwanted shape alterations. Therefore, the implementation of straightening processes becomes imperative to ensure the requisite dimensional accuracy, especially for slender components such as linear guide rails. These components are notably sensitive to residual stress changes following profile grinding.

Laser treatment and deep rolling represent promising paths for systematically and significantly mitigating workpiece distortion in metallic components. Importantly, these processes can be seamlessly integrated into existing manufacturing workflows, including conventional CNC machines. In the context of profile grinding within V-grooves, where high thermal effects can lead to substantial shape alterations, numerical modeling proves indispensable for analyzing and predicting these changes. The incorporation of optimization algorithms and artificial neural networks, combined with simulation techniques, exhibits great potential for reducing unavoidable workpiece deformations resulting from thermal loads. These methods also offer a means to explore the interplay of coupled processes, advancing our understanding of controlled thermal and mechanical straightening procedures.

Thus, the identified challenges associated with workpiece distortions and the potential for their control underscore the necessity for action. They form the foundational basis for the research approach detailed in Chapter 4.

4 Research Approach

4.1 Chapter overview

This chapter presents the scientific objectives of this thesis, the research approach, and the methodological approach to distortion control after profile grinding by laser machining and deep rolling. The requirements for the method to be developed are specified, and scientific objectives, including sub-objectives, are derived based on the state of the art described in Chapter 3. The integration of the five publications that form the research focus of this thesis is also described.

4.2 Scientific objectives

This work aims to identify and implement effective methods and approaches for distortion compensation when grinding slender workpieces with a V-groove. In this context, targeted measures for the induction of residual stresses are investigated, which can minimize or completely compensate for the resulting distortion after a profile grinding process.

To achieve these goals, the focus is initially set on a feasibility analysis and a successive enhancement of the process know-how concerning the relevant strain mechanisms. Simulation approaches for modeling the compensation measures based on laser processing and deep rolling are subsequently developed, and their applicability is verified. An additional focus is placed on analyzing and modeling the interactions and distortion effects caused by thermal, mechanical, and thermometallurgical influences on the workpiece surface.

Experimental investigations validate the effectiveness of the derived compensation strategies and improve the quality of the simulation results. The process-relevant influencing variables are identified and weighted to enable a computer-aided design of the compensation strategies. A goal-oriented enhancement of existing simulation approaches from the literature is used to represent the complex thermometallurgical and thermomechanical interactions of post-treatment processes for distortion compensation and to achieve a continuous increase in the quality of the numerical result concerning the occurrence of dimensional workpiece changes.

A slender workpiece with a V-profile (replacement of a linear guide rail) made of quenched and tempered AISI 4140 steel is used as the exemplary geometry. The boundary zone of this

sample is strongly influenced thermally and mechanically so that the effects of the investigated approaches for distortion compensation can be studied in detail. The computer-aided design of those strategies allows for the analysis of the residual stress and deformation phenomena and the process-specific interactions to be controlled. Existing limitations in post-treatment processes and, hence, missing representation of straightening processes after profile grinding can thus be eliminated.

The following list of four sub-objectives (SO) characterizes the necessary actions for this thesis:

SO 1 Numerical modeling of the profile grinding process

First, the initial state of the AISI 4140 workpieces with a V-groove must be assessed experimentally. It must be implemented in an FE simulation to enable numerical modeling along the manufacturing process chain. Afterwards, experimental investigations should provide an adaptation of the model concerning the distortion prediction based on the given mechanical and thermal boundary conditions during the grinding process. The occurring thermomechanical effects on the workpiece distortions must be studied with varying process parameters.

SO 2 Laser processing as a thermal distortion compensation method

Experimental studies of laser processing for the systematic induction of tensile stresses are required to design a thermal distortion compensation strategy after profile grinding of the workpiece with a V-groove. These studies will be used to set up and calibrate an appropriate numerical model of this process concerning distortion control.

SO 3 Deep rolling as a mechanical distortion compensation method

A numerical design of the deep rolling process to control workpiece distortions must be carried out corresponding to SO 2. Experimental investigations will define the boundary conditions of this mechanical process and calibrate the submodel for the combined distortion compensation strategy to be realized in SO 4 for profile grinding of workpieces with a V-groove.

SO 4 Design of the combined thermal and mechanical distortion compensation strategies

It is consequently necessary to combine the analyzed approaches from laser processing and deep rolling for the compensation of workpiece distortions occurring from profile grinding so that the occurring interactions can be analyzed and their specific capacities can be used sequentially. Finally, the coupled models and

simulations must be adapted, and optimal strategies must be identified using the numerical approach.

Section 4.3 presents the research approach that results from the aforementioned sub-objectives.

4.3 Methodological approach

According to their thematic focus in alignment with the research objectives stated in Section 4.2, the publications developed during the author's research activities are categorized here in Section 4.3. While Section 5.2 details the main findings, Figure 20 summarizes the classification and incorporation of the articles into the methodology. It also presents a schematic illustration of the connection between the SOs.

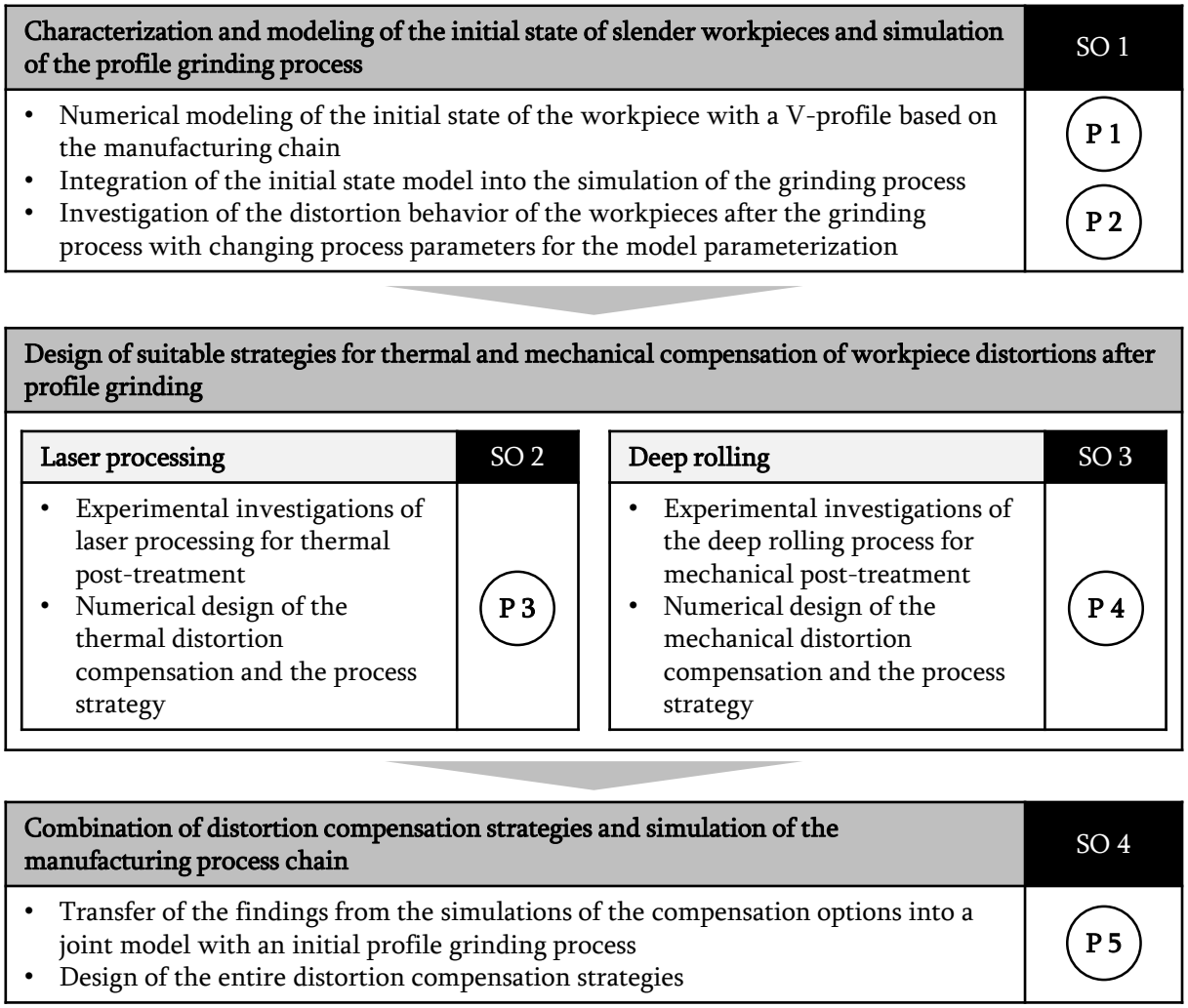

Figure 20: The methodological approach of publications P 1 to P 5, the conceptual organization, and the thematic focus in alignment with the stated sub-objectives (SOs) listed in Section 4.2

Characterization and modeling of the initial state of slender workpieces and simulation of the profile grinding process

The first SO of the methodology includes the characterization and modeling of the initial state of workpieces, the simulation of the grinding process, and the validation of the simulation results through experiments with different grinding parameters. Achievement of SO 1 enables the evaluation of the distortion of 250-mm-long workpieces due to the induced tensile stresses caused by the heat generated in the contact zone during a profile grinding process in a V-groove, longitudinally embedded at the top surface.

For this evaluation, after peripheral milling, all workpieces were first subjected to heat pretreatment to create a stress-free condition. This specification provides a reference value and allows for an accurate prediction of the deformation since the parts have gone through the entire manufacturing process chain, including soft machining and stress relieving, but do not yet have any additional distortions due to the actual grinding process. Therefore, the shape deviations were subsequently measured by a coordinate measuring machine. The material properties and geometric data of the relevant workpieces were also collected.

Using the information obtained from the characterization and pretreatment steps, as well as the clamping properties presented in Publication 1, a developed model can be used to predict workpiece distortions based on temperature and stress–strain history. The numerical boundary conditions were changed according to the variations of the grinding process parameters, namely the depth of cut and feed rate. The simulation was performed for each set of parameter values to predict the resulting distortion.

The simulation predictions are validated through experimental results obtained by examining the processed workpieces. The sample was fixed using a magnetic clamping plate on the bottom for the grinding process under investigation. Since this substantially prevents deformation of the workpiece, the distortion to be compensated for occurs immediately after unclamping. In these experiments, the geometry had to be subjected to the same simulated grinding process, and the deformation of the parts had to be measured. However, the process parameters should be selected such that significant and comparable distortions are caused. The experiments were performed with grinding parameters, commonly used for manufacturing steel components, to confirm the validity of the simulation results. The aim was to achieve an alteration in the related material removal rate from low (mechanically dominating effect) to high values (thermally dominating effect). The depth of cut, the feed rate, and the cutting speed were varied on three levels to cover non-linear effects. For statistical validation, three measurements of the 250-mm-long workpieces were taken for each test point. This procedure increases the prediction quality of the models used concerning component distortion. Furthermore, the data determined experimentally with respect to

SO 2 and SO 3 for the compensation strategies were integrated into the simulations in parallel to model the complete manufacturing process chain later on, starting with the condition after heat treatment up to thermal and mechanical post-treatment.

The results of the simulations and experiments were analyzed and interpreted to build knowledge about the relationship between the grinding process parameters and the resulting deformation. Therefore, the simulation results had to be compared to the experimental results, and deviations had to be investigated. The analysis also includes identifying trends or patterns in the data that may provide insights into the mechanisms behind the deformation.

Based on the simulation and experimental results, a conclusion is drawn regarding the effects of grinding process parameters on the resulting distortion, and recommendations for possible compensation approaches are derived in Publication 2.

Design of suitable strategies for thermal and mechanical compensation of workpiece distortions after profile grinding

The effect of the mechanical and thermal machining processes for distortion compensation is first determined through simulation. The result is validated via an experimental implementation by considering, in parallel, the feasibility of minimization strategies by thermal (SO 2: Local heat input) and mechanical (SO 3: Deep rolling) processes in post-treatment after profile grinding. The distortion is again evaluated through the coordinate measuring technique.

Laser processing

As already explained in the chapter on the state of the art, straightening processes with thermal loads on a workpiece are suitable for counteracting unwanted sample deformation due to grinding by laser processing. To implement the geometry with a V-groove considered here, the profiled guide rail was clamped upside down and subjected to an NC-guided heat source on the side facing away from the grinding process. It should be noted that tensile stresses are induced due to thermally induced plastic deformation. The induced distortion potential depends on the intensity (laser power) and effective duration (laser feed rate) of the laser. The thermal post-treatment design must first be based on the defined FE model. On the one hand, this helps to avoid a high experimental effort; on the other hand, it allows for an investigation at which locations of the component residual stress profiles have to be imposed. It can also be used to determine the required intensity and, respectively, the numerical control (NC) trajectories to minimize the distortion and to prevent a possible overcompensation. The post-treatment was implemented in the test environment by building on the findings from the simulation, which include identified variables and parameters as

boundary conditions for determining the thermal process effect due to laser reworking. The experimentally determined data regarding the residual stress profiles due to laser treatment and the resulting component distortion must be used to validate the simulation. This ensures that the model reflects the actual process as accurately as possible and can be used for SO 4. The description of the model is presented in Publication 3.

Deep rolling

In addition to the previously described investigations regarding straightening processes with thermal effects, the possibility of mechanical post-treatment by deep rolling of workpieces for distortion compensation is examined. The resulting compressive stresses were induced on both workpiece surfaces next to the V-groove while the bottom side of the specimen was clamped.

Since the deep rolling process induces compressive stresses and the amount of the respective stress depends on the treated area and the rolling track numbers, the design of the compensation strategy is based on existing models from the literature. To predict the caused workpiece distortions and to investigate the suitability of deep rolling as a correction method, the numerical model of the workpiece had to be extended by the corresponding boundary conditions of the process, i.e., the transient mechanical load and the clamping.

The experimentally determined data regarding the workpiece distortions due to deep rolling are used to validate the simulation so that an adjustment or calibration of the thermometallurgical and thermomechanical material data is possible. The combined numerical and experimental approach of deep rolling as a distortion compensation strategy is explained in Publication 4.

Combination of distortion compensation strategies and simulation of the manufacturing process chain

Finally, to pursue SO 4, the numerical simulation extensions of the mechanical and thermal post-treatment processes developed in SO 2 and SO 3 are integrated into an overall model to allow for a description of the entire process chain, from the initial state to the application of the compensation methods. Thus, a successful distortion compensation is designed. After identification of a suitable process strategy and prediction of a reasonable parameter space of the process variables using the FE simulation, the evaluation of this strategy for the application follows. The distortion of the test workpieces with a V-profile is compensated for as accurately as it is possible while avoiding a negative influence on the material properties. Experimentally obtained results were used to validate, calibrate, and adapt the FE simulation. The selected compensation strategies were numerically implemented after an optimal process plan and the best process parameters were identified based on a comparison of the

effects of the individual compensation steps and their interactions. The model also predicts how mechanical and thermal processes can be combined to counteract workpiece distortion caused by profile grinding. The strategies derived are discussed in Publication 5.

4.4 Embedded publications

The five publications, P 1 to P 5, are shown as an overview in Figure 21, along with the authors, titles, and media. Appendix B contains a list of the papers that are integrated into this dissertation.

The German Research Foundation financed the research titled “Distortion Control during Grinding by Computer-aided Design of Distortion Compensation Strategies.” The Leibniz Institute for Material-Oriented Technologies (IWT), Bremen — collaborator on the previous research effort — provided the experimental results unless otherwise noted. The IWT test environment used for this purpose, including the associated measurement and analysis technology, was described and published in the project-specific documents.

P 1	C. Schieber ● M. Hettig ● M. F. Zaeh ● C. Heinzel	*3D modeling and simulation of thermal effects during profile grinding*	*Production Engineering (2020)*
P 2 SO 1	C. Schieber ● M. Hettig ● M. F. Zaeh ● C. Heinzel	*Evaluation of approaches to compensate the thermo-mechanical distortion effects during profile grinding*	*Proceedia CIRP: 18th CIRP Conference on Modeling of Machining Operations (2021)*
P 3 SO 2	C. Schieber ● M. Hettig ● V. Müller ● M. F. Zaeh ● C. Heinzel	*Modeling of laser processing as a distortion compensation strategy for profile grinding*	*Production Engineering (2022)*
P 4 SO 3	C. Schieber ● M. Hettig ● M. F. Zaeh ● C. Heinzel	*Modeling of deep rolling as a distortion compensation strategy during profile grinding*	*Key Engineering Materials (2022)*
P 5 SO 4	C. Schieber ● M. Hettig ● M. F. Zaeh ● C. Heinzel	*Combination of thermal and mechanical strategies to compensate for distortion effects during profile grinding*	*Metals (2022)*

Figure 21: Overview of the publications related to the four identified SOs

5 Research Findings

5.1 Chapter overview

Following the methodological approach described in Chapter 4, Chapter 5 now presents the individual publications that contain the research findings within the scope of this dissertation. The publications are summarized below with a brief recapitulation, presenting the knowledge gained and the main conclusions. Likewise, the author's contributions are defined.

5.2 Recapitulation of the embedded publications

5.2.1 Publication 1—"3D modeling and simulation of thermal effects during profile grinding"

The first publication serves as the foundation for subsequent numerical modeling of profile grinding for slender AISI 4140 workpieces with V-grooves to predict residual stress-induced distortions. Before grinding, the initial condition of the workpieces was characterized by analyzing the geometrical dimensions and material properties in the boundary zone over the defined process chain (SCHIEBER ET AL. 2020).

In the initial phase, the experimental design of the grinding process aimed to generate targeted workpiece distortions, requiring suitable material conditions and workpiece geometries. For better comparability, the specimens were peripherally milled (23 mm × 38 mm × 250 mm ($h_w \times w_w \times l_w$)), and then machined with a V-groove (8.67 mm × 19 mm ($h_v \times w_v$)) along the entire length, using a stock removal of 0.6 mm (Figure 22). To ensure a uniform contact area during distortion-generating grinding experiments, the same grinding wheel (Baystate 9A60-H16-VCF2 profile grinding wheel with a diameter of 400 mm and a grit size of 60 (mesh openings per linear inch)) was used for distortion analysis in Publication 2. After semi-finished production, stress relief and heat treatment (quenched and tempered (QT) at 200 °C, 55 HRC) were performed to attain the hardened microstructure condition for the experiments. The initial state was then characterized through numerical modeling, taking into account the manufacturing history and relevant material parameters of AISI 4140 steel. Initial grinding tests were conducted, varying the depth of cut and grinding wheel feed rate, with power measurements and tangential (F_t) and normal (F_n) forces

monitored using a dynamometer. These measurements were utilized to analyze the heat flux density distribution in the contact zone, used for defining boundary conditions in the simulation (Publication 2).

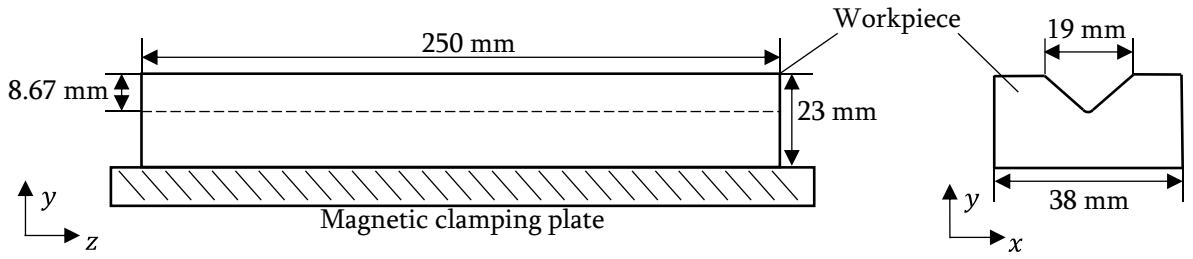

Figure 22: Drawing of the workpiece with a V-groove on a magnetic clamping plate for profile grinding (based on SCHIEBER ET AL. (2023))

The result of this publication was the preliminary design of the numerical distortion prediction model during profile grinding of slender workpieces with a V-groove. This design was realized by successfully characterizing the initial condition and analyzing (a) the geometric contact zones between the workpiece and the tool and (b) the heat flux density distribution during the machining process, depending on the grinding wheel feed rates and the depths of cut.

Main findings

F 1 Adequate geometrical dimensions and a process chain for the semi-finished product (acting as a guide rail substitute) were selected to achieve comparable experimental distortion data after the machining process in Publication 2, considering the high thermal loads in the V-groove and the microstructure transformation effects during profile grinding.

F 2 Geometrical contact conditions during the grinding process within the V-groove were analytically calculated, providing a starting point for subsequent numerical modeling.

F 3 The experimental determination of the tangential contact load in the contact zone for different depths of cut and feed rates of the grinding wheel yielded properties of the heat flux density distribution.

Contributions of the authors

This publication was developed and written under the leadership of Christian Schieber. He pursued the analytical interpretation of the heat flux density distribution depending on the

process parameters. Matthias Hettig planned and coordinated the acquisition of experimental data at the Leibniz Institute for Material-Oriented Technologies (IWT), which were evaluated and interpreted by Christian Schieber to define boundary conditions in the simulation of grinding for distortion prediction. The manuscript was edited by Matthias Hettig, Michael F. Zaeh, and Carsten Heinzel. All authors discussed the results derived from the evaluations.

5.2.2 Publication 2—"Evaluation of approaches to compensate the thermo-mechanical distortion effects during profile grinding"

Building on Publication 1, this study investigated the effects of distortion in profile grinding by varying the process parameters. The machining and the workpiece distortion were simulated, considering the model representation of the initial condition (SCHIEBER ET AL. 2021).

First, the material parameters identified in Publication 1 were transferred to the FE model. A critical transient boundary condition in the time-dependent process simulation was the heat flux density distribution which was analytically calculated from force measurements for different parameter combinations of grinding wheel feed rate (v_{ft} = 1,500–6,000 mm/min) and depth of cut (a_e = 0.2–0.8 mm), with a constant cutting speed v_c of 35 m/s (Figure 23).

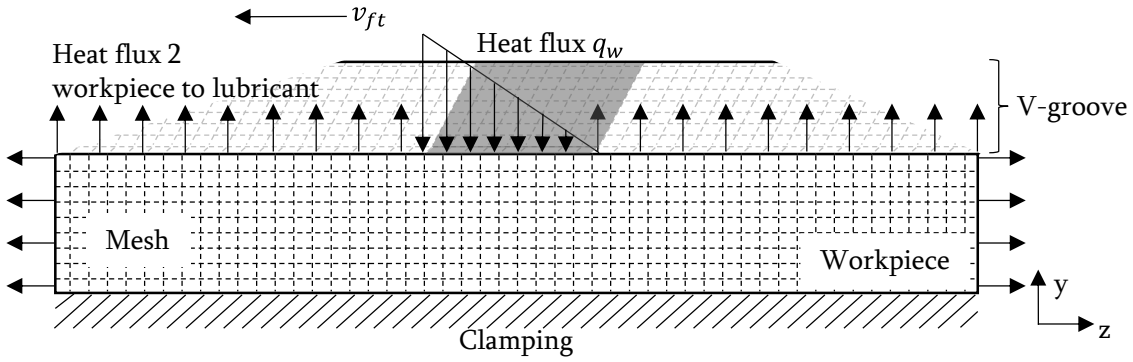

Figure 23: Finite element model of the profile grinding process with defined boundary conditions (based on (SCHIEBER ET AL. 2022c))

For each combination, three experiments were conducted to ensure reliable average values in the distortion determination using a coordinate measuring machine. To maintain consistency, the tool was dressed with a diamond dressing roll (dressing parameters: radial dressing feed a_{ed} = 30 µm, speed ratio q_d = 0.7) before each test. The choice of the process parameters varied the thermomechanical load spectrum in the contact zone, with cooling and lubrication provided by an oil (Houghton, Cut-Max 906-10) supplied through a central nozzle at a flow rate of 50 l/min.

The peak-to-valley value ΔPV, representing the deformation difference from the workpiece center point at the bottom before and after machining, was used to calibrate the numerical FE model. This enabled a detailed evaluation and analysis of the thermomechanical effects that occurred.

After calibration, the experimentally determined ΔPV values aligned well with the simulated results for different grinding wheel feed rates and depths of cut. While increasing v_{ft} caused only slight deformation, a higher a_e significantly amplified it due to the increased heat input in the contact zone. The distortion model resulting from this publication provides the basis and initial strategies for using laser-based treatment and hard rolling as distortion compensation strategies after profile grinding.

Main findings

F 1 The analytically determined heat flux density distribution and the initial condition of the workpiece were integrated into the grinding process simulation.

F 2 The test results were used to calibrate and validate the thermal and mechanical boundary conditions of the profile grinding simulation model, optimizing the prediction accuracy of the resulting workpiece distortions.

F 3 Increases in grinding wheel feed rate and depth of cut during profile grinding in the V-groove resulted in significantly larger peak-to-valley distortions ΔPV of the workpiece due to increased heat input.

F 4 The thermomechanically coupled model was adapted to incorporate the laser-based treatment and deep rolling as distortion compensation strategies.

Contributions of the authors

Christian Schieber defined the numerical requirements and the boundary conditions for the profile grinding simulation model. Together with Matthias Hettig, he was responsible for the experimental designs of the different processes and their execution. The main author analyzed the experimental grinding forces and workpiece distortions data provided by Matthias Hettig. The manuscript was written by Christian Schieber and edited by Matthias Hettig, Michael F. Zaeh, and Carsten Heinzel. They all discussed the results. Christian Schieber presented the findings at the 18th CIRP Conference on Modelling of Machining Operations (CIRP CMMO) in Ljubljana, Slovenia, over a virtual platform.

5.2.3 Publication 3—"Modeling of laser processing as a distortion compensation strategy for profile grinding"

In the third publication, the possibility of laser processing on long slender steel workpieces to control distortion was investigated (SCHIEBER ET AL. 2023). The goal was to systematically induce tensile stresses on the opposing side of the V-groove using double passes to counteract residual stresses after profile grinding and compensate for workpiece distortions. A simulation model was created based on experimental boundary conditions, and measured distortion values were used to calibrate the FE simulation. Metallographic investigations, such as hardness measurements near the surface, were also conducted to analyze material phase changes. The objective was to develop numerical strategies for controlled distortion generation and to gain a comprehensive understanding of heat treatment through laser processing as a process strategy for deformation compensation after profile grinding.

The thermal process was successfully implemented using a defocused, annular laser spot (TruDisk 4001 from Trumpf, Ditzingen, Germany) with a diameter d_l of 15 mm and a wavelength of emitted light λ of 1,030 nm. The laser was applied to the bottom side of the workpiece with two total passes, $N_l = 2$, to induce uniformly distributed tensile stresses. The laser parameters, such as feed rate v_l (ranging from 0.6 to 0.9 m/min) and laser power P_l (ranging from 2,000 to 3,100 W), significantly influenced the distortion values of the workpiece (Figure 24). Increasing P_l and decreasing v_l resulted in higher local heat input and, consequently, more significant deformations. The laser experiments were repeated twice for each parameter combination to average the distortions from three workpieces. Microstructural transformation processes on the surfaces due to the high temperatures were confirmed through hardness measurements and micrographic examinations. Compared to the maximum deformations obtained after profile grinding, laser processing generated a much higher opposing distortion of the workpiece.

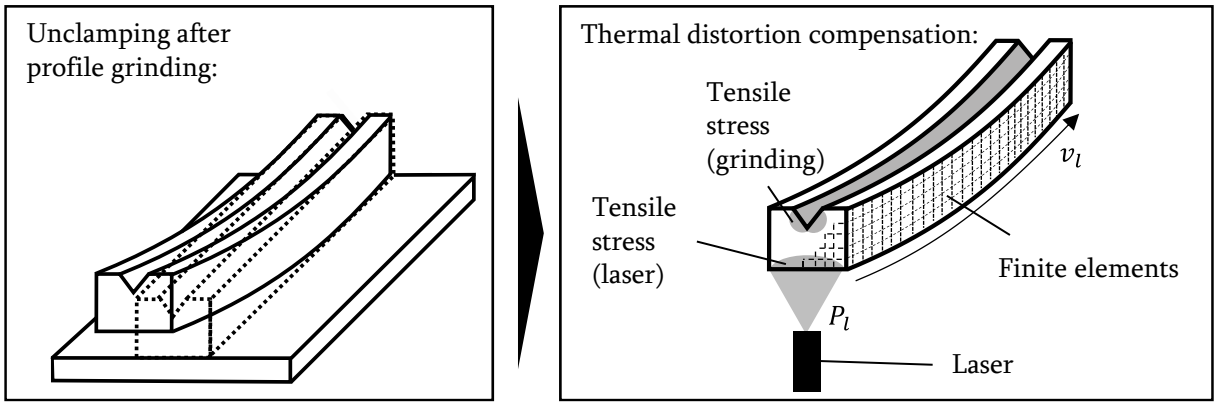

Figure 24: The distorted workpiece after profile grinding due to tensile stress in the V-groove with the compensation strategy utilizing laser processing (based on SCHIEBER ET AL. (2023))

The results partially contributed to the overall compensation strategy presented in the final publication, which involved defining relevant boundary conditions, calibrating simulations experimentally, and evaluating the suitability of distortion compensation processes for slender components with a ground profile.

Main findings

F 1 Controlled laser processing can effectively control workpiece distortions caused by a profile grinding process. Suitable parameter ranges of laser feed rate and laser power were identified for this purpose.

F 2 A finite element model of the thermal process was established with relevant boundary conditions and validated with experiments. Key aspects included defining the beam geometry and temperature-dependent material parameters.

F 3 Hardness measurements and micrograph examinations provided valuable insights into microstructural transformation processes in the workpiece due to laser processing, enhancing the overall understanding.

F 4 To comprehensively analyze thermomechanical effects after the grinding process and to define compensation steps in the workpiece, it is recommended to create a valid overall prediction model combining all material treatments.

Contributions of the authors

Christian Schieber, the author of this thesis, wrote the manuscript. He developed the idea for the double-track thermal treatment of the workpiece with a defocused, annular laser source and was responsible for evaluating the measurement data and the numerical model. Valentin Müller assisted with his master's thesis project in the execution of the experiments, which were conducted at the *iwb*. The manuscript was edited by Michael F. Zaeh, Carsten Heinzel, and Matthias Hettig, who also measured the workpiece distortions after the experiments. All authors discussed the data.

5.2.4 Publication 4—"Modeling of deep rolling as a distortion compensation strategy during profile grinding"

In addition to the laser machining process mentioned above for distortion reduction in profile grinding, Publication 4 addressed deep rolling (SCHIEBER ET AL. 2022b). The study

focused on evaluating the influences of the compressive stresses induced in the workpiece through deep rolling and their suitability for offsetting distortions caused by grinding.

The deep rolling tool (Ecoroll HG 13 with a sphere diameter of 13 mm) was employed to process the top surfaces of the workpiece adjacent to the V-groove. The ball was pressed vertically onto the surface and rolled along the length of the specimen at a rolling speed v_{dr} of 1,000 mm/min, causing plastic deformation of the material underneath. The expansion due to volume constancy resulted in a relief of in-plane tensile stresses, producing distortions opposite to those caused by tensile stresses in the V-groove after grinding. A numerical model was developed, starting from the initial state of the workpiece, to predict these effects. The simulation was validated using experimental measurements of the distortions, and thermometallurgical and thermomechanical material data were calibrated accordingly. Distortions were obtained based on the number of rolling tracks N_{dr} (ranging from 1 to 50) with a lateral feed f_{dr} (ranging from 0 to 1.0 mm) on the two lateral surfaces using a 4,200 N deep rolling force F_{dr} of the tool. The transient load distribution by the rolling tool on the surfaces was successfully modeled by defining appropriate numerical boundary conditions (Figure 25). The simulation and experimental results indicated that the achievable opposing distortions do not significantly increase above a certain number of rolling tracks N_{dr} and are not sufficient to compensate for high distortions caused by profile grinding. For extended calibration of the FE model, a reference deformation of a ground sample with maximum range from previous investigations in Publication 2 was selected for a combined process of grinding and subsequent deep rolling.

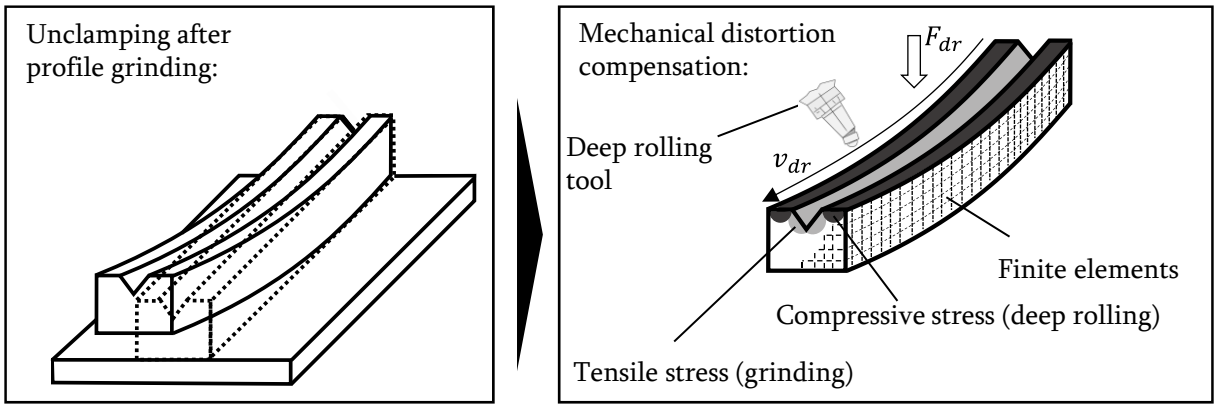

Figure 25: The distorted workpiece after profile grinding due to tensile stress in the V-groove with the compensation strategy utilizing a deep rolling process (based on SCHIEBER ET AL. (2022b))

This publication aimed to extend the know-how of deep rolling of slender components and to analyze its suitability as a distortion compensation strategy. The established submodel was subsequently combined with the laser machining simulation as part of Publication 5.

Main findings

F 1 Utilizing deep rolling on the top surfaces next to the V-groove, affected by tensile stresses, effectively counteracts deformations resulting from profile grinding.

F 2 The numerical modeling for distortion prediction was enabled through the modeling of the transient load distribution by the deep rolling tool and the consideration of appropriate boundary conditions from clamping as well as of material parameters.

F 3 An increase in the number of rolling tracks on both top surfaces of the workpiece adjacent to the V-groove, along with a simultaneous lateral feed, resulted in higher levels of distortion compared to those induced by grinding.

F 4 The systematic application of compressive stresses has its limitations, and the maximum achievable distortion increases only marginally above a certain number of tracks.

Contributions of the authors

Christian Schieber proposed developing a numerical model of the deep rolling process. This created the possibility to predict distortion effects due to tensile stresses in workpieces. He calibrated the model and evaluated the results of the experimental data provided by Matthias Hettig at the IWT. Christian Schieber elaborated the publication, whereas Matthias Hettig, Michael F. Zaeh, and Carsten Heinzel reviewed and edited the manuscript. All authors commented on the results.

5.2.5 Publication 5—"Combination of thermal and mechanical strategies to compensate for distortion effects during profile grinding"

In the four previous publications, the numerical modeling of the three machining processes, namely profile grinding, laser processing, and deep rolling, was limited to separate procedures. Finally, in Publication 5 (SCHIEBER ET AL. 2022a), the two compensation strategies were combined, and the simulation of the manufacturing process chain was validated.

The manuscript describes the analysis and results of distortion compensation processes in profile grinding. Submodels for the three operations were defined and explained, including the thermomechanical structure model representing the laser and deep rolling process. The simulation considered all relevant influences of the environment, the compensation system, and the compliant heat-conducting periphery, including clamping and cooling lubricants,

where applicable. Optimal process parameters for distortion minimization of the workpiece were derived by identifying suitable process strategies with the selection of thermal and mechanical compensation options. The strategies were numerically implemented, predicting a reasonable parameter space of the process variables, followed by an optimization to achieve the minimum residual distortion within tolerance limits.

The main objective was to simulate the complete manufacturing process chain, allowing the design of mechanical and thermal post-treatment processes for successful distortion compensation. The simulation calibration demonstrated accurate predictions for each process step, leading to the creation of a valid overall deformation compensation model. The superposition of the effects from laser-based machining and deep rolling was also considered, resulting in two effective strategies.

Firstly, the correction of grinding distortions was achieved exclusively with laser machining due to the high opposing deformations that could be achieved. Secondly, in a different strategy, distortions after machining were initially minimized by deep rolling. However, deep rolling alone was not suitable as a final manufacturing process due to the high number of rolling tracks and the lower maximum distortions. Therefore, continuous laser power adjustment and the laser feed rate were used to provide the necessary final laser processing for finishing correction. Combining mechanical and thermal methods after the grinding process for distortion compensation adds strain to the workpiece at a lower magnitude, and it has the advantage of reducing or reliably preventing lasting damage to the workpieces that could result from the sole effect of a single strategy.

Main findings

F 1 A novel FEM-based method was presented for compensating workpiece distortions after profile grinding by utilizing laser machining and deep rolling. The approach enabled the numerical modeling of the machining process and the two downstream compensation options and their implementation in the process chain.

F 2 The developed 3D FEM model allowed for the thermomechanical analysis of form deviations caused by tensile and compressive stresses. Definitions of the relevant surface loads and the material properties of the workpiece were provided.

F 3 Two process strategies were identified from the coupled submodels for laser processing and deep rolling, and process parameters were optimized to reduce distortions after profile grinding, ensuring that the remaining workpiece distortions were within the defined tolerance limits.

Contributions of the authors

Christian Schieber defined the boundary conditions of the numerical modeling of the profile grinding and the compensation strategies. He also analyzed the experimental data, derived the compensation strategies, and elaborated on the manuscript. The experiments were performed at the laser processing facility operated by Christian Schieber at *iwb*. Matthias Hettig implemented the grinding, the deep rolling, and the distortion measurements at IWT. The final publication was edited by Matthias Hettig, Michael F. Zaeh, and Carsten Heinzel, all of whom commented on the results.

5.3 Discussion

This section discusses the scientific relevance of this dissertation, utilizing the five previously presented publications and the state of the art in distortion compensation. The research primarily focused on the numerical simulation of three processes: profile grinding, laser processing, and deep rolling, along with their experimental validation. The subdivision into individual publications was driven by the description and combination of these processes for distortion control.

The initial investigation involved surface grinding, for which FÖCKERER (2015) employed a numerical simulation approach using transient temperature fields and thermomechanical phenomena to predict residual stresses. Notably, the consideration of temperature- and phase-dependent material behavior was crucial for accurate predictions (FOECKERER ET AL. 2012). Building upon this foundation, the current work extended the model to the machining of slender AISI 4140 workpieces with V-grooves, enabling the prediction of distortions after grinding. Previous studies by THATER ET AL. (2015) and KRAUS (2020) explored the use of lasers to induce tensile stresses in metallic workpieces. Although they did not consider subsequent thermal processes combined with grinding, their research demonstrated the beneficial systematic application of lasers for inducing tensile stresses.

In contrast to laser processing, the literature has shown limited exploration of deep rolling for distortion control. HETTIG & MEYER (2020) investigated the change in compressive stresses in AISI 4140 workpieces due to different mechanical loads. In this dissertation, the distinct impacts of multiple contacts and load sequences on the top surfaces of the workpieces after deep rolling were explicitly leveraged to apply resulting deformations as distortion compensation after profile grinding. This process also offers the added advantage of increasing fatigue strength, thus mitigating the risk of cracking (KLOCKE & MADER 2005). The combination of these two compensation methods was considered in this work to

achieve effective workpiece distortion control. On one hand, precise heat is applied via a laser, and on the other hand, structural damage due to high thermal loads is reduced through additional deep rolling. The computer-aided design of distortion control allowed for the estimation of respective process parameters using a decoupling approach for structural, process, and material simulations (RADAJ 2002). Strategies for minimizing unavoidable workpiece deformations, driven by thermomechanical effects and the influences of processes or process chains, were developed by BAYERLEIN (2020) and BELITZKI (2018), combining optimization algorithms with numerical approaches.

The three processes and their combination were considered and elaborated on to realize the individual contents within this dissertation. Thereby, the following conceptual phases (CPs) were completed as part of this work to obtain the main results:

CP 1 In Publication 1, an analytical three-dimensional heat source model was developed for thermometallurgical finite element simulation of profile grinding. This model includes geometrical and material analyses, as well as the adjustment of process parameters during the machining of the profiled steel workpiece. It extends surface grinding models from the literature to simulate workpiece distortions.

CP 2 Publication 2 presents an FE-based model to predict the deformation of slender workpieces with V-grooves after a profile grinding process, considering different parameters. The simulation was calibrated using experimental data, yielding reasonable deformation accuracy, and thus serving as a valid overall model for predicting deformations.

CP 3 For Publication 3, laser-induced deformation of workpieces, like linear guide rails, was experimentally investigated to calibrate a numerical prediction model for distortions. A defocused annular laser source was employed for the thermal treatment of the workpieces, and the temperature behavior was linked to material parameters and mechanical behavior.

CP 4 Publication 4 explored the possibility of using deep rolling to systematically induce compressive stresses for distortion compensation after profile grinding of workpieces. Effects and predictions were investigated through the creation and qualification of an FE simulation.

CP 5 For Publication 5, a method was developed to compensate for workpiece distortion after profile grinding by combining laser processing and deep rolling. Then numerical submodels were linked, and experimental results were gathered for validation. Optimized process chains for distortion compensation after profile grinding were

identified, showing promising outcomes for improving accuracy and precision, with a high potential for a successful industrial implementation.

6 Conclusion, economic evaluation, and outlook

6.1 Conclusion

Within this research work, a simulation methodology for predicting workpiece deformation caused by initial and process-induced residual stresses was successfully developed and validated. Residual stress-induced distortion in machined workpieces has been a significant challenge in the industry, leading to iterative reduction methods or manual straightening, lacking computer-aided control. This dissertation addressed this issue by creating a simulation methodology based on the Finite Element Method (FEM) to predict and minimize shape deviations in machining processes. By modeling compensation processes such as laser machining and deep rolling and coupling the models with grinding simulations, potential methods for correcting workpiece deformations were explored. The main goal was to enable the prediction of distortions and to design effective thermal and mechanical compensation strategies.

The first sub-objective focused on creating and fitting a numerical model for an AISI 4140 V-groove workpiece, representing a linear guide rail, based on its manufacturing history. The simulation was calibrated using experimental data to improve distortion prediction after the grinding process for various feed rates and depths of cut. Thermomechanical effects on the workpiece deformations were also investigated by varying the process parameters.

As Sub-objective 2, laser processing was investigated as a compensation method for thermal distortions after grinding. A numerical model was designed and calibrated to induce tensile stresses in the workpiece by adjusting laser feed rate and power. This allowed for precise positioning of the transient heat flux on the workpiece surface, compensating for thermal deformations after grinding.

Similarly, Sub-objective 3 meant to explore deep rolling as a mechanical compensation method. After the grinding process, deep rolling induced compressive stresses on the workpiece surfaces adjacent to the V-groove. The numerical simulation was extended to incorporate deep rolling as a distortion control method.

Finally, as Sub-objective 4, both thermal and mechanical compensation methods were combined in two strategies, and their industrial applicability was evaluated.

Overall, this study provides valuable insights for industrial applications by offering consistent methods for selecting and designing efficient thermal and mechanical processes to compensate for distortions after profile grinding. The results also lead to a significant reduction of experimental efforts. However, further research is necessary to validate the generalizability of these findings and to optimize the compensation methods. Nevertheless, this study represents a significant advancement in understanding grinding processes and potential approaches for addressing deformations in slender workpieces.

6.2 Economic evaluation

Deformations of linear guide rails occuring during production processes can significantly affect the performance and durability of the final product. Therefore, manufacturers must produce high-quality workpieces that are free of distortions. Cost-intensive reworking is typically necessary after the machining operation, and the methods developed according to Chapters 4 and 5 provide economic potential with reduced experimental work. The publications demonstrated how a computer-aided distortion compensation parameter can be determined for laser processing and deep rolling of a workpiece with a V-groove with complex thermometallurgical effects after grinding. The numerical results showed satisfactory qualitative and quantitative agreement with the experiments. The differences between the measured and the numerically determined peak-to-valley values were within the tolerance of industrial standards. This led to the conclusion that simulative approaches do not have to be limited to gaining knowledge or validating experimental investigations. The established models can be extended by optimization algorithms or with neural networks relying on real-time process data so that strategies for distortion compensation utilizing laser processing and deep rolling could be derived, and post-processing parameters could be determined. This option is suitable for industrial production to save personnel and monetary resources, particularly for complex component geometries, such as linear guide rails with a V-groove. Long-term damage to a workpiece due to high thermal loads during laser processing can be counteracted by the combined use with deep rolling after the grinding process. In this way, the shape deviations from thermally and mechanically induced residual stresses near the surfaces can be reduced.

The accuracy of the predicted workpiece distortions after profile grinding and the necessary straightening parameters depend on various factors. First, the quality of the data provided is of decisive importance. Here, the material parameters are particularly relevant, as they form the input for the simulation. An inaccurate determination of these characteristic values can lead to significant deviations in predicting component distortions. Calibration of heat sources and load profiles is also necessary. These system components must be

accurately determined, as they form the basis of the entire process; inaccurate calibration can lead to errors and inaccurate prediction of the component distortion. In addition, the overall simulation must consist of several partially simplified submodels that build on one another to enable the prediction of part deformations. They must be integrated to avoid errors. High accuracy in predicting component distortions can only be guaranteed in this way.

An economic evaluation based on the abovementioned experience is helpful to decide whether a computer-aided strategy for distortion compensation is cost-effective compared with a conventional experimental approach to minimization. Such a benchmarking exercise enables one to weigh the costs and benefits of the two approaches and thus make an informed decision. Several assumptions should be made, for example regarding the availability of the technical equipment and the types and amounts of incurred costs. These assumptions may vary depending on the application scenario and must be carefully considered to ensure a reasonable comparison. Considering the long-term effects of the two approaches is also essential. Moreover, factors such as personnel skill requirements associated with each approach should be addressed.

The conventional approach to minimizing distortion of slender workpieces after grinding is often based on established thermal processes such as flame straightening. In addition to the extra raw material when using gas torches with, for example, an oxy-acetylene gas mixture, these procedures also require an experienced welding specialist. To minimize deformation, the operator can selectively apply the straightening flame to the proper workpiece positions. This method is relatively inexpensive but time-consuming and may not provide consistent results.

The use of automated straightening processes such as laser processing utilizing a robot and a fixed rolling tool in a CNC machining center can help the manufacturer to reduce costs in the long term due to a computer-aided design. The new acquisition of a computational cluster for distortion prediction and identification of the compensation parameters is not necessary for many large companies, as they usually already have departments with the related equipment for FE simulations. In addition, license fees must be incurred to use the necessary software for the implementation, and an expert FEM engineer is required to implement the method correctly. The automated approach is more efficient and can produce more consistent results than the conventional approach, but it requires the purchase and maintenance of a robot, a laser system, and a deep rolling tool.

For both cases, the costs of a CNC machining center, a coordinate measuring machine, and a technician to clamp and control the machines are neglected, as are application-related maintenance and operating costs. The machines and the technician for operation are

necessary for both cases due to the preliminary grinding process and can be ignored in the calculation.

This study compares the costs of using a laser mounted on a robot and a fixed rolling tool with manual flame straightening to minimize distortions in linear guide rails. Regarding the availability of the technical equipment and the associated cost types, the following assumptions according to Table 1 are made.

Table 1: List of exemplary cost types and costs generated by computer-aided distortion control or manual straightening[1]

Cost description	Symbol	Computer-aided distortion control	Manual straightening	Unit
Material (flame straightening)	M_G	–	30	€/h
Welding specialist	P_{WS}	–	60	€/h
FEM engineer	P_{FE}	120	–	€/h
FEM software	C_{FE}	8,000	–	€
Computer cluster	C_C	10,000	–	€
Laser equipment	C_L	90,000	–	€
Deep rolling tool	C_D	15,000	–	€
Laser equipment maintenance	M_L	10,000	–	€/a

For the conventional approach, a welding torch has material costs M_G of 30 €/h and total costs of €40,000 per year for a welding specialist with an hourly wage P_{WS} of 60 €/h. The number t_M of working hours per year is 1,600 h/a. The total annual costs A_M for the conventional approach with an assumed 100 % utilization of a welding specialist are thus as follows:

$$A_M = (M_G + P_{WS}) \cdot t_M = (30\ €/h\ + 60\ €/h\ ) \cdot 1{,}600\ h/a = 144{,}000\ €/a. \tag{6-1}$$

[1] These estimations are based on data provided by experts from *iwb*, Ecoroll AG Werkzeugtechnik, Precitec KG, and TRUMPF Laser GmbH + Co. KG.

For the computer-aided distortion control, the one-time acquisition costs of the computer cluster C_C of €10,000, the FE simulation software C_{FE} of €8,000, the deep rolling tool C_D of €15,000, and the laser equipment C_L of €90,000 with annual maintenance costs M_L of €10,000 are initially assumed. For the total personnel costs of an FEM engineer with a 70-h time investment t_C for the design of the deformation compensation strategies at an hourly wage P_{FE} of 120 €/h, the result is €8,400. Based on these assumptions, the total costs A_C for the computer-aided distortion control for the first year are as follows:

$$\begin{aligned} A_C &= C_C + C_{FE} + C_D + C_L + M_L + (t_C \cdot P_{FE}) \\ &= 10{,}000\ € + 8{,}000\ € + 15{,}000\ € + 90{,}000\ € + 10{,}000\ € \\ &+ (70\ h \cdot 120\ €/h\ ) \\ &= 141{,}400\ €. \end{aligned} \tag{6-2}$$

In subsequent years, only €10,000 in maintenance costs for the laser equipment are to be added. Figure 26 compares the costs of manual straightening and computer-aided distortion control from Table 1 over six years. The straightening effort per working day is assumed to be either 100 %, 75 %, or 50 % of the welding operator's working time, depending on the workload and capacity. The graphs indicate that the computer-aided design would be worthwhile after 1.06 years if 100 % of the technician's workday is spent using the conventional method.

The high financial savings potential compared with the cost-intensive manual straightening processes, especially for high production volumes and over a more extended manufacturing period, justifies the use of the method despite the possible occurrence of random scatter. These results are significant to manufacturers, as they can aid in optimizing production procedures and reducing costs. However, further research is needed to fully understand the trade-offs between the different methods and to investigate other factors that may affect the costs and efficiency of manufacturing high-quality linear guide rails.

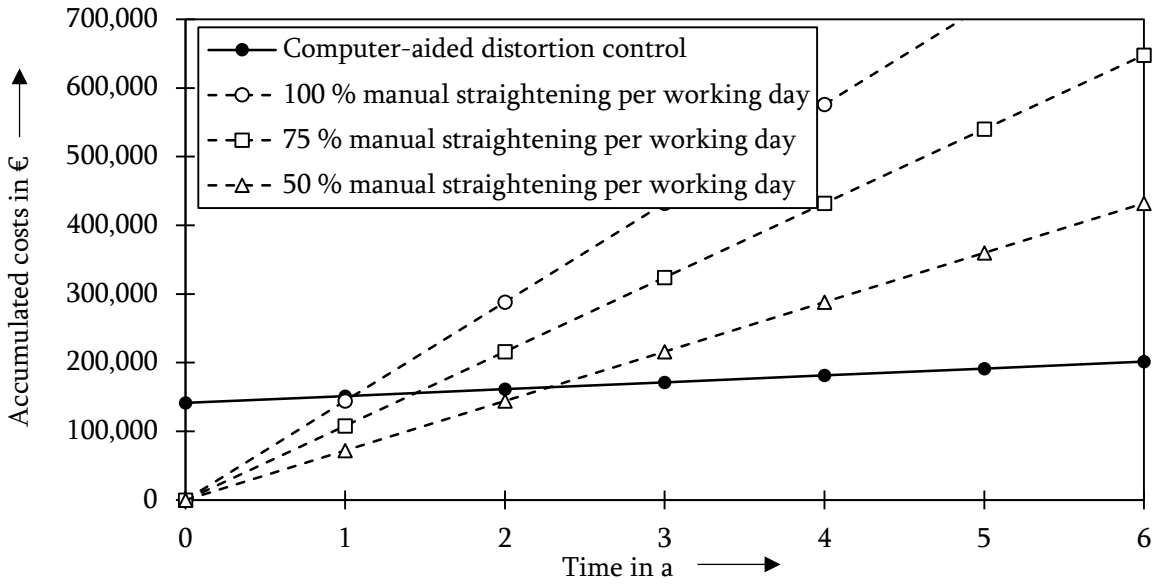

Figure 26: Cost development for manual straightening by a welding specialist as well as for computer-aided methods for distortion control of linear guide rails after profile grinding based on the assumptions listed in Table 1

6.3 Outlook

The control of distortion after grinding, as demonstrated in this dissertation with a simplified linear guide rail with a V-groove, can be extended to other workpieces through numerical approaches. Comprehensive models for predicting and correcting deformations in slender profiled workpieces after various grinding processes can be developed based on the findings of this study.

Further research is required to verify the generalizability of these findings to other materials and workpiece geometries. Additionally, optimizing laser machining and deep rolling to address asymmetric and rotational distortion and investigating the benefits of combining these processes with localized distortion due to random scattering in production would be valuable. Such an investigation would necessitate a detailed understanding of the mechanisms involved in thermal and mechanical processes and their interactions with the workpiece material.

Future investigations could also focus on developing effective compensation strategies for other manufacturing processes involving high thermal or mechanical stresses on component surfaces, leading to deformation. Processes such as milling and welding could potentially benefit from similar approaches explored in this work.

Overall, this study highlights the importance of understanding and eliminating the causes of slender workpiece deformation to enhance the quality and performance of final components. By developing comprehensive models and effective compensation strategies, the

efficiency and effectiveness of manufacturing processes can be significantly improved, resulting in high-quality components with minimal defects. To achieve such outcomes, further research, innovative methods, and new approaches are essential, and this study lays a solid foundation for future work.

It is expected that the knowledge gained in this dissertation can be readily applied to industrial production of linear guide rails. The findings on distortion compensation in grinding processes are expected to enhance manufacturing quality and to lead to economic savings for companies.

7 References

ABRÃO ET AL. 2014
Abrão, A. M.; Denkena, B.; Breidenstein, B.; Mörke, T.: Surface and subsurface alterations induced by deep rolling of hardened AISI 1060 steel. Production Engineering 8 (2014) 5, pp. 551-558.

ACHMUS ET AL. 1997
Achmus, C.; Betzold, J.; Wohlfahrt, H.: Messung von Festwalzeigenspannungsverteilungen an Bauteilen [engl.: Measurement of deep rolling stress distributions on components]. Materials Science and Engineering Technology 28 (1997) 4, pp. 153-157.

ACHMUS 1999
Achmus, C.: Messung und Berechnung des Randschichtzustands komplexer Bauteile nach dem Festwalzen [engl.: Measurement and calculation of the surface layer condition of complex components after deep rolling]. Diss. Technical University of Braunschweig. 1st Ed. Clausthal-Zellerfeld: Papierflieger 1999. ISBN: 978-3897202764.

AFAZOV ET AL. 2017
Afazov, S.; Denmark, W. A.; Lazaro Toralles, B.; Holloway, A.; Yaghi, A.: Distortion prediction and compensation in selective laser melting. Additive Manufacturing 17 (2017) 12, pp. 15-22.

ALTENBERGER 2002
Altenberger, I.: Alternative mechanical surface treatments: microstructures, residual stresses and fatigue behavior. International Conference on Shot Peening (ICSP) 8 (2002) 1, pp. 421-434.

ALTENBERGER 2005
Altenberger, I.: Deep rolling. The past, the present and the future. International Conference on Shot Peening (ICSP) 9 (2005) 1, pp. 144-155.

ANDERSON ET AL. 2011
Anderson, D.; Warkentin, A.; Bauer, R.: Experimental and numerical investigations of single abrasive-grain cutting. International Journal of Machine Tools and Manufacture 51 (2011) 12, pp. 898-910.

AVALLONE & BAUMEISTER 1996
Avallone, Eugene A.; Baumeister, Theodore (Editor): Mark's standard handbook for mechanical engineers. Revised by a staff of specialists. 10th Ed. New York: Mc Graw Hill 1996. ISBN: 0070049971.

BATHE 2002
Bathe, K.-J.: Finite-Elemente-Methoden. 2nd Ed. Berlin, Heidelberg: Springer 2002. ISBN: 978-3-54066-806-0.

BAYERLEIN ET AL. 2015
Bayerlein, F.; Zeller, C.; Zaeh, M. F.; Weirather, J.; Wunderer, M.; Seidel, C.: Improving cost effectiveness in additive manufacturing. Increasing dimensional accuracy in laser beam melting by means of a simulation-supported process chain. ANSYS Conference & 33. CADFEM Users' Meeting (2015).

BAYERLEIN ET AL. 2016
Bayerlein, F.; Zeller, C.; Wunderer, M.; Weirather, J.; Zaeh, M. F.; Schmid, M.; Schlick, G.; Hessert, R.;Hofmann, Michael; Uihlein, Thomas: Validation of modeling assumptions for the buildup simulation of laser beam melting on the basis of the residual stress distribution. In: Papadrakakis, M. (Editor): Proceedings of the VII European Congress on Computational Methods in Applied Sciences and Engineering (ECCOMAS Congress 2016), VII European Congress on Computational Methods in Applied Sciences and Engineering. Crete Island, Greece, 05.06.2016 - 10.06.2016. Athens: Institute of Structural Analysis and Antiseismic Research School of Civil Engineering National Technical University of Athens (NTUA) Greece 2016, pp. 469-479. ISBN: 978-618-82844-0-1.

BAYERLEIN ET AL. 2018
Bayerlein, F.; Bodensteiner, F.; Zeller, C.; Hofmann, M.; Zaeh, M. F.: Transient development of residual stresses in laser beam melting – A neutron diffraction study. Additive Manufacturing 24 (2018) 1, pp. 587-594.

BAYERLEIN 2020
Bayerlein, F.: Managing form deviation in laser beam melting by pre-deformation. Diss. Technical University of Munich. 2020.

BEER & JOHNSTON 2002
Beer, F. P.; Johnston, E. R.: Mechanics of materials. 3rd Ed. Singapore: McGraw 2002. ISBN: 0071210601.

BELITZKI 2018
Belitzki, A.: Rechnergestützte Minimierung des Verzugs laserstrahlgeschweißter Bauteile [engl.: Computer-aided minimization of the distortion of laser-welded components]. Diss. Technical University of Munich: Utz GmbH 2018. ISBN: 9783831673759.

BELITZKI & ZAEH 2016
Belitzki, A.; Zaeh, M. F.: Accuracy of calculated component distortions using the weld pool length to calibrate the heat source. Journal of Laser Applications 28 (2016) 2, p. 22424.

BENYOUNIS & OLABI 2008
Benyounis, K. Y.; Olabi, A. G.: Optimization of different welding processes using statistical and numerical approaches – A reference guide. Advances in Engineering Software 39 (2008) 6, pp. 483-496.

BERSTEIN 1979
Berstein, G.: Oberflächenfeinwalzen und Festwalzen. Grundlagen und Anwendung [engl.: Surface fine rolling and deep rolling. Basics and application]. Eßlingen. 1979.

BERSTEIN & FUCHSBAUER 1982
Berstein, G.; Fuchsbauer, B.: Festwalzen und Schwingfestigkeit [engl.: Deep rolling and fatigue strength]. Materials Science and Engineering Technology 13 (1982) 3, pp. 103-109.

BREIDENSTEIN 2011
Breidenstein, B.: Oberflächen und Randzonen hoch belasteter Bauteile [engl.: Surfaces and edge zones of highly stressed components]. Diss. University of Hannover. Garbsen: PZH Produktionstechn. Zentrum 2011. ISBN: 9783943104318.

BRINKSMEIER 1982
Brinksmeier, E.: Randzonenanalyse geschliffener Werkstücke [engl.: Boundary zone analysis of ground workpieces]. VDI-Verlag 1982. ISBN: 3181450022.

BRINKSMEIER ET AL. 1982
Brinksmeier, E.; Cammett, J. T.; König, W.; Leskovar, P.; Peters, J.; Tönshoff, H. K.: Residual stresses. Measurement and causes in machining processes. CIRP Annals 31 (1982) 2, pp. 491-510.

BRINKSMEIER 1990
Brinksmeier, E.: Eigenspannungsanalyse zur Prozessgestaltung beim Schleifen [engl.: Residual stress analysis for process design during grinding]. Journal of Heat Treatment and Materials 45 (1990) 6, pp. 348-355.

BRINKSMEIER 1991
Brinksmeier, E.: Prozess- und Werkstückqualität in der Feinbearbeitung [engl.: Process and workpiece quality in fine machining]. Düsseldorf: VDI-Verlag 1991. ISBN: 3181434027. (IFW-Produktionstechnik Nr. 234).

BRINKSMEIER ET AL. 2002
Brinksmeier, E.; Klocke, F.; Giwerzew, A.; Vučetić, D.: Spanbildungsmechanismen beim Schleifen mit niedrigen Schnittgeschwindigkeiten [engl.: Chip formation mechanisms when grinding at low cutting speeds]. Industrial Diamond Review 36 (2002) 4, pp. 346-356.

BRINKSMEIER ET AL. 2003
Brinksmeier, E.; Heinzel, C.; Boehm, C.; Wilke, T.: Simulation of the temperature distribution and metallurgical transformations in grinding by using the finite-element-method. Production Engineering Research and Development 10 (2003) 1, pp. 9-14.

BRINKSMEIER ET AL. 2005
Brinksmeier, E.; Minke, E.; Wilke, T.: Investigations on surface layer impact and grinding wheel performance for industrial grind-hardening applications. Production Engineering–Research and Development (Annals of WGP) 12 (2005) 1, pp. 35-40.

BRINKSMEIER ET AL. 2006
Brinksmeier, E.; Aurich, J. C.; Govekar, E.; Heinzel, C.; Hoffmeister, H.-W.; Klocke, F.; Peters, J.; Rentsch, R.;Stephenson, David J.; Uhlmann, Eckhart; Weinert, Klaus; Wittmann, Michael: Advances in modeling and simulation of grinding processes. CIRP Annals 55 (2006) 2, pp. 667-696.

BRINKSMEIER & BROCKHOFF 1994
Brinksmeier, E.; Brockhoff, T.: Randschicht-Wärmebehandlung durch Schleifen [engl.: Surface layer heat treatment by grinding]. Journal of Heat Treatment and Materials 49 (1994) 5, pp. 327-330.

BRINKSMEIER & BROCKHOFF 1996
Brinksmeier, E.; Brockhoff, T.: Utilization of grinding heat as a new heat treatment process. CIRP Annals 45 (1996) 1, pp. 283-286.

BRINKSMEIER & BROCKHOFF 1997
Brinksmeier, E.; Brockhoff, T.: Spanende Kurzzeitmetallurgie. Kurzzeitmetallurgische Effekte in der Hartbearbeitung [engl.: Machining short-time metallurgy. Short-term metallurgical effects in hard machining]. wt Werkstattstechnik online 87 (1997) 9/10, pp. 463-466.

BRINKSMEIER & GIWERZEW 2003
Brinksmeier, E.; Giwerzew, A.: Chip formation mechanisms in grinding at low speeds. CIRP Annals - Manufacturing Technology 52 (2003) 1, pp. 253-258.

BRINKSMEIER & HEINZEL 1998
Brinksmeier, E.; Heinzel, C.: Optimierter Kühlschmierstoffeinsatz beim Schleifen [engl.: Optimized use of cooling lubricant during grinding]. In: Tawakoli, T. (Editor): 2. Seminar Moderne Schleiftechnologie und Feinstbearbeitung [engl.: Modern grinding technology and superfinishing] 1998, 5.1-5.35.

BRINKSMEIER & MINKE 1993
Brinksmeier, E.; Minke, E.: High-performance surface grinding. The influence of coolant on the abrasive process. CIRP Annals 42 (1993) 1, pp. 367-370.

BROCKHOFF 1998
Brockhoff, T.: Schleifprozesse zur martensitischen Randschichthärtung von Stählen [engl.: Grinding processes for martensitic surface hardening of steels]. Diss. University of Bremen: Shaker 1998. ISBN: 3826560205.

BROCKHOFF & BRINKSMEIER 1999
Brockhoff, T.; Brinksmeier, E.: Grind-hardening: A comprehensive view. CIRP Annals 48 (1999) 1, pp. 255-260.

BROGGIATO ET AL. 2008
Broggiato, G. B.; Campana, F.; Cortese, L.: The chaboche nonlinear kinematic hardening model. Calibration methodology and validation. Meccanica 43 (2008) 2, pp. 115-124.

BROSZEIT 1984
Broszeit, E.: Grundlagen der Schwingfestigkeitssteigerung durch Fest- und Glattwalzen [engl.: Basics of increasing fatigue strength through deep rolling and roller burnishing]. Materials Science and Engineering Technology 15 (1984) 12, pp. 416-420.

BRUNA-ROSSO ET AL. 2021
Bruna-Rosso, C.; Mergheim, J.; Previtali, B.: Finite element modeling of residual stress and geometrical error formations in selective laser melting of metals. Proceedings of the Institution of Mechanical Engineers, Part C: Journal of Mechanical Engineering Science 235 (2021) 11, pp. 2022-2038.

BÜHLER & BUCHHOLTZ 1933
Bühler, H.; Buchholtz, H.: Die Wirkung von Eigenspannungen auf die Biegeschwingungsfestigkeit [engl.: The effect of residual stresses on bending fatigue strength]. Stahl und Eisen 53 (1933) 51, pp. 1330-1332.

CAMACHO & ORTIZ 1997
Camacho, G. T.; Ortiz, M.: Adaptive Lagrangian modelling of ballistic penetration of metallic targets. Computer Methods in Applied Mechanics and Engineering 142 (1997) 3-4, pp. 269-301.

CARSLAW & JAEGER 1959
Carslaw, H. S.; Jaeger, J. C.: Conduction of heat in solids. 2nd Ed. Oxford: Clarendon 1959. ISBN: 0198533039.

CHEN ET AL. 2000
Chen, X.; Rowe, W. B.; McCormack, D. F.: Analysis of the transitional temperature for tensile residual stress in grinding. Journal of Materials Processing Technology 107 (2000) 1-3, pp. 216-221.

CHICHKOV ET AL. 1996
Chichkov, B. N.; Momma, C.; Nolte, S.; Alvensleben, F.; Tünnermann, A.: Femtosecond, picosecond and nanosecond laser ablation of solids. Applied Physics A Materials Science & Processing 63 (1996) 2, pp. 109-115.

CHOI 1986
Choi, H.-Z.: Beitrag zur Ursachenanalyse der Randzonenbeeinflussung beim Schleifen [engl.: Contribution to the root cause analysis of boundary zone influence during grinding]. Diss. Universität Hannover. Düsseldorf: VDI-Verlag 1986. ISBN: 3181419028. (Fortschritt-Berichte VDI Reihe 2 119).

COOK ET AL. 2002
Cook, R. D.; Malkus, D. S.; Plesha, M. E.; Witt, R. J.: Concepts and applications of finite element analysis. 4th Ed. New York, NY: Wiley 2002. ISBN: 0471356050.

DAI & SHAW 2002
Dai, K.; Shaw, L.: Distortion minimization of laser-processed components through control of laser scanning patterns. Rapid Prototyping Journal 8 (2002) 5, pp. 270-276.

DENKENA ET AL. 2003
Denkena, B.; Jung, M.; Müller, C.; Walden, L.: Charakterisierung weißer Schichten nach mechanischer und thermischer Einwirkung durch Fertigungsverfahren [engl.: Characterization of white layers after mechanical and thermal impact by manufacturing processes]. Journal of Heat Treatment and Materials 58 (2003) 4, pp. 211-217.

DENKENA ET AL. 2012
Denkena, B.; Köhler, J.; Kästner, J.: Chip formation in grinding: an experimental study. Production Engineering 6 (2012) 2, pp. 107-115.

DENKENA & TÖNSHOFF 2011
Denkena, B.; Tönshoff, H. K.: Spanen. Grundlagen [engl.: Machining. Basics]. Wiesbaden: Springer Fachmedien 2011. ISBN: 978-3-642-19771-0. (VDI-Buch).

DES RUISSEAUX & ZERKLE 1970
Des Ruisseaux, N. R.; Zerkle, R. D.: Thermal analysis of the grinding process. Journal of Engineering for Industry 92 (1970) 2, pp. 428-433.

DOMAN 2008
Doman, D. A.: Rubbing & plowing phases in single grain grinding. Diss. Dalhousie University Canada. 2008.

DOMAN ET AL. 2009
Doman, D. A.; Warkentin, A.; Bauer, R.: Finite element modeling approaches in grinding. International Journal of Machine Tools and Manufacture 49 (2009) 2, pp. 109-116.

DREIER ET AL. 2016
Dreier, S.; Brüning, J.; Denkena, B.: Simulation based reduction of residual stress related part distortion. Materials Science and Engineering Technology 47 (2016) 8, pp. 710-717.

DUSCHA ET AL. 2010
Duscha, M.; Klocke, F.; d'Entremont, A.; Linke, B.; Wegner, H.: Investigation of temperatures and residual stresses in speed stroke grinding via FEA simulation and practical tests. Manufacturing Systems 5 (2010) 1/1-10, pp. 1-6.

DUSCHA ET AL. 2011
Duscha, M.; Eser, A.; Klocke, F.; Broeckmann, C.; Wegner, H.; Bezold, A.: Modeling and Simulation of Phase Transformation during Grinding. Advanced Materials Research 223 (2011) 1, pp. 743-753.

ENGEIL & SPEIDEL 1969
Engeil, H.-J.; Speidel, M. O.: Ursachen und Mechanismen der Spannungsrißkorrosion [engl.: Causes and mechanisms of stress corrosion cracking]. Materials and Corrosion 20 (1969) 4, pp. 281-300.

EWELLIX 2023
Ewellix: Präzisionsschienenführungen [engl.: Precision rail guides]. <https://www.ewellix.com/de/produkte/linearfuhrungen/prazisionsschienenführungen/prazisionsschienenfuhrungen-mit-gleitbeschichtung-lwrpm/v> - 03.04.2023.

FANINGER 1976
Faninger, G.: Thermisch bedingte Eigenspannungen. Sonderheft: Spannungsermittlung mit Röntgenstrahlen [engl.: Thermally induced residual stresses. Special issue: Stress determination with X-rays] (1976) 1+2, pp. 48-51.

DIN 8589-11:2003-09
DIN Deutsches Institut für Normung e.V. 8589-11:2003-09: Fertigungsverfahren Spanen - Teil 11: Schleifen mit rotierendem Werkzeug; Einordnung, Unterteilung, Begriffe [engl.: Cutting manufacturing processes - Part 11: Grinding with rotating tools; classification, subdivision, terms]. Berlin: Beuth Verlag GmbH 2003.

DIN EN 8580:2003-09
DIN Deutsches Institut für Normung e.V. 8580:2003-09: Fertigungsverfahren: Begriffe, Einteilung [engl.: Manufacturing processes: Terms, classification]. Berlin: Beuth Verlag GmbH 2003.

DIN EN ISO 6507-1:2018-07
DIN Deutsches Institut für Normung e.V. 6507-1:2018-07: Metallische Werkstoffe - Härteprüfung nach Vickers - Teil 1: Prüfverfahren [engl.: Metallic materials - Vickers hardness test - Part 1: Test method] (ISO 6507-1:2018); Deutsche Fassung EN ISO 6507-1:2018. Berlin: Beuth Verlag GmbH 2018.

FÖCKERER 2015
Föckerer, T.: Methode zur rechnergestützten Prozessgestaltung des Schleifhärtens [engl.: Method for computer-aided process design of grinding hardening]. Diss. Technical University of Munich: Utz GmbH 2015. ISBN: 3831644489.

FOECKERER ET AL. 2010
Foeckerer, T.; Huntemann, J.-W.; Heinzel, C.; Brinksmeier, E.; Zaeh, M. F.: Experimental and numerical analysis of the influences on part distortion as a result of the grind-hardening process. 7th CIRP International Conference on Intelligent Computation in Manufacturing Engineering (ICME). Capri, Italy, 23.-25.06.2010 2010.

FOECKERER ET AL. 2012

Foeckerer, T.; Kolkwitz, B.; Heinzel, C.; Zaeh, M. F.: Experimental and numerical analysis of transient behavior during grind-hardening of AISI 52100. Production Engineering 6 (2012) 6, pp. 559-568.

FOECKERER ET AL. 2013
Foeckerer, T.; Zaeh, M. F.; Zhang, O. B.: A three-dimensional analytical model to predict the thermo-metallurgical effects within the surface layer during grinding and grind-hardening. International Journal of Heat and Mass Transfer 56 (2013) 1-2, pp. 223-237.

FRIESECKE & DOLZMANN 1997
Friesecke, G.; Dolzmann, G.: Implicit time discretization and global existence for a quasilinear evolution equation with nonconvex energy. SIAM Journal on Mathematical Analysis 28 (1997) 2, pp. 363-380.

GAO ET AL. 2020
Gao, H.; Ma, B.; Singh, R. P.; Yang, H.: Areal surface roughness of AZ31B magnesium alloy processed by dry face turning. An experimental framework combined with regression analysis. MDPI Materials 13 (2020) 10.

GIWERZEW 2003
Giwerzew, A.: Spanbildungsmechanismen und tribologisches Prozeßverhalten beim Schleifen mit niedrigen Schnittgeschwindigkeiten [engl.: Chip formation mechanisms and tribological process behavior during grinding at low cutting speeds]. Diss. University of Bremen. Aachen: Shaker 2003. ISBN: 978-3-8322-1685-6.

GOLDAK ET AL. 1984
Goldak, J.; Chakravarti, A.; Bibby, M.: A new finite element model for welding heat sources. Metallurgical Transactions B 15 (1984) 2, pp. 299-305.

GORGELS 2011
Gorgels, C.: Entstehung und Vermeidung von Schleifbrand beim diskontinuierlichen Zahnflankenprofilschleifen [engl.: Formation and prevention of grinding burn during discontinuous tooth flank profile grinding]. Diss. Techn. Hochsch. Aachen: Apprimus 2011. ISBN: 9783863590192.

GROSS & HAUGER 1998
Gross, D.; Hauger, W.: Technische Mechanik, Band 2: Elastostatik [engl.: Engineering Mechanics, Volume 2: Elastostatics]. 6th Ed. Berlin, Heidelberg: Springer 1998. ISBN: 3540641475.

GUO & MALKIN 1995
Guo, C.; Malkin, S.: Analysis of energy partition in grinding. Journal of Engineering for Industry 117 (1995) 1, p. 55.

GUO & MALKIN 2000
Guo, C.; Malkin, S.: Energy partition and cooling during grinding. Journal of manufacturing processes 2 (2000) 3, pp. 151-157.

HADAD & SADEGHI 2012
Hadad, M.; Sadeghi, B.: Thermal analysis of minimum quantity lubrication-MQL grinding process. International Journal of Machine Tools and Manufacture 63 (2012) 1, pp. 1-15.

HAHN 1966
Hahn, R. S.: On the mechanics of the grinding process under plunge cut conditions. Journal of Engineering for Industry 88 (1966) 1, pp. 72-79.

HAMDI ET AL. 2003
Hamdi, H.; Dursapt, M.; Zahouani, H.: Characterization of abrasive grain's behavior and wear mechanisms. Wear 254 (2003) 12, pp. 1294-1298.

HEEß 2012
Heeß, K.: Maß- und Formänderungen infolge Wärmebehandlung von Stählen. Grundlagen - Ursachen – Praxisbeispiele [engl.: Dimensional and shape changes due to heat treatment of steels. Basics - causes - practical examples]. 4th Ed. Renningen: Expert-Verlag 2012. ISBN: 9783816930679.

HEINZEL 2009
Heinzel, C.: Schleifprozesse verstehen. Zum Stand der Modellbildung und Simulation sowie unterstützender experimenteller Methoden [engl.: Understanding grinding processes. On the status of modeling and simulation as well as supporting experimental methods]. Habil. University of Bremen. Aachen: Shaker 2009. ISBN: 9783832286149.

HETTIG & MEYER 2020
Hettig, M. A.; Meyer, D.: Sequential multistage deep rolling under varied contact conditions. Procedia CIRP 87 (2020) 1, pp. 291-296.

HINTZE 2021
Hintze, W.: Laserstrahlbearbeitung von CFK und artverwandter Faserverbundkunststoffe [engl.: Laser beam processing of CFRP and related fiber composites]. In: Hintze, W. (Editor): CFK-Bearbeitung [engl.: CFRP processing]. Berlin, Heidelberg: Springer Berlin Heidelberg 2021, pp. 351-388. ISBN: 978-3-662-63264-2.

HORNFECK 2008
Hornfeck, T.: Laserstrahlbiegen komplexer Aluminiumstrukturen für Anwendungen in der Luftfahrtindustrie [engl.: Laser beam bending of complex aluminum structures for applications in the aviation industry]. 1st Ed.: Herbert Utz Verlag 2008. ISBN: 9783831608263.

HÜGEL & GRAF 2009
Hügel, H.; Graf, T.: Laser in der Fertigung. Strahlquellen, Systeme, Fertigungsverfahren [engl.: Lasers in manufacturing. Beam sources, systems, manufacturing processes]. 2nd Ed. Wiesbaden: Vieweg + Teubner 2009. ISBN: 978-3-83510-005-3.

INOUE & ARIMOTO 1997
noue, T.; Arimoto, K.: Development and implementation of cae system “hearts” for heat treatment simulation based on metallo-thermo-mechanics. Journal of Materials Engineering and Performance 6 (1997) 1, pp. 51-60.

JAEGER 1942
Jaeger, J. C.: Moving sources of heat and the temperature of sliding contacts. Proceedings of the royal society of New South Wales 76 (1942) 3, pp. 203-224.

JERMOLAJEV ET AL. 2016
Jermolajev, S.; Epp, J.; Heinzel, C.; Brinksmeier, E.: Material modifications caused by thermal and mechanical load during grinding. Procedia CIRP 45 (2016) 1, pp. 43-46.

JIANG ET AL. 2016
Jiang, J.; Ge, P.; Sun, S.; Wang, D.; Wang, Y.; Yang, Y.: From the microscopic interaction mechanism to the grinding temperature field: An integrated modelling on the grinding process. International Journal of Machine Tools and Manufacture 110 (2016) 1, pp. 27-42.

JIN ET AL. 2002
Jin, T.; Rowe, W. B.; McCormack, D.: Temperatures in deep grinding of finite workpieces. International Journal of Machine Tools and Manufacture 42 (2002) 1, pp. 53-59.

JIN ET AL. 2017
Jin, T.; Yi, J.; Li, P.: Temperature distributions in form grinding of involute gears. The International Journal of Advanced Manufacturing Technology 88 (2017) 9-12, pp. 2609-2620.

JIN & CAI 2001
Jin, T.; Cai, G. Q.: Analytical thermal models of oblique moving heat source for deep grinding and cutting. Journal of Manufacturing Science and Engineering 123 (2001) 2, p. 185.

JOHANSSON 1998
Johansson, T. G.: Controlled peen forming (1998) 65, p. 124.

JOHNSON & COOK 1983
Johnson, G. R.; Cook, W. H.: A constitutive model and data for metals subjected to large strains, high strain rates and high temperatures. Proceedings of the International Symposium on Ballistics 7 (1983) 1, pp. 541-547.

JÖNSSON 1998
Jönsson, R.: Richten wärmebehandelter Werkstücke [engl.: Straightening of heat-treated workpieces]. Journal of Heat Treatment and Materials 53 (1998) 1, pp. 5-8.

JORDAN ET AL. 1998
Jordan, R.; Kinderlehrer, D.; Otto, F.: The variational formulation of the Fokker-Planck equation. SIAM Journal on Mathematical Analysis 29 (1998) 1, pp. 1-17.

JUNG 1996
Jung, U.: FEM-Simulation und experimentelle Optimierung des Festwalzens bauteilähnlicher Proben unterschiedlicher Grösse [engl.: FEM simulation and experimental optimization of the deep rolling of component-like samples of different sizes]. Diss. Technical University of Darmstadt: Shaker 1996. ISBN: 3826518616.

JUNG ET AL. 1996
Jung, U.; Kaiser, B.; Kloos, K. H.; Berger, C.: Festwalz-Eigenspannungen per Computer-Simulation bestimmen [engl.: Determine residual stresses in deep rolling using computer simulation]. Materials Science and Engineering Technology 27 (1996) 4, pp. 159-164.

KANE ET AL. 1999
Kane, C.; Repetto, E. A.; Ortiz, M.; Marsden, J. E.: Finite element analysis of nonsmooth contact. Computer Methods in Applied Mechanics and Engineering 180 (1999) 1-2, pp. 1-26.

KANNAPPAN & MALKIN 1972
Kannappan, S.; Malkin, S.: Effects of grain size and operating parameters on the mechanics of grinding. Journal of Engineering for Industry 94 (1972) 3, pp. 833-842.

KARPUSCHEWSKI ET AL. 2008
Karpuschewski, B.; Knoche, H.-J.; Hipke, M.: Gear finishing by abrasive processes. CIRP Annals 57 (2008) 2, pp. 621-640.

KEßLER ET AL. 1998
Keßler, O.; Brockhoff, T.; Hoffmann, E.; Brinksmeier, E.; Mayr, P.: Maß- und Formänderungen bei der Randschichtwärmebehandlung durch Schleifen [engl.: Dimensional and shape changes during surface layer heat treatment by grinding]. Journal of Heat Treatment and Materials 53 (1998) 1, pp. 9-13.

KLOCKE ET AL. 2005
Klocke, F.; Brinksmeier, E.; Weinert, K.: Capability profile of hard cutting and grinding processes. CIRP Annals 54 (2005) 2, pp. 22-45.

KLOCKE 2018
Klocke, F.: Fertigungsverfahren 2. Zerspanung mit geometrisch unbestimmter Schneide [engl.: Manufacturing process 2. Machining with geometrically indefinite cutting edge]. 6th Ed. Berlin, Heidelberg: Springer 2018. ISBN: 978-3-662-58091-2.

KLOCKE & KÖNIG 2005
Klocke, F.; König, W.: Fertigungsverfahren 2. Schleifen, Honen, Läppen [engl.: Manufacturing process 2. Grinding, honing, lapping]. 4th Ed. Berlin: Springer 2005. (VDI-Buch Bd. 2).

KLOCKE & MADER 2005
Klocke, F.; Mader, S.: Fundamentals of the deep rolling of compressor blades for turbo aircraft engines. steel research international 76 (2005) 2-3, pp. 229-235.

KOERDT ET AL. 2008
Koerdt, M.; Beren, J. D.; Schilf, M.; Vollertsen, F.: Richten mit dem Laserstrahl [engl.: Straightening with the laser beam]. Schiffbau und Schiffstechnik 2 (2008) 2, pp. 64-67.

KOISTINEN & MARBURGER 1959
Koistinen, D. P.; Marburger, R. E.: A general equation prescribing the extent of the austenite-martensite transformation in pure iron-carbon alloys and plain carbon steels. Acta Metallurgica 7 (1959) 1, pp. 59-60.

KOLKWITZ ET AL. 2011
Kolkwitz, B.; Foeckerer, T.; Heinzel, C.; Zaeh, M. F.; Brinksmeier, E.: Experimental and numerical analysis of the surface integrity resulting from outer-diameter grind-hardening. Procedia Engineering 19 (2011) 1, pp. 222-227.

KOMERLA ET AL. 2020
Komerla, K.; Gach, S.; Akyel, F.; Vossel, T.; Reisgen, U.; Bleck, W.: Finite element simulation of residual stress induced by high energy beam welding in dual phase steel. Lasers in Manufacturing and Materials Processing 7 (2020) 2, pp. 154-176.

KÖNIG ET AL. 1978
König, W.; Steffens, K.; Lauer-Schmaltz, H.: Spanbildung und Trennpunktlage beim Schleifen [engl.: Chip formation and separation point position during grinding]. Industrie-Anzeiger 100 (1978) 73, pp. 49-50.

KÖNIG ET AL. 1985
König, W.; Ludewig, T.; Steffens, K.: Single grit tests to reveal the fundamental mechanism in grinding. ASME Grinding Symposium (1985).

KRAUS 2020
Kraus, J.: Laserstrahlumformen von Profilen [engl.: Laser forming of profiles]. Meisenbach (2020).

KRAUSS & ZAEH 2013
Krauss, H.; Zaeh, M. F.: Multi-target optimization and process window analysis in selective laser melting of high-performance parts. International Conference on Production Research ICPR 22 - Conference Proceedings. Iguassu Falls, Brazil, July 28–August 1 2013.

KUSCHEL ET AL. 2016
Kuschel, S.; Kolkwitz, B.; Sölter, J.; Brinksmeier, E.; Heinzel, C.: Experimental and numerical analysis of residual stress change caused by thermal loads during grinding. Procedia CIRP 45 (2016) 1, pp. 51-54.

LANGHORST ET AL. 2012
anghorst, M.; Deimling, C. von; Zäh, M. F.: Verzugsminimierung beim Laserstrahlschweißen [engl.: Minimizing distortion during laser beam welding]. ZWF Zeitschrift für wirtschaftlichen Fabrikbetrieb 107 (2012) 3, pp. 127-132.

LANGHORST 2016
Langhorst, M.: Beherrschung von Schweißverzug und Schweißeigenspannungen [engl.: Control of welding distortion and residual welding stresses]. Diss. Technical University of Munich: Utz GmbH 2016. ISBN: 9783831671977.

LEBLOND & DEVAUX 1984
Leblond, J. B.; Devaux, J.: A new kinetic model for anisothermal metallurgical transformations in steels including effect of austenite grain size. Acta Metallurgica 32 (1984) 1, pp. 137-146.

LEÓN GARCÍA 2010
León García, L. R. de: Residual stress and part distortion in milled aerospace aluminium. Diss. University of Hannover. Garbsen: PZH Produktionstechn. Zentrum 2010. ISBN: 9783941416437.

LI & AXINTE 2017
Li, H. N.; Axinte, D.: On a stochastically grain-discretised model for 2D/3D temperature mapping prediction in grinding. International Journal of Machine Tools and Manufacture 116 (2017) 1, pp. 60-76.

LIAO ET AL. 2000
Liao, Y. S.; Luo, S. Y.; Yang, T. H.: A thermal model of the wet grinding process. Journal of Materials Processing Technology 101 (2000) 1-3, pp. 137-145.

LIEDTKE 2004
Liedtke, D.: Wärmebehandlung. Grundlagen und Anwendungen für Eisenwerkstoffe [engl.: Heat treatment. Fundamentals and applications for ferrous materials]. 6th Ed. Renningen: Expert-Verlag 2004. ISBN: 978-3816924173. (Kontakt & Studium 349).

LIU ET AL. 1997
Liu, X.; Du, D.; Mourou, G.: Laser ablation and micromachining with ultrashort laser pulses. IEEE Journal of Quantum Electronics 33 (1997) 10, pp. 1706-1716.

LORTZ 1975
Lortz, W.: Schleifscheibentopographie und Spanbildungsmechanismus beim Schleifen [engl.: Grinding wheel topography and chip formation mechanism during grinding]. Diss. Techn. Hochsch. Aachen. 1975.

LOWIN 1980
Lowin, R.: Schleiftemperaturen und ihre Auswirkungen im Werkstück [engl.: Grinding temperatures and their effects on the workpiece]. Diss. Techn. Hochsch. Aachen: Shaker 1980.

LYUBENOVA 2020
Lyubenova, N.: Comprehensive characterisation and modelling of the surface integrity by deep rolling on flat surface. Diss. Saarland University. 2020.

MA ET AL. 2010
Ma, K.; Goetz, R.; Srivatsa, S. K.: Modeling of residual stress and machining distortion in aerospace components. In: Furrer, D. U. et al. (Editor): Metals Process Simulation: ASM International 2010, pp. 386-407. ISBN: 978-1-62708-197-9.

MAGALHÃES ET AL. 2017
Magalhães, F. C.; Abrão, A. M.; Denkena, B.; Breidenstein, B.; Mörke, T.: Analytical modeling of surface roughness, hardness and residual stress induced by deep rolling. Journal of Materials Engineering and Performance 26 (2017) 2, pp. 876-884.

MAHDI & ZHANG 1998
Mahdi, M.; Zhang, L.: Residual stresses in ground components caused by coupled thermal and mechanical plastic deformation. Journal of Materials Processing Technology 95 (1998) 1-3, pp. 238-245.

MAHDI & ZHANG 1999
Mahdi, M.; Zhang, L.: Applied mechanics in grinding – VII. Residual stresses induced by the full coupling of mechanical deformation, thermal deformation and phase transformation. International Journal of Machine Tools and Manufacture 39 (1999) 8, pp. 1285-1298.

MAHDI & ZHANG 2000
Mahdi, M.; Zhang, L.: A numerical algorithm for the full coupling of mechanical deformation, thermal deformation and phase transformation in surface grinding. Computational Mechanics 26 (2000) 2, pp. 148-156.

MAIER 2008
Maier, B.: Beitrag zur thermischen Prozessmodellierung des Schleifens [engl.: Contribution to the thermal process modeling of grinding]. Diss. Techn. Hochsch. Aachen. 2008.

MAKSOUD 2005
Maksoud, T.: Heat transfer model for creep-feed grinding. Journal of Materials Processing Technology 168 (2005) 3, pp. 448-463.

MALKIN 1974
Malkin, S.: Thermal aspects of grinding: part 2. Surface temperatures and workpiece burn. Journal of Engineering for Industry 96 (1974) 4, pp. 1184-1191.

MALKIN 1978
Malkin, S.: Burning limit for surface and cylindrical grinding of steels. CIRP Annals - Manufacturing Technology 27 (1978) 1, pp. 233-236.

MALKIN & GUO 2007
Malkin, S.; Guo, C.: Thermal analysis of grinding. CIRP Annals 56 (2007) 2, pp. 760-782.

MALKIN & GUO 2008
Malkin, S.; Guo, C.: Grinding technology. Theory and applications of machining with abrasives. 2nd Ed. New York, NY: Industrial Press 2008. ISBN: 9780831132477.

MARINESCU ET AL. 2004
Marinescu, I. D.; Rowe, W. B.; Dimitrov, B.; Inasaki, I.: Tribology of abrasive machining processes. Norwich, NY: Andrew 2004. ISBN: 0815514905.

MARTIN & YEGENOGLU 1992
Martin, K.; Yegenoglu, K.: HSG-Technologie : Handbuch zur praktischen Anwendung [engl.: HSG technology : manual for practical application]. Frohnstetten: Guehring Automation GmbH (1992).

MARUSICH ET AL. 2008
Marusich, T. D.; Usui, S.; Marusich, K. J.: Finite element modeling of part distortion. In: Xiong, C. et al. (Editor): Intelligent robotics and applications. First international conference, ICIRA 2008, Wuhan, China, October 15-17, 2008; Proceedings. Berlin: Springer 2008, pp. 329-338. ISBN: 978-3-540-88516-0.

MARUSICH & ORTIZ 1995
Marusich, T. D.; Ortiz, M.: Modelling and simulation of high-speed machining. International Journal for Numerical Methods in Engineering 38 (1995) 21, pp. 3675-3694.

MERCELIS & KRUTH 2006
Mercelis, P.; Kruth, J.-P.: Residual stresses in selective laser sintering and selective laser melting. Rapid Prototyping Journal 12 (2006) 5, pp. 254-265.

MISHRA & PRASAD 1985
Mishra, A.; Prasad, T.: Residual stresses due to a moving heat source. International Journal of Mechanical Sciences 27 (1985) 9, pp. 571-581.

MISHRA & YADAVA 2015
Mishra, S.; Yadava, V.: Laser Beam MicroMachining (LBMM). A review. Optics and Lasers in Engineering 73 (2015) 1, pp. 89-122.

MITZE 2010
Mitze, M.: Richten wärmebehandelter Bauteile [engl.: Straightening of heat-treated components]. Journal of Heat Treatment and Materials 65 (2010) 2, pp. 110-117.

MOULIK ET AL. 2001
Moulik, P. N.; Yang, H. T.; Chandrasekar, S.: Simulation of thermal stresses due to grinding. International Journal of Mechanical Sciences 43 (2001) 3, pp. 831-851.

MUGWAGWA ET AL. 2018
Mugwagwa, L.; Dimitrov, D.; Matope, S.; Yadroitsev, I.: Influence of process parameters on residual stress related distortions in selective laser melting. Procedia Manufacturing 21 (2018) 1, pp. 92-99.

NACHMANI 2008
Nachmani, Z.: Randzonenbeeinflussung beim Schnellhubschleifen [engl.: Boundary zone influencing during high-speed stroke grinding]. Diss. Techn. Hochsch. Aachen: Apprimus 2008. ISBN: 978-3-452268-07-5.

NGUYEN & ZHANG 2010
Nguyen, T.; Zhang, L.: Grinding–hardening using dry air and liquid nitrogen: Prediction and verification of temperature fields and hardened layer thickness. International Journal of Machine Tools and Manufacture 50 (2010) 10, pp. 901-910.

NOYEN 2008
Noyen, M.: Analyse der mechanischen Belastungsverteilung in der Kontaktzone beim Längs-Umfangs-Planschleifen [engl.: Analysis of the mechanical load distribution in the contact zone during longitudinal peripheral surface grinding]. Essen: Vulkan-Verlag 2008. ISBN: 3802787447.

ORTIZ & REPETTO 1999
Ortiz, M.; Repetto, E.: Nonconvex energy minimization and dislocation structures in ductile single crystals. Journal of the Mechanics and Physics of Solids 47 (1999) 2, pp. 397-462.

ORTIZ & STAINIER 1999
Ortiz, M.; Stainier, L.: The variational formulation of viscoplastic constitutive updates. Computer Methods in Applied Mechanics and Engineering 171 (1999) 3-4, pp. 419-444.

PAPADAKIS 2008
Papadakis, L.: Simulation of the structural effects of welded frame assemblies in manufacturing process chains. Diss. Technical University of Munich: Utz GmbH 2008. ISBN: 9783831608133.

PEITER 1992
Peiter, Arnold (Editor): Handbuch Spannungsmeßpraxis. Experimentelle Ermittlung mechanischer Spannungen [engl.: Manual of stress measurement practice. Experimental determination of mechanical stresses]. Braunschweig, Wiesbaden: Vieweg 1992. ISBN: 3528064285.

PERENDA ET AL. 2015
Perenda, J.; Trajkovski, J.; Žerovnik, A.; Prebil, I.: Residual stresses after deep rolling of a torsion bar made from high strength steel. Journal of Materials Processing Technology 218 (2015) 1, pp. 89-98.

PERENDA ET AL. 2016
Perenda, J.; Trajkovski, J.; Žerovnik, A.; Prebil, I.: Modeling and experimental validation of the surface residual stresses induced by deep rolling and presetting of a torsion bar. International Journal of Material Forming 9 (2016) 4, pp. 435-448.

PITTNER ET AL. 2010
Pittner, A.; Schwenk, C.; Weiss, D.; Rethmeier, M.: An efficient solution of the inverse heat conduction problem for welding simulation. In: Cerjak, H.-H. (Editor): Mathematical modelling of weld phenomena 9. Graz: Verlag der Techn. Univ. Graz 2010, pp. 761-791. ISBN: 978-3-85125-127-2.

POPRAWE 2005
Poprawe, R.: Lasertechnik für die Fertigung. Grundlagen, Perspektiven und Beispiele für den innovativen Ingenieur [engl.: Laser technology for manufacturing. Basics, perspectives and examples for the innovative engineer]. Berlin, Heidelberg: Springer 2005. ISBN: 978-3-54021-406-9. (VDI-Buch).

PREVÉY, P., HOMBACH, D. & MASON 1997
Prevéy, P., Hombach, D.; Mason, P.: Thermal residual stress relaxation and distortion in surface enhanced gas turbine engine components. Proceedings of the Heat Treating Society Conference 17 (1997) 1, pp. 3-12.

PRINZ ET AL. 2004
Prinz, C.; Sotirov, N.; Keßler, O.; Hoffmann, F.: Thermische Nachbehandlung der laserstrahlgeschweißten Al-Legierung AlSi1MgMn* [engl.: Thermal post-treatment of the laser-welded Al alloy AlSi1MgMn*]. Journal of Heat Treatment and Materials 59 (2004) 1, pp. 45-50.

RABINOWICZ 1995
Rabinowicz, E.: Friction and wear of materials. 2nd Ed. New York, NY: Wiley 1995. ISBN: 978-0-471-83084-9.

RADAJ 1988
Radaj, D.: Wärmewirkungen des Schweißens. Temperaturfeld, Eigenspannungen, Verzug [engl.: Thermal effects of welding. Temperature field, residual stresses, distortion]. Berlin, Heidelberg: Springer 1988. ISBN: 978-3-54018-695-3.

RADAJ 2002
Radaj, D.: Eigenspannungen und Verzug beim Schweißen. Rechen- und Meßverfahren [engl.: Residual stresses and distortion during welding. Calculation and measurement methods]. Düsseldorf: Verlag für Schweißen und Verwandte Verfahren DVS-Verlag 2002. ISBN: 978-3-87155-194-9. (Fachbuchreihe Schweißtechnik 143).

RADOVITZKY & ORTIZ 1999
Radovitzky, R.; Ortiz, M.: Error estimation and adaptive meshing in strongly nonlinear dynamic problems. Computer Methods in Applied Mechanics and Engineering 172 (1999) 1-4, pp. 203-240.

RATCHEV ET AL. 2011
Ratchev, S. M.; Afazov, S. M.; Becker, A. A.; Liu, S.: Mathematical modelling and integration of micro-scale residual stresses into axisymmetric FE models of Ti6Al4V alloy in turning. CIRP Journal of Manufacturing Science and Technology 4 (2011) 1, pp. 80-89.

ROBINSON ET AL. 2016
Robinson, J. W.; Zhou, Y.; Bhattacharya, P.; Erck, R.; Qu, J.; Bays, J. T.; Cosimbescu, L.: Probing the molecular design of hyper-branched aryl polyesters towards lubricant applications. Scientific reports 6 (2016) 1, p. 18624.

RODRÍGUEZ ET AL. 2012
Rodríguez, A.; López de Lacalle, L. N.; Celaya, A.; Lamikiz, A.; Albizuri, J.: Surface improvement of shafts by the deep ball-burnishing technique. Surface and Coatings Technology 206 (2012) 11-12, pp. 2817-2824.

ROOS & MAILE 2004
Roos, E.; Maile, K.: Werkstoffkunde für Ingenieure. Grundlagen, Anwendung, Prüfung [engl.: Materials science for engineers. Fundamentals, application, testing]. 2nd Ed. Berlin, Heidelberg: Springer 2004. ISBN: 978-3540220343.

ROSENTHAL 1946
Rosenthal, D.: The theory of moving sources of heat and its applicatioin to metal treatments. Materials Sciences and Applications 68 (1946) 8, pp. 849-866.

ROSS 1999
Ross, C. T.: Mechanics of solids. Chichester: Horwood Pub 1999. ISBN: 9780857099716. (Horwood Series in Engineering Science).

RÖTTGER 2003
Röttger, K.: Walzen hartgedrehter Oberflächen [engl.: Rolling of hard turned surfaces]. Diss. Techn. Hochsch. Aachen. 2003. ISBN: 3832211772.

RÖTTGER & FRICKE 2014
Röttger, K.; Fricke, S.: Deep rolling of bore holes with a diameter of 3 mm with a hydrostatic tool. International Conference on Shot Peening (ICSP) 12 (2014) 1, pp. 381-385.

ROWE ET AL. 1996
Rowe, W. B.; Morgan, M. N.; Black, S.; Mills, B.: A simplified approach to control of thermal damage in grinding. CIRP Annals 45 (1996) 1, pp. 299-302.

ROWE 2001
Rowe, W. B.: Thermal analysis of high efficiency deep grinding. International Journal of Machine Tools and Manufacture 41 (2001) 1, pp. 1-19.

ROWE & JIN 2001
Rowe, W. B.; Jin, T.: Temperatures in high efficiency deep grinding (HEDG). CIRP Annals 50 (2001) 1, pp. 205-208.

RYKALIN 1957
Rykalin, N. N.: Berechnung der Wärmevorgänge beim Schweißen [engl.: Calculation of heat processes during welding]. Berlin: VEB Verlag Technik 1957.

SADROSSADAT & JOHANSSON 2008
Sadrossadat, M.; Johansson, S.: S175 The effects of casting parameters and heat treatment on residual stress and microstructure variations of an Al-Si alloy. Powder Diffraction 23 (2008) 2, p. 186.

SATHIYA ET AL. 2012
Sathiya, P.; Panneerselvam, K.; Abdul Jaleel, M. Y.: Optimization of laser welding process parameters for super austenitic stainless steel using artificial neural networks and genetic algorithm. Materials & Design 36 (2012) 1, pp. 490-498.

SCHENK 2011
Schenk, T.: Modelling of welding distortion. The influence of clamping and sequencing. Diss. Technical University of Delft. 2011.

SCHIEBER ET AL. 2020
Schieber, C.; Hettig, M.; Zaeh, M. F.; Heinzel, C.: 3D modeling and simulation of thermal effects during profile grinding. Production Engineering 14 (2020) 5, pp. 655-665.

SCHIEBER ET AL. 2021
Schieber, C.; Hettig, M.; Zaeh, M. F.; Heinzel, C.: Evaluation of approaches to compensate the thermo-mechanical distortion effects during profile grinding. Procedia CIRP 102 (2021) 1, pp. 331-336.

SCHIEBER ET AL. 2022a
Schieber, C.; Hettig, M.; Zaeh, M. F.; Heinzel, C.: Combination of thermal and mechanical strategies to compensate for distortion effects during profile grinding. MDPI Machines 10 (2022) 1240, pp. 1-18.

SCHIEBER ET AL. 2022b
Schieber, C.; Hettig, M.; Zaeh, M. F.; Heinzel, C.: Modeling of deep rolling as a distortion compensation strategy during profile grinding. Key Engineering Materials 926 (2022) 1, pp. 897-905.

SCHIEBER ET AL. 2022c
Schieber, C.; Hettig, M.; Zäh, M. F.; Heinzel, C.: Verzugskompensation beim Profilschleifen mittels simulativ ausgelegter thermischer und mechanischer Oberflächenbearbeitung [engl.: Distortion compensation during profile grinding by means of simulatively designed thermal and mechanical surface treatment]. In: Hoffmeister, H.-W. et al. (Editor): Jahrbuch Schleifen, Honen, Läppen und Polieren. Verfahren und Maschinen [engl.: Yearbook of grinding, honing, lapping and polishing. Processes and machines]. 70th Ed. Aufl. Essen: Vulkan-Verlag GmbH 2022, pp. 2-19. ISBN: 978-3-8027-3176-1.

SCHIEBER ET AL. 2023
Schieber, C.; Hettig, M.; Müller, V.; Zaeh, M. F.; Heinzel, C.: Modeling of laser processing as a distortion compensation strategy for profile grinding. Production Engineering 17 (2023) 1, pp. 47-56.

SCHIMANSKI ET AL. 2010
Schimanski, K.; Karsten, O.; Hehl, A. von; Zoch, H.-W.: Wirkung der Wärmebehandlung auf den Verzug geschweißter Aluminiumstrukturen – eine Herausforderung für den Flugzeugbau [engl.: Effect of heat treatment on the distortion of welded aluminum structures – a challenge for aircraft construction]. Journal of Heat Treatment and Materials 65 (2010) 3, pp. 172-177.

SCHLATHER ET AL. 2019
Schlather, F.; Zapata, A.; Oefele, F.; Zaeh, M. F.: Determination of process forces during remote laser beam welding for the design of fastening features. Journal of Laser Applications 31 (2019) 4, p. 42006.

SCHOLTES 1991
Scholtes, B.: Eigenspannungen in mechanisch randschichtverformten Werkstoffzuständen. Ursachen, Ermittlung und Bewertung [engl.: Residual stresses in mechanically surface layer deformed material states. Causes, determination and evaluation]. Materials Science and Engineering Technology 22 (1991) 12, pp. 435-474.

SCHOLTES & MACHERAUCH 1986
Scholtes, B.; Macherauch, E.: Auswirkungen mechanischer Randschichtverformungen auf das Festigkeitsverhalten metallischer Werkstoffe [engl.: Effects of mechanical surface layer deformations on the strength behavior of metallic materials]. Zeitschrift für Metallkunde 77 (1986) 5, pp. 322-327.

SCHREIBER 1973
Schreiber, E.: Umwandlungseigenspannungen. Sonderheft zur röntgenographische Spannungsermittlung [engl.: Conversion residual stresses. Special issue on radiographic stress determination]. Journal of Heat Treatment and Materials 3 (1973) 28, pp. 186-200.

SCHUH ET AL. 2007
Schuh, A.; Zeller, C.; Holzwarth, U.; Kachler, W.; Wilcke, G.; Zeiler, G.; Eigenmann, B.; Bigoney, J.: Deep rolling of titanium rods for application in modular total hip arthroplasty. Journal of biomedical materials research. Part B, Applied biomaterials 81 (2007) 2, pp. 330-335.

SCHUHMANN & BIERMANN 2012

Schuhmann, S.; Biermann, D.: Herausforderungen bei der Modellierung von Schleifprozessen mittels der Finite-Elemente-Methode. Teil 3: Ermittlung der thermomechanischen Belastungen in Abhängigkeit der Werkstückgeschwindigkeit und Kontaktlänge [engl.: Challenges in the modeling of grinding processes using the finite element method. Part 3: Determination of thermomechanical loads as a function of workpiece speed and contact length]. Diamond Business 43 (2012) 4, pp. 56-63.

SCHULZE 2009

Schulze, G.: Die Metallurgie des Schweißens. Eisenwerkstoffe, nichteisenmetallische Werkstoffe [engl.: The metallurgy of welding. Ferrous materials, non-ferrous materials]. 4th Ed.: Springer-Verlag 2009. ISBN: 978-3-64203-183-0.

SEYFFARTH 2007

Seyffarth, P.: Entwicklung neuer Verfahren und Werkzeuge zum thermischen Richten im Schiffbau (Schlussbericht). Verfahrenstechnische Untersuchungen zum Richten von Feldbeulen an schiffbaulichen Strukturen mittels Mikroplasmastrahl [engl.: Development of new processes and tools for thermal straightening in shipbuilding (final report). Process engineering investigations into the straightening of field dents on shipbuilding structures using microplasma jets]. Technische Informationsbibliothek u. Universitätsbibliothek 2007.

SHAH ET AL. 2012

Shah, S. M.; Nélias, D.; Zain-ul-abdein, M.; Coret, M.: Numerical simulation of grinding induced phase transformation and residual stresses in AISI-52100 steel. Finite Elements in Analysis and Design 61 (2012), pp. 1-11.

SHAW 1992

Shaw, M. C.: Metal cutting principles. 1st Indian Ed. New Delhi: CBS Publishers & Distributors 1992. ISBN: 9788123901367. (Oxford series on advanced manufacturing).

SIM 2010

Sim, W. M.: Challenges of residual stress and part distortion in the civil airframe industry. International Journal of Microstructure and Materials Properties 5 (2010) 4/5, p. 446.

SNOEYS ET AL. 1978

Snoeys, R.; Leuven, K. U.; Maris, M.; Wo, N. F.; Peters, J.: Thermally induced damage in grinding. CIRP Annals - Manufacturing Technology 27 (1978) 2, pp. 571-581.

SOCHALSKI-KOLBUS ET AL. 2015
Sochalski-Kolbus, L. M.; Payzant, E. A.; Cornwell, P. A.; Watkins, T. R.; Babu, S. S.; Dehoff, R. R.; Lorenz, M.; Ovchinnikova, O.; Duty, C.: Comparison of residual stresses in inconel 718 simple parts made by electron beam melting and direct laser metal sintering. Metallurgical and Materials Transactions A 46 (2015) 3, pp. 1419-1432.

SÖLTER 2010
Sölter, J.: Ursachen und Wirkmechanismen der Entstehung von Verzug infolge spanender Bearbeitung [engl.: Causes and mechanisms of distortion due to machining]. Diss. University of Bremen. Aachen: Shaker 2010. ISBN: 9783832288242.

SÖLTER ET AL. 2016
Sölter, J.; Eckebrecht, J.; Kolkwitz, B.; Heinzel, C.: Analysis of the distortion and compensation potential in grind-hardening of linear guides. Materials Science and Engineering Technology 47 (2016) 8, pp. 726-734.

SOMMER ET AL. 2014
Sommer, K.; Heinz, R.; Schöfer, J.: Verschleiß metallischer Werkstoffe. Erscheinungsformen sicher beurteilen [engl.: Wear of metallic materials. Assessment of manifestations]. 2nd Ed. Wiesbaden: Springer Vieweg 2014. ISBN: 9783834824646.

SPINU ET AL. 2011
Spinu, S.; Frunza, G.; Diaconescu, E.: Numerical simulation of elastic-plastic non-conforming contact. In: Angermann, L. (Editor): Numerical Simulations - Applications, Examples and Theory: InTech 2011. ISBN: 978-953-307-440-5.

STÖHR 2008
Stöhr, R.: Untersuchung und Entwicklung des Innenrundschleifhärtens [engl.: Investigation and development of internal cylindrical grinding hardening]. Shaker 2008. ISBN: 3832271074.

TAKAZAWA 1966
Takazawa, K.: Effects of grinding variables on surface structure of hardened steel. Bulletin of the Japan Society of Precision Engineering 2 (1966) 1, pp. 14-21.

THATER ET AL. 2015
Thater, R.; Pittner, A.; Rethmeier, M.: Einsatz der Schweißsimulation zur Verzugsoptimierung an Praxisbauteilen [engl.: Use of welding simulation to optimize distortion on practical components]. Deutscher Verband für Schweißen und Verwandte Verfahren, DVS Congress (2015), pp. 892-895.

TÖNSHOFF 1965
Tönshoff, H. K.: Eigenspannungen und plastische Verformungen im Werkstück durch spanende Bearbeitung [engl.: Residual stresses and plastic deformation in the workpiece due to machining]. 1965.

TOTTEN ET AL. 2002
Totten, George E.; Howes, Maurice A. H.; Inoue, Tatsuo (Editor): Handbook of residual stress and deformation of steel. ebrary, Inc. Materials Park, OH: ASM International 2002. ISBN: 978-0871707291.

TOTTEN 2007
Totten, G. E.: Steel heat treatment. 2nd Ed. Boca Raton: CRC 2007. ISBN: 978-0849384554. (Steel heat treatment handbook).

VDI 3411
Verein Deutscher Ingenieure 3411: Hochleistungsschleifen metallischer Werkstoffe mit CBN-Schleifscheiben und erhöhten Schnittgeschwindigkeiten [engl.: High-performance grinding of metallic materials with CBN grinding wheels and increased cutting speeds]. Berlin: Beuth Verlag GmbH 2000.

VITS 1985
Vits, R.: Technologische Aspekte der Kühlschmierung beim Schleifen [engl.: Technological aspects of cooling lubrication during grinding]. Diss. Techn. Hochsch. Aachen: Apprimus. 1985.

VUČETIĆ 2008
Vučetić, D.: Zerspan- und Verschleißmechanismen beim Verzahnungshonen [engl.: Cutting and wear mechanisms in gear honing]. Diss. Techn. Hochsch. Aachen: Apprimus 2008. ISBN: 9783940565204.

WERNER 1971
Werner, G.: Kinematik und Mechanik des Schleifprozesses [engl.: Kinematics and mechanics of the grinding process]. Diss. Techn. Hochsch. Aachen: Apprimus. 1971.

WILKE 2008
Wilke, T.: Energieumsetzung und Gefügebeeinflussung beim Schleifhärten [engl.: Energy conversion and influence on microstructure during grinding hardening]. Diss. University of Bremen. Aachen: Shaker 2008. ISBN: 9783832278755.

WIMMER ET AL. 2018
Wimmer, S.; Loehe, J.; Zaeh, M. F.: Coupling analytical and numerical models to simulate thermomechanical interaction during the milling process of thin-walled workpieces. Lecture Notes in Production Engineering (2018), pp. 321-346.

WITTMANN ET AL. 2006
Wittmann, M.; Brinksmeier, E.; Heinzel, C.: Einfluss des Kühlschmierstoff-Zufuhrsystems auf die Wirkmechanismen im Schleifspalt [engl.: Influence of the cooling lubricant supply system on the mechanisms of action in the grinding gap]. In: Technische Akademie Esslingen et al. (Editor): Automotive and industrial lubrication. 15. International Colloquium Tribology, January 17 - 19, 2006. ISBN: 3-924813-62-0.

WITTMANN 2007
Wittmann, M.: Bedarfsgerechte Kühlschmierung beim Schleifen [engl.: Cooling lubrication on demand during grinding]. Diss. University of Bremen: Shaker 2007. ISBN: 3832261974.

YEGENOGLU & THURNBICHLER 1995
Yegenoglu, K.; Thurnbichler, M.: CBN-Schleifscheiben als wichtige Systemkomponente beim Hochleistungsschleifen [engl.: CBN grinding wheels as an important system component for high-performance grinding]. wt-Produktion und Management 85 (1995) 10, pp. 517-522.

YEN ET AL. 2005
Yen, Y.; Sartkulvanich, P.; Altan, T.: Finite element modeling of roller burnishing process. CIRP Annals 54 (2005) 1, pp. 237-240.

ZAEH ET AL. 2009
Zaeh, M. F.; Brinksmeier, E.; Heinzel, C.; Huntemann, J.-W.; Föckerer, T.: Experimental and numerical identification of process parameters of grind-hardening and resulting part distortions. Production Engineering 3 (2009) 3, pp. 271-279.

ZAEH & BRANNER 2010
Zaeh, M. F.; Branner, G.: Investigations on residual stresses and deformations in selective laser melting. Production Engineering 4 (2010) 1, pp. 35-45.

ZEPPENFELD 2005
Zeppenfeld, C.: Schnellhubschleifen von Gamma-Titanaluminiden [engl.: Fast-stroke grinding of gamma titanium aluminides]. Diss. Techn. Hochsch. Aachen. 2005.

ZHANG ET AL.
Zhang, J.; Xu, H.; Yu, Y.; Wei, Z.: FEM based numerical analysis on the temperature field in grind-hardening. International Conference on Computational 2009, pp. 615-618.

ZHANG ET AL. 1992
Zhang, L.; Suto, T.; Noguchi, H.; Waida, T.: An overview of applied mechanics in grinding. Manufacturing Review 5 (1992) 4, pp. 261-273.

ZHANG ET AL. 2017
Zhang, J.; Wang, G. C.; Pei, H. J.: Effects of grinding parameters on residual stress of 42CrMo steel surface layer in grind-hardening. Proceedings of the International Symposium on Mechanical Engineering and Material Science (2017), pp. 42-45.

ZHANG & MAHDI 1995
Zhang, L.; Mahdi, M.: Applied mechanics in grinding - IV. The mechanism of grinding induced phase transformation. International Journal of Machine Tools and Manufacture 35 (1995) 10, pp. 1397-1409.

ZHAO ET AL. 2013
Zhao, J. Y.; Fu, Y. C.; Xu, J. H.; Tian, L.; Yang, L.: Forces and chip morphology of nickel-based superalloy inconel 718 during high speed grinding with single grain. Key Engineering Materials 589-590 (2013) 1, pp. 209-214.

ZHONGYI & YUNQIAO 2010
Zhongyi, M.; Yunqiao, W.: Analyzing distortion of aircraft Structural part in NC machining based on FEM simulation. 2nd International Conference on Mechanical and Electrical Technology (ICMET). Singapore, Singapore, 10.09.2010 - 12.09.2010: IEEE 2010, pp. 1-5. ISBN: 978-1-4244-8100-2.

ZOCH 1995
Zoch, H.-W.: Randschichtverfestigung – Verfahren und Bauteileigenschaften [engl.: Surface hardening – Process and component properties]. Journal of Heat Treatment and Materials 50 (1995) 5, pp. 287-293.

ZOCH 2012
Zoch, H.-W.: Distortion engineering. Interim results after one decade research within the Collaborative Research Center. Materials Science and Engineering Technology 43 (2012) 1-2, pp. 9-15.

ZÖLTZER ET AL. 2001
Zöltzer, G.; Altenberger, I.; Scholtes, B.: Einfluss von Eigenspannungen auf die Mikrohärteverteilung in elastisch-plastisch gebogenen Stäben aus C80 [engl.: Influence of residual stresses on the microhardness distribution in elastic-plastic bent bars made of C80]. Journal of Heat Treatment and Materials 56 (2001) 5.

ZUM GAHR 1983
zum Gahr, K. H. (Editor): Reibung und Verschleiß. Mechanismen, Prüftechnik, Werkstoffeigenschaften [engl.: Friction and wear. Mechanisms, testing technology, material properties]. DGM Informationsgesellschaft Verlag 1983.

8 Appendix

A. List of supervised students

Within the scope of this dissertation project, multiple student theses were created at the Institute for Machine Tools and Industrial Management (*iwb*) of the TUM. The author of this thesis guided them scientifically, technically, and in terms of content. Various issues regarding simulative distortion control after profile grinding were investigated in those theses. Numerical and experimental results have been partially incorporated into the present work. The author would like to take this opportunity to express his sincere thanks to all students for their excellent support of this scientific work as well as for the inspiring discussions and ideas regarding the strategic design of process models and straightening techniques. The student work is listed below.

Table 2: Students' names, titles, and dates of author-supervised research projects, including submission dates and *iwb*-reference numbers

Name of student	Title and date of student thesis
Liu, Wenzhe	*Investigation of the influence of temperature-dependent, metallurgical and mechanical material properties on the result of the distortion simulation during profile grinding* Semester's thesis (September 14th, 2020; *iwb*-No.: 2020/55692)
Hofmann, Thomas	*Computer-aided design of a strategy for thermal distortion compensation of profiled workpieces by a laser* Semester's thesis (October 15th, 2020; *iwb*-No.: 2020/55691)
Helmer, Nicholas	*Computer-aided design of a strategy for mechanical distortion compensation of profiled workpieces by deep rolling* Bachelor's thesis (October 15th, 2020; *iwb*-No.: 2020/55690)
Zhang, Jiawei	*Data-based deep learning during profile grinding* Semester's thesis (November 10th, 2021; *iwb*-No.: 2021/60200)

Müller, Valentin Nikolaus	*Simulative, experimental and AI-based investigation of laser-assisted distortion compensation after grinding processing* Master's thesis (December 31st, 2021; *iwb*-No.: 2021/61097)
Hannl, Leonard Cedric	*Development of a data-driven force model for a five-axis machine tool* Master's thesis (August 26th, 2022; *iwb*-No.: 2022/62789)

B. Publications of the author

The following is a chronological list of the author's publications that were elaborated upon during the writing of this dissertation.

- **Schieber, C.**; Hettig, M.; Zaeh, M. F.; Heinzel, C.: 3D modeling and simulation of thermal effects during profile grinding. Production Engineering 14 (2020) 5, pp. 655–665. https://doi.org/10.1007/s11740-020-00983-8. **Publication 1 of this dissertation.**
- **Schieber, C.**; Hettig, M.; Zaeh, M. F.; Heinzel, C.: Evaluation of approaches to compensate the thermo-mechanical distortion effects during profile grinding. Procedia CIRP 102 (2021) 1, S. 331–336. https://doi.org/10.1016/j.procir.2021.09.057. **Publication 2 of this dissertation.**
- **Schieber, C.**; Hettig, M.; Zaeh, M. F.; Heinzel, C.: Modeling of deep rolling as a distortion compensation strategy during profile grinding. Key Engineering Materials 926 (2022) 1, S. 897–905. https://doi.org/10.4028/p-kl033k. **Publication 4 of this dissertation.**
- **Schieber, C.**; Hettig, M.; Müller, V.; Zaeh, M. F.; Heinzel, C.: Modeling of laser processing as a distortion compensation strategy for profile grinding. Production Engineering 17 (2022) 1. https://doi.org/10.1007/s11740-022-01144-9. **Publication 3 of this dissertation.**
- **Schieber, C.**; Hettig, M.; Zaeh, M.F.; Heinzel, C. Combination of thermal and mechanical strategies to compensate for distortion effects during profile grinding. MDPI Machines 10 (2022) 1240, 1240. https://doi.org/10.3390/machines10121240. **Publication 5 of this dissertation.**

Other publications

- **Schieber, C.**; Hettig, M.-A.; Zäh, F. M.; Heinzel, C.: Verzugskompensation beim Schleifen/Distortion compensation during grinding. Computer-aided modelling of

distortion compensation strategies. wt Werkstattstechnik online 110 (2020) 03, S. 159–165. https://doi.org/10.37544/1436-4980-2020-03-75.

- **Schieber, C.**; Hettig, M.; Zäh, F. M.; Heinzel, C.: Verzugskompensation beim Profilschleifen mittels simulativ ausgelegter thermischer und mechanischer Oberflächenbearbeitung. In: Hoffmeister, H.-W.; Denkena, B.: Schleifen, Honen, Läppen und Polieren 70 (2022). ISBN: 978-3-8027-3176-1.